

THESIS FOR THE DEGREE OF DOCTOR OF PHILOSOPHY

**FUEL CONVERSION IN A DUAL FLUIDIZED BED GASIFIER**

**- EXPERIMENTAL QUANTIFICATION AND IMPACT ON PERFORMANCE**

**Anton Larsson**

Department of Energy and Environment

CHALMERS UNIVERSITY OF TECHNOLOGY

Göteborg, Sweden 2014

Fuel Conversion in a Dual Fluidized Bed Gasifier  
- Experimental Quantification and Impact on Performance  
Anton Larsson  
ISBN 978-91-7597-074-5

© Anton Larsson 2014

Doktorsavhandling vid Chalmers tekniska högskola  
Ny serie Nr. 3755  
ISSN 0346-718X

Department of Energy and Environment  
Division of Energy Technology  
Chalmers University of Technology  
SE-412 96 Gothenburg  
Sweden  
Telephon +46 (0)31-772 1000

Chalmers Reproservice  
Göteborg 2013

# FUEL CONVERSION IN A DUAL FLUIDIZED BED GASIFIER

## - EXPERIMENTAL QUANTIFICATION AND IMPACT ON PERFORMANCE

Anton Larsson  
Division of Energy Technology  
Chalmers University of Technology  
SE-412 96 Gothenburg, Sweden

### Abstract

The present work is motivated by increasing demands and political goals to establish the commercial production of biofuels. Dual fluidized bed (DFB) gasification is a promising route for the production of biofuels through synthesis. The efficiency of biofuel production is limited by the conversion of biomass into syngas. The goal of the present work is to contribute to the understanding and description of the DFB gasification process, so as to facilitate the efficient conversion of biomass to a syngas. Towards this goal, an evaluation procedure is proposed that enables a comprehensive evaluation of the fuel conversion and efficiency of DFB gasifiers. This procedure is used to evaluate the Chalmers 2–4-MWth gasifier, and it is shown that important parameters, such as the yield of organic compounds (OC), char conversion, oxygen transport, and syngas yield, can be quantified online. Further, the dynamics of the loop seals were investigated to quantify the steam entering the gasifier and to ensure that there is no gas leakage through the loop seals into the gasifier.

To increase the fuel conversion in the Chalmers gasifier, it is investigated how individual changes in the level of fluidization, bed material, and layout of the gasifier affect the fuel conversion rate and heat demands of the process. The results obtained show that increasing the level of steam used for fluidization has a positive effect on the conversion of OC. However, increasing the level of steam also increases the heat demand of the system, and only when sufficient heat is available does this measure have a positive effect on the chemical efficiency of the process. Another way to reduce the yield of OC is to use a catalytic material. In the present work, catalytic metal-oxide bed materials are tested and compared with silica sand, used as reference. Metal-oxide materials can transport oxygen from the combustion side to the gasification side of the DFB system. If too much oxygen is transported, the efficiency of the gasifier suffers, since part of the gas is combusted. The investigation shows that ilmenite transports too much oxygen to be used in a DFB gasifier without additional measures, while bauxite and olivine show good potentials with lower oxygen-carrying capacities than ilmenite and higher OC conversion rates than silica sand. To increase the conversion of char, a change in the layout of the gasifier was investigated that involved the addition of a baffle, which was placed across the surface of the bubbling bed in the gasifier. After introduction of the baffle, the degree

of char conversion was effectively increased by 8%–15%, which can be explained by an increase in average residence time and of by forcing the char into areas with low levels of volatiles.

Using the evaluation procedure proposed in this work, different measures that affect the performance of the gasifier can be assessed, and the results can be exploited to reveal the optimal design and operational parameters for DFB gasifiers to ensure efficient production of biofuels based on biomass.

## Appended Publications

---

This thesis is an introduction to and a summary of the following publications, referred to in the text by Roman numbers:

- I. Anton Larsson, Martin Seemann, Daniel Neves, Henrik Thunman. Evaluation of Performance of Industrial-Scale Dual Fluidized Bed Gasifiers Using the Chalmers 2–4-MW<sub>th</sub> Gasifier. *Energy & Fuels*, 2013, 27, 6665-6680
- II. Anton Larsson, Mikael Israelsson, Fredrik Lind, Martin Seemann, Henrik Thunman. Using Ilmenite to Reduce the Tar Yield in a Dual Fluidized Bed Gasification System. *Energy & Fuels*, 2014, 28, 2632-2644
- III. Anton Larsson, Erik Sette, David Pallarés, Claes Breitholtz, Henrik Thunman. Char Conversion in the Chalmers 2–4-MW<sub>th</sub> Dual Fluidized Bed Gasifier. *To be submitted*
- IV. Anton Larsson, Henrik Ström, Srdjan Sasic, Henrik Thunman. Experimental and Numerical Investigation of the Dynamics of a Loop Seal Operating under Hot Conditions in a Large-Scale Dual Fluidized-Bed System. *To be submitted to AIChE*
- V. Mikael Israelsson, Anton Larsson, Henrik Thunman. Online Measurement of Elemental Yields, Oxygen Transport, Condensable Compounds, and Heating Values in a Gasification System. *Accepted for publication in Energy & Fuels*.
- VI. Daniel Neves, Henrik Thunman, Luís Tarelho, Anton Larsson, Martin Seemann, Arlindo Matos. Method for online measurement of the CHON composition of raw gas from biomass gasifier. *Applied Energy*, 2014, 113, 932-945

## Author's details

Professor Henrik Thunman, who was the main academic supervisor of this work, contributed with ideas and discussions and to the editing of **Papers I-VI**. Dr. Martin Seemann was the assistant academic supervisor of this work and contributed with experimental expertise and discussions for **Papers I-VI**. He has also contributed to the discussion and editing of **Papers I, II, and VI**. The financial support for this work was secured by Professor Henrik Thunman.

Anton Larsson is the lead author of **Papers I-IV**, and has been responsible for conducting the experiments and the evaluation of the results. For **Paper I**, Daniel Neves contributed with measurements of the pyrolysis yield. For **Paper II**, Mikael Israelsson was responsible for the tar analysis, and both he and Dr. Fredrik Lind contributed to the editing of the paper. For **Paper III**, Erik Sette was responsible for the measurements performed in the cold flow model, and both he and Dr. David Pallarès contributed to the editing of the paper. Claes Breitholtz contributed to the construction of the baffle used in the experiments under the hot condition, the performance of the experiments, and the editing of the paper. For **Paper IV**, Henrik Ström and Srdjan Sasic were responsible for the implementation of the CFD model and contributed to the editing of the paper. For **Paper V**, Mikael Israelsson is the main author and has been responsible for the design of the experimental equipment, data analysis, and experiments. Anton Larsson contributed to the experiments, analysis of the data, and editing of the paper. For **Paper VI**, Daniel Neves is the main author and has been responsible for the design of the experimental equipment, together with his academic supervisors Luís Tarelho, Arlindo Matos, and Henrik Thunman. Anton Larsson contributed to the experiments, analysis of the data, and editing of the paper.

## Publications not included in the thesis

- Anton Larsson, David Pallarés, Daniel Neves, Martin Seemann, Henrik Thunman. Zero-dimensional modeling of indirect fluidized bed gasification. Peer reviewed conference article, *Fluidization XIII*, 2010, Gyeong-ju, Korea.
- Anton Larsson, Martin Seemann, Henrik Thunman. Measurement of gas and carbon conversion in chalmers 2-4 MW<sub>th</sub> DFB Biomass Gasifier. Poster at the international conference on thermochemical conversion science, *tcbiomass2013*, Chicago, 2013.
- Henrik Thunman and Anton Larsson. The effect of oxygen transport by catalytic bed material in a biomass gasifier. Poster at the international conference on thermochemical conversion science, *tcbiomass2013*, Chicago, 2013.

## Acknowledgments

---

I hereby express my sincere gratitude to my main academic supervisor professor Henrik Thunman. Thank you for sharing your great knowledge and your enthusiasm of our field, and thank you for all the time you have dedicated to supervise me. Dr. Martin Seemann, thank you for sharing your experimental expertise and all the work you have put in to make the experiments in the Chalmers gasifier possible.

To my dear colleagues in the gasification group, thank you all for your support and good friendship, it has been a pleasure to work with you. Special thanks to; my friend Mikael Israelsson, thanks for good collaboration and for all the small debates, we have had; to Mr Lind for always taking time and finding a straight forward solution, to my “roomie” Jelena Marinkovic, always eager to discuss the importance of ash components, to my friend Patrick Moldenhauer, you always find another perspective on things; Claes Breitholtz, I have learned a lot from you; and to all my coauthors, thanks for a good collaboration.

I would like to acknowledge Rustan Marberg, Jessica Bohwalli and Johannes Öhlin, thanks for your excellent work in the power central. Thanks also to the operating staff at Akademiska Hus: Per, Mikael, Raymond, Robert and Malin for your fine work with running power plant and for your patience during experiments. Thanks to all colleagues at the division of Energy Technology, it has been a good experience to work with you all.

Thanks to my family and friends for supporting me and being the lovely people that you are. Kerstin and Ingemar, Erika och Jörgen, Frida och Calle, thanks for all your support, Albin, Axel, Thore and Linn thanks for giving me perspective on life. Finally, I want to thank my wonderful betrothed Helena Wallström, you are my love and my friend, thanks for your support and for believing in me.

This work was supported by Akademiska Hus, Göteborg Energi AB, Valmet Power AB, the Swedish Energy Agency, the Swedish Gasification Center (SFC), and The Centre for Combustion Science and Technology (CECOST). The CFD computations were performed using the resources of the Chalmers Centre for Computational Science and Engineering (C3SE), provided by the Swedish National Infrastructure for Computing (SNIC).



# Table of Contents

---

1	Introduction.....	1
1.1	Thermochemical conversion of biomass .....	1
1.2	Synthesis of biofuels.....	4
1.3	Gasification.....	9
1.4	Gasification Techniques .....	12
1.5	Development towards a comercial SNG plant .....	18
1.6	Aim of the present work .....	19
1.7	Methodology.....	20
2	Evaluation of the Performance of a DFB Gasifier.....	21
2.1	The Chalmers 2–4-MW <sub>th</sub> Gasifier .....	21
2.2	Process and Performance Parameters .....	25
2.3	Evaluation Procedures .....	27
2.4	Conclusions .....	48
3	Fuel conversion in DFB Gasifiers.....	51
3.1	OC Conversion .....	51
3.2	Char Conversion .....	60
3.3	Conclusions .....	64
4	Concluding Remarks and Outlook.....	65
5	Nomenclature.....	67
6	References.....	71



# 1 INTRODUCTION

---

Currently, the vehicle fleet in Sweden is dependent upon imported fossil fuels, and the consumption of these fuels contributes to emissions of greenhouse gases (mainly carbon dioxide (CO<sub>2</sub>)). To reduce the release of greenhouse gases, decrease dependency on imported fossil fuels, and secure employment levels in the energy sector, the Swedish government has set the goal of a fossil-free vehicle fleet in Sweden by Year 2030[1]. One of the issues addressed by the Government of Sweden towards the achievement of this goal is the production of renewable and efficient biofuels, with the condition that the production of biofuels should not compete with food production. Second-generation biofuels are defined as biofuels that are based on waste, rest products, cellulose from nonfood-based sources, lignocellulosic biomass, and algae. Biomass that is suitable for producing second-generation biofuels can be converted using bacteria or enzymes, or by means of thermochemical conversion, which includes pyrolysis, gasification and combustion. Thermochemical conversion is distinguished from the other processes by its ability to convert the lignin fraction of lignocellulosic feedstock. Given the potential for efficient conversion and the large available feedstock of lignocellulosic biomass, the present work focuses on the thermochemical conversion of lignocellulosic biomass, and more specifically, on dual fluidized bed gasification. To place the dual fluidized bed gasification technology in perspective, this section provides a general description of the thermochemical conversion of biomass into energy-rich intermediate products, as well as the pathways being explored towards the production of second-generation biofuels *via* gasification.

## 1.1 THERMOCHEMICAL CONVERSION OF BIOMASS

Thermochemical conversion of biomass yields a variety of intermediate products, which include solid-, liquid-, and gas-phase components, the distribution of which is highly dependent upon the process used[2]. The thermochemical conversion of biomass can be divided into three steps:

1. Drying
2. Pyrolysis/devolatilization
3. Char conversion and reforming of volatile components

Drying is a heat-requiring process in which the moisture content of the fuel is converted to steam; this step mainly affects the heat demand of the fuel conversion. When the temperature of the dry biomass is increased (to >130°C), volatile components are released as pyrolysis starts. During pyrolysis, the biomass decomposes into a wide range of components, which can be categorized as solids, liquids or gases, referring to the aggregation state of the products under ambient

conditions. The term *pyrolysis* refers to the decomposition of biomass in the absence of oxygen, while *devolatilization* refers to the release of volatile products independent of the surrounding atmosphere. During devolatilization, the net flow of gases is from the biomass and as such, the pyrolysis yields represent the yields achieved through devolatilization in the absence of gas-phase reactions. Therefore, the pyrolysis yields are hereinafter used to describe the second step of the thermochemical conversion.

The fraction of the fuel that remains in the solid state after pyrolysis is referred to as the char. Char consists of a carbon-rich matrix that contains hydrogen, oxygen, and ash components.[3] The mixture of gas components, consisting of species that have up to three carbon atoms ( $C_3$ ). Organic components with 2 or 3 carbon atoms are referred to as  $C_xH_y$  throughout this work. The liquids consist of water ( $H_2O$ ) and a range of condensable organic compounds (OC). Since organic compounds larger than  $C_3$  are not included in the group of gases, they are defined as OC components and assigned to the liquids group even though some of these compounds are unlikely to condense under ambient conditions, making the naming of this group somewhat ambiguous. Hereinafter, the abbreviation ‘OC’ is used to refer to all organic compounds that are not included in the cold gas (larger than  $C_3$ ), and ‘liquids’ refers to OC plus  $H_2O$ . Aromatic organic compounds (included in the OC) are commonly referred to as tar. Tar compounds condense at the temperatures higher than the ambient and cause problems related to fouling[4]. At high temperature some of the organic compounds can polymerize to form particles, which are referred to as soot[5]. As part of the cold gas can be used for the synthesis of a variety of products[2], it is referred to as syngas, which contains hydrogen ( $H_2$ ), carbon monoxide (CO), and  $CO_2$ . Figure 1.1 summarizes the different groups used in the present work to describe the yields from the thermochemical conversion of biomass.

Notation	Components																
	$N_2$	$H_2$	CO	$CO_2$	$CH_4$	$C_2$	$C_3$	...	$C_6$	...	$C_8$	...	$C_{16}$	...	soot	$H_2O$	solids
Cold gas																	
$C_xH_y$																	
Liquids																	
OC																	
Char																	
Raw gas																	
Tar																	
Syngas																	
Soot																	

Figure 1.1: The different products from a gasifier and the groupings used to describe these products. The notations  $C_2$ ,  $C_3$ ,  $C_6$  (and so on) represent organic compounds with 2, 3, 6 (and so on) carbon atoms, respectively, and the heading ... represents all component between the adjacent components.

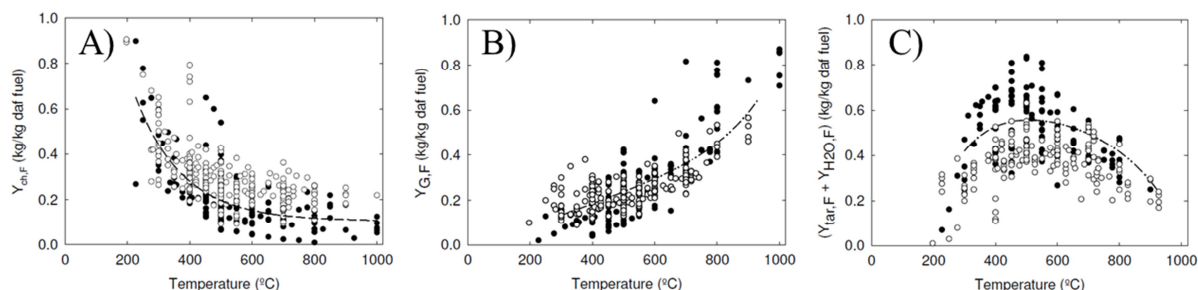


Figure 1.2: Yields of pyrolysis products as a function of temperature. A) Char ( $Y_{ch,F}$ ); B) cold gas ( $Y_{G,F}$ ); and C) liquids (tar and  $H_2O$ ,  $Y_{tar,F} + Y_{H_2O,F}$ ). Adapted from Neves *et al.*[6]

The yields of pyrolysis products depend on the fuel properties and operational conditions. The operational parameters that have the strongest impacts on product yield are the temperature of the reactor and the heating of the fuel. Figure 1.2 shows the typical yields of pyrolysis products as a function of temperature, as summarized by Neves *et al.*[6] for a large variety of biomasses, using either low heating rates (open symbols) or high heating rates (filled symbols). The yield of char decreases with temperature, and this trend is strongest up to a temperature of  $\sim 600^\circ\text{C}$ . The yield of gas increases continuously with temperature, whereas the yield of liquids peaks at around  $500^\circ\text{C}$ . Pyrolysis with a low heating rate yields more char and less liquid compounds than pyrolysis with high heating rates. Briefly, this can be explained by the dehydration of cellulose, which occurs mainly in the temperature range of  $200^\circ\text{--}300^\circ\text{C}$ , forming char and  $H_2O$  at slow heating rates, whereas at high heating rates, this reaction does not occur to the same extent[7].

The finding that the yields of char, liquids, and gases are flexible opens up possibilities for specialized processes, (Table 1.1). For example, torrefaction processes applies a low heating rate and low temperatures to maximize the yield of char.[8] If liquids are the main products, it is beneficial to have a high heating rate and a slightly higher temperature than is used for torrefaction.[9] For gasification and combustion, the benefits of using a specific heating rate are less clear, as neither liquids nor solids are the desired fractions.

The gas produced by thermochemical conversion of biomass can be used to produce heat and power or biofuels[2]. For heat and power production, the pyrolysis products are combusted, whereas for biofuel production, syngas is produced through gasification. The highest yield of gas is obtained through pyrolysis conducted at a higher temperature ( $>750^\circ\text{C}$ ) than is used for liquids or solids production.

Table 1.1: Examples of processes based on thermochemical conversion of biomass

	Torrefaction	Pyrolysis	Gasification	Combustion
Phase of main product	Solid	Liquid	Gas	Gas (for heat and power production)
Main products	Char	OC	$H_2$ , $CO$ , $CO_2$	$CO_2$ and $H_2O$
Typical temperatures	$200^\circ\text{--}300^\circ\text{C}$	$300^\circ\text{--}600^\circ\text{C}$	$>750^\circ\text{C}$	$>750^\circ\text{C}$
Beneficial heating rate	Low	High	Low/High	Low/High

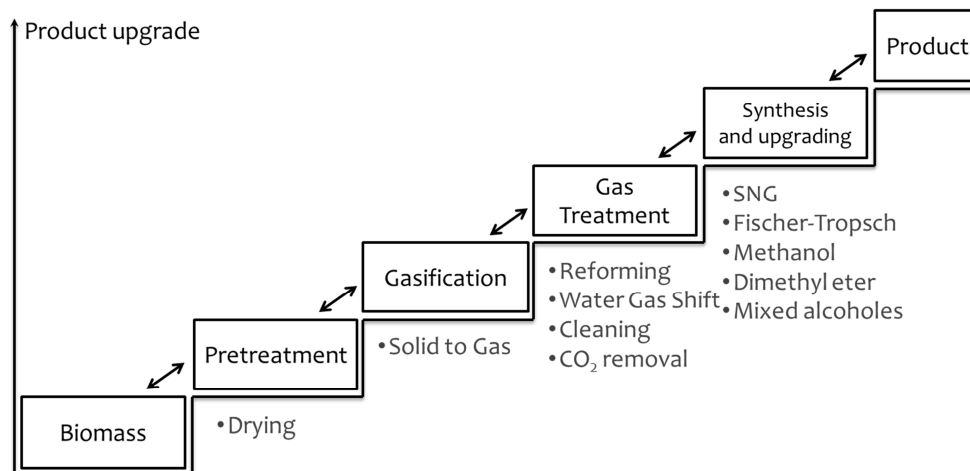


Figure 1.3: Simplified production chain for second-generation biofuels using gasification.

To increase the yield of gas beyond that obtained by pyrolysis, the char and liquids need to be converted in a third conversion step, which involves char conversion and reforming of the volatile components (as elaborated in section 1.3). For production of biofuels, the conversion process should be outlined to maximize the yield of syngas and the variety of biofuels, and the different synthetic processes place different requirements on the gas[10]. Therefore, conditioning of the raw gas from the gasifier is required to enable the synthesis (Figure 1.3). However, to minimize the complexity and investment costs for gas conditioning and losses related to by-products, the gas composition required by the synthesis process should be considered when outlining a gasification process. Therefore, the following section gives a summary of the different synthetic processes and the requirements that they place on the gas composition prior to the description of the gasification process so that the reactions in the gasifier can be discussed with knowledge of the gas requirements.

## 1.2 SYNTHESIS OF BIOFUELS

This section gives an overview of some relevant fuel synthesis processes and the requirements that the different static processes place on gas quality. The biofuels considered in this work are: substitute natural gas (SNG); methanol (MeOH); dimethyl ether (DME); mixed alcohols; and Fischer-Tropsch (FT) crude. The gas requirements are summarized in Table 1.2.

The main gas components to consider for the synthesis processes are H<sub>2</sub> and CO, and to achieve a high level of efficiency in the synthetic process, the H<sub>2</sub>/CO-ratio should lie within a specified range. For methanol and mixed alcohol production, CO<sub>2</sub> is required in addition to the H<sub>2</sub> and CO, and for these processes the (H<sub>2</sub>-CO<sub>2</sub>)/(CO+CO<sub>2</sub>)-ratio is used instead of the H<sub>2</sub>/CO-ratio. When synthesizing alcohols, the concentration of CO<sub>2</sub> should be between 4–8%, otherwise the reaction is inhibited. For the other synthetic processes, CO<sub>2</sub> dilutes the gas so its level should be minimized to avoid large reactors and low yields and to prevent high concentrations the CO<sub>2</sub> is separated from the gas prior to the synthesis.

Table 1.2: Summary of a selected range of synthetic processes and main process parameters, and the requirements that different applications exhibit for the gas produced through gasification.

Biofuel	FT crude[11]	MeOH[11]	SNG[12-15]	DME (one-step)[16]	Mixed Alcohols[11]
Main Product	Olefins	CH <sub>3</sub> OH	CH <sub>4</sub>	CH <sub>3</sub> OCH <sub>3</sub>	Mixed Alcohols
Catalyst	Paraffin's Co	Cu/ZnO/Al <sub>2</sub> O <sub>3</sub>	Variety of metal-based catalysts, Ni is considered for commercial plants	Variety of metal-based catalysts	Alkali/variety of metal-based catalysts
Type	Fixed bed	Fixed bed	Fixed bed	Multi-Fixed bed/slurry	Fixed bed
Temperature range (°C)	300–350	220–275	200–450	240–280	260–425
Pressure range (bar)	20–40	50–100	Atmospheric or higher	30–70	
H <sub>2</sub> /CO-ratio	0.6 –1.7	Unimportant	3	~1	1.0–1.2
(H <sub>2</sub> -CO <sub>2</sub> )/(CO+CO <sub>2</sub> )-ratio	Unimportant	>2	Unimportant	Unimportant	Dependent on the catalyst; range, 0–2
CO <sub>2</sub>	<5%	4%–8% (slow without, but inhibition with too much)	Low (CO <sub>2</sub> requires more hydrogen)	Low (by-product )	~5%
H <sub>2</sub> O	Low (slowly oxidizes catalysts, large amount inhibits Fe-based synthesis)	Low (can block active sites)	Low, reduces the CH <sub>4</sub> at equilibrium	By-product, needed for WGSR, accumulation leads to deactivation	Low
N <sub>2</sub>	Low (dilutes)	Low (dilutes)	Low (dilutes, can form NH <sub>3</sub> )	Low (dilutes)	Low (dilutes)
CH <sub>4</sub>	<2% (dilutes)	Low (dilutes)	Product		Low (dilutes)
C <sub>2</sub>	Low (dilutes)	Low (dilutes)	Low, causes deactivation through carbon deposition	no data	Low (dilutes)
Hydrocarbons C <sub>3</sub> –C <sub>6</sub>	Recycle to produce smaller molecules (to improve efficiency)	Recycle to produce smaller molecules (to improve efficiency)	Causes deactivation through carbon deposition	no data	Recycle to produce smaller molecules (to improve efficiency)
Tar	Concentrations below the dew-point	Concentrations below the dew-point	Causes deactivation through carbon deposition	Concentrations below the dew-point	Concentrations below the dew-point

Gases such as nitrogen ( $N_2$ ) and saturated gaseous hydrocarbons [e.g., methane ( $CH_4$ ), and ethane ( $C_2H_6$ )] cannot be utilized in the synthetic process, and in similarity to  $CO_2$ , the concentrations of these gases should be minimized to avoid unnecessary investment costs related to building a larger reactor. An exception is the SNG process, where  $CH_4$  is the main product and therefore the presence of a high concentration of  $CH_4$  already in the gas from the gasifier is desirable. Unsaturated hydrocarbons can cause deactivation of catalysts by forming carbon deposits, which should be avoided by hydration to saturate the molecules.

All the considered synthesis reactors are operated at temperatures in the range of  $200^\circ$ – $430^\circ C$ , which is considerably lower than the gasification temperature ( $>750^\circ C$ ), which means that the gas needs to be cooled upon entering the synthesis reactor. The low temperatures of the synthesis processes impose a restraint on the tar content of the gas, as the concentration must be less than the dew-point to avoid fouling in the gas cooling and synthesis steps. A high concentration of  $H_2O$  should be avoided in most synthetic processes and in such a case, the gas should be cooled below the dew-point of  $H_2O$  before reheating to attain the temperature for synthesis. In addition, the reactions that occur during the synthesis are generally exothermic. Together, these features make heat recovery and process integration important aspects of synthetic processes, the consequences of which are elaborated in Sections 1.4 and 1.5.

Table 1.2 gives the main operational parameters and components based on the compounds that contain the elements C, H, and O. For the implementation of such a system, aspects, such as the presence of particles, sulfur, alkali, chlorine, and trace elements, must be considered in addition those listed in Table 1.2[11], both in terms of the required cleaning steps and the temperature required by such temperatures and how they can be thermally integrated.

In summary, the syngas compositions required for the different synthetic processes are listed in Figure 1.4. The gas components considered in Figure 1.4 are  $H_2$ ,  $CO$ , and  $CO_2$ , as they are desired components of the synthetic processes. The composition is here visualized in terms of H/C-coordinates and O/C-coordinates on molar basis (van Krevelen diagram[17]). This enables the consideration of the three elemental components carbon (C), hydrogen (H) and oxygen (O) with only two axes, and this type of plot is used throughout this work to describe differences and changes in the gas composition.

The main components desired for the synthesis are  $CO$  and  $H_2$ , and a mixture of these gives an O/C-ratio of 1, which sets the lower limit of the  $x$ -axis. If the  $CO_2$  fraction is high, as happens during complete combustion, the O/C-ratio tends toward the value of 2, which therefore is the upper limit of the O/C-ratio. The upper limit of the H/C-ratio is based on the required  $H_2/CO$ -ratio.

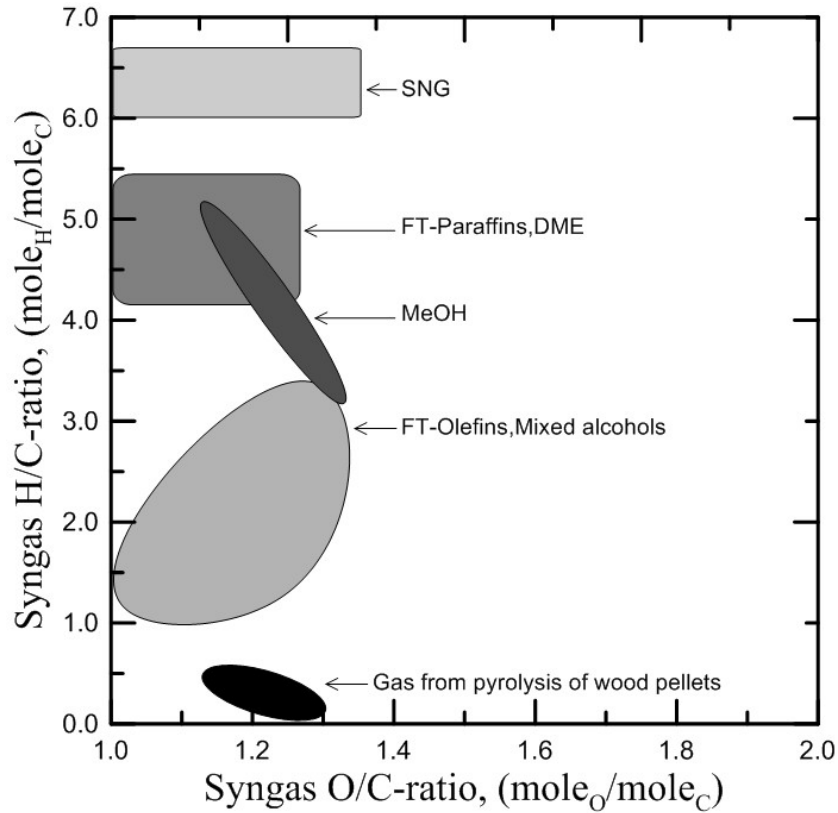


Figure 1.4: The H/C- and O/C-ratios of the syngas required by different synthetic processes (areas with different shades of gray) as compared with the coordinates that are typical for gas produced by pyrolysis of wood pellets (black area).

Figure 1.4 shows the required syngas composition (areas with different shades of gray) and the typical composition of a syngas produced by pyrolysis of woody biomass in the temperature range of 600°–840°C (black area). By comparing the composition of the syngas produced by pyrolysis with the syngas composition required by the synthetic processes, it becomes clear that an increase in the H/C ratio is required, while the O/C-ratio lies within the required range.

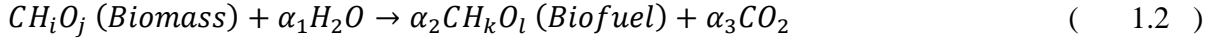
## EFFICIENCY OF BIOFUEL PRODUCTION

The choice of biofuel also affects the efficiency with which the biofuel can be produced. The chemical efficiency of a biofuel,  $\eta_b$ , can be estimated based on the lower heating value as:

$$\eta_b = \mu_{C,b} \frac{LHV_b/Y_{C,b}}{LHV_{daf}/Y_{C,daf}} \quad ( 1.1 )$$

where  $LHV_b$  is the lower heating value of the biofuel,  $LHV_{C,daf}$  is the lower heating value of the dry ash-free fuel,  $Y_{C,b}$  is the carbon fraction of the biofuel, and  $Y_{C,daf}$  is the carbon fraction of the dry ash-free fuel.

The yield of C in the biofuel,  $\mu_{C,b}$ , can be estimated by assuming that steam is available in abundance during all steps of the process. Biofuel production can be described in terms of a global reaction based on the elemental components C, H, and O as follows:



where  $\alpha_{1-3}$  are the numbers of moles required to balance the reaction,  $i$  and  $j$  are the moles of H and O, respectively, related to the C in the biomass, and  $k$  and  $l$  are the moles of H and O, respectively, related to the C in the biomass. Then, the mass balances for C, H, and O are:

$$1 = \alpha_2 + \alpha_3 \quad , (C - \text{balance}) \quad (1.3)$$

$$\gamma = (j + \alpha_1 - \alpha_2 l)/2 \quad , (O - \text{balance}) \quad (1.4)$$

$$i + 2\alpha_1 = \alpha_2 k \quad , (H - \text{balance}) \quad (1.5)$$

Rearranging Eqs (1.3–1.5), the yield of C in the biofuel,  $\mu_{C,b,theo}$ , can be estimated as:

$$\mu_{C,b,theo} = \left(4 - 2(O/C)_{daf} + (H/C)_{daf}\right) / \left(4 - 2(O/C)_b + (H/C)_b\right) \quad (1.6)$$

where  $(O/C)_{daf}$  and  $(H/C)_{daf}$  are the molar ratios for the dry ash-free fuel, and  $(O/C)_b$  and  $(H/C)_b$  are the molar ratios for the biofuel. However, for a real-life process, losses coupled to the heat demand of the process and losses coupled to the yield of by-products should be considered. With derivation equivalent to that for Eq. (1.6) the yield of C in the biofuel,  $\mu_{C,b}$ , can be estimated for a real-life process as:

$$\mu_{C,b} = \left(4 - 2(O/C)_{daf} + (H/C)_{daf} - \vartheta_{hd} - \vartheta_{bp}\right) / \left(4 - 2(O/C)_b + (H/C)_b\right) \quad (1.7)$$

where  $\vartheta_{hd}$  is the loss-term coupled to the heat demand of the process, and  $\vartheta_{bp}$  is the loss-term coupled to by-products that are not converted into biofuel. The loss-terms are defined as:

$$\vartheta_j = -\sum(4\dot{n}_{C,i} - 2\dot{n}_{O,i} + \dot{n}_{H,i}) / \dot{n}_{C,daf} = -\sum\left(\left(4 - 2(O/C)_i + (H/C)_i\right) \dot{n}_{C,i} / \dot{n}_{C,daf}\right) \quad (1.8)$$

where  $j = bp$  and  $hd$ , and  $i$  are components that are added to or removed from the process and  $\dot{n}_C$ ,  $\dot{n}_H$ ,  $\dot{n}_O$ , are the molar flows of C, H, and O, respectively. Added mass flows (such as oxygen) are treated as positive molar flows, while removed mass flows (e.g., a removed by-product) are treated as negative molar flows. These loss-terms are described further in the following sections, together with an explanation of how they are coupled to the reactions in a gasifier.

Table 1.3: Summary of the H/C-ratios and O/C-ratios used for estimations of the theoretical yields of C in different biofuels based on wood pellets;  $(O/C)_{daf} = 0.65$ ,  $(H/C)_{daf} = 1.43$ , and  $LHV_{daf}/Y_{C,daf} = 38 \text{ MJ/kg}_C$ .

	FT-O*	FT-P**	SNG	MeOH	Direct DME	Mixed alcohols***
H/C-ratio	2	~3	4	4	3	4
O/C-ratio	0	0	0	1	0.5	0.25
$\mu_{C,b} [\text{kg}_{C,b}/\text{kg}_{C,daf}]$	$0.69 - \frac{\partial_{hd}}{6} - \frac{\partial_{rp}}{6}$	$0.59 - \frac{\partial_{hd}}{7} - \frac{\partial_{rp}}{7}$	$0.52 - \frac{\partial_{hd}}{8} - \frac{\partial_{rp}}{8}$	$0.69 - \frac{\partial_{hd}}{6} - \frac{\partial_{rp}}{6}$	$0.69 - \frac{\partial_{hd}}{6} - \frac{\partial_{rp}}{6}$	$0.55 - \frac{\partial_{hd}}{7.5} - \frac{\partial_{rp}}{7.5}$
$LHV_b/Y_{C,b} [\text{MJ/kg}_C]$	~56	~46	67	53	55	~49
$\eta_b [\text{MJ}_b/\text{MJ}_{daf}]$	$1.02 - \frac{\partial_{hd}}{0.16} - \frac{\partial_{rp}}{0.16}$	$0.72 - \frac{\partial_{hd}}{0.13} - \frac{\partial_{rp}}{0.13}$	$0.92 - \frac{\partial_{hd}}{0.19} - \frac{\partial_{rp}}{0.19}$	$0.97 - \frac{\partial_{hd}}{0.15} - \frac{\partial_{rp}}{0.15}$	$1.00 - \frac{\partial_{hd}}{0.16} - \frac{\partial_{rp}}{0.16}$	$0.71 - \frac{\partial_{hd}}{0.14} - \frac{\partial_{rp}}{0.14}$

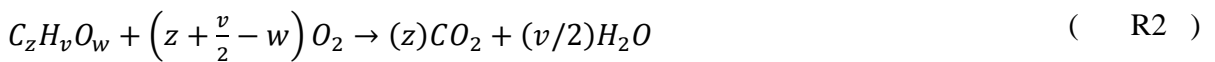
\* $C_nH_{2n}$ ; \*\* $C_nH_{2n+2}$ ; \*\*\*Example with butanol as the average.

Equation (1.6) indicates that a high yield of C can be achieved with a biofuel that has a low H/C-ratio and high O/C-ratio. To demonstrate how the choice of biofuel influences the chemical efficiency of the conversion of biomass to biofuel, an example based on wood pellets and the biofuels included in Table 1.3 is given here. Using wood pellets with  $(O/C)_{daf} = 0.65$ ,  $(H/C)_{daf} = 1.43$ , and  $LHV_{daf}/Y_{C,daf} = 38 \text{ MJ/kg}_C$ , the yield of C in the biofuel and the chemical efficiency can be estimated (Table 1.3). This shows that the loss-terms have less impact on chemical efficiency for biofuels with high H/C-ratios and low O/C-ratios, than for biofuels with low H/C-ratios and low O/C-ratios.

## 1.3 GASIFICATION

This section summarizes the main reactions occurring in a gasifier that are central to heat production and to the conversion of by-products that are formed during pyrolysis into syngas. Figure 1.5 illustrates the fuel conversion steps, where  $Y$  represents the yields from pyrolysis and  $X$  represents the degrees of conversion. The production of gas in a gasifier is restricted by the degree of char conversion,  $X_{ch}$ , and unconverted char leaves the gasifier in the form of solids. The composition of the volatile components formed during pyrolysis is reformed in the gas phase where the conversion of OC components,  $X_{OC}$ , into syngas or  $\text{CH}_4$  is of major importance.

To produce the heat needed to maintain the temperature of the process, part of the raw gas (represented as  $C_zH_vO_w$ ) or the char (represented as  $C(s)$ ) can be combusted by the addition of oxygen:



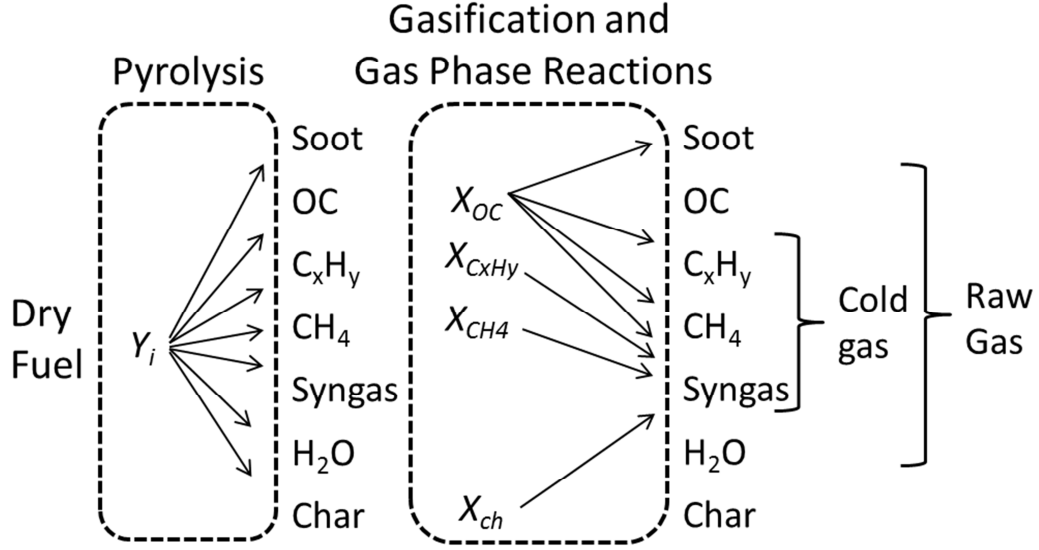


Figure 1.5: Illustration of and notations for the yields from pyrolysis ( $Y_i$ ) and the degrees of conversion ( $X$ ) of OC,  $C_xH_y$ , and  $CH_4$ .

The loss-term coupled to the oxygen added for heat production can be estimated with a simplification of Eq. 1.8:

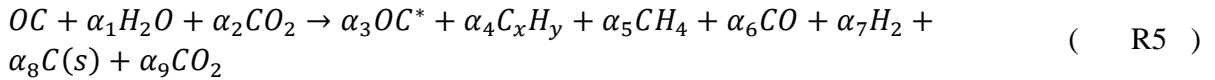
$$\vartheta_{hd} = 2\dot{n}_O / \dot{n}_{C,daf} \quad ( 1.9 )$$

where  $\dot{n}_O$  is the molar flow of oxygen, and  $\dot{n}_{C,daf}$  is the molar flow of carbon in the daf fuel.

The intermediate products from the pyrolysis are converted together with  $CO_2$  and  $H_2O$  into syngas. The char can be gasified through reactions with  $CO_2$  and  $H_2O$ , and the global reactions can be summarized as:



The conversion of OC can be summarized as the following global reaction:



where  $\alpha_{1-9}$  indicates the molar amount of the different components related to the OC, and  $OC^*$  represents a changed composition of the remaining OC. The yields of the different components

can change with the level of conversion, the available reactants, and the presence of catalytic materials.

Additional gas-phase reactions that should be considered are steam reforming of the hydrocarbons that are included in the cold gas,  $CH_4$  and  $C_xH_y$ :



The syngas compounds produced through reactions R1–R9, as well as the syngas formed during pyrolysis react with steam through the water gas-shift reaction (WGSR):



The change in the composition of the syngas due to reactions R1–R10 is illustrated in Figure 1.6. The example shown is based on the measured gas composition from pyrolysis of wood pellets in a bench-scale fluidized reactor operated at 840°C. The arrows in Fig. 1.6 indicate the changes in the O/C- and H/C-coordinates caused by the reactions. The gas requirements for the synthesis of different biofuels, as shown in Fig. 1.4, are included, so as to illustrate those reactions that reduce the need for conditioning of the gas by changing the syngas composition in line with the gas requirements. In Fig. 1.6, the conversion of OC is illustrated as a striped area, as the composition of the syngas generated by the conversion can differ depending on whether the OC arises through cracking reactions or reforming reactions. However, the OC conversion generally causes an increase in the H/C-ratio (especially if  $H_2O$  is included in the reaction). Due to the rather low oxygen contents of organic compounds that are thermally stable above 800°C[18, 19], the O/C-ratio can be expected to approach the value of 1 when OC is converted through steam reforming.

An important observation from Eq. (1.8) is that adding or removing  $H_2O$  has no impact on the loss-factor. Thus, the vector of the WGSR can be used as a reference to indicate whether a change in syngas composition has a positive or negative effect on the loss-factors compared to the reference case (in this case the pyrolysis gas). Using the syngas from the pyrolysis as reference point, conversion of char, OC,  $CH_4$ ,  $C_xH_y$  or  $CH_4$  are required to yield a coordinate above the WGSR vector, which is associated with a decreases of the loss-factors as indicated by Eq. (1.8). Correspondingly, addition of oxygen or addition of  $CO_2$  (e.g. as a purge gas for the fuel feed) is required to yield a coordinate below the WGSR vector, which is associated with an increase of the loss-factor related to the heat demands.

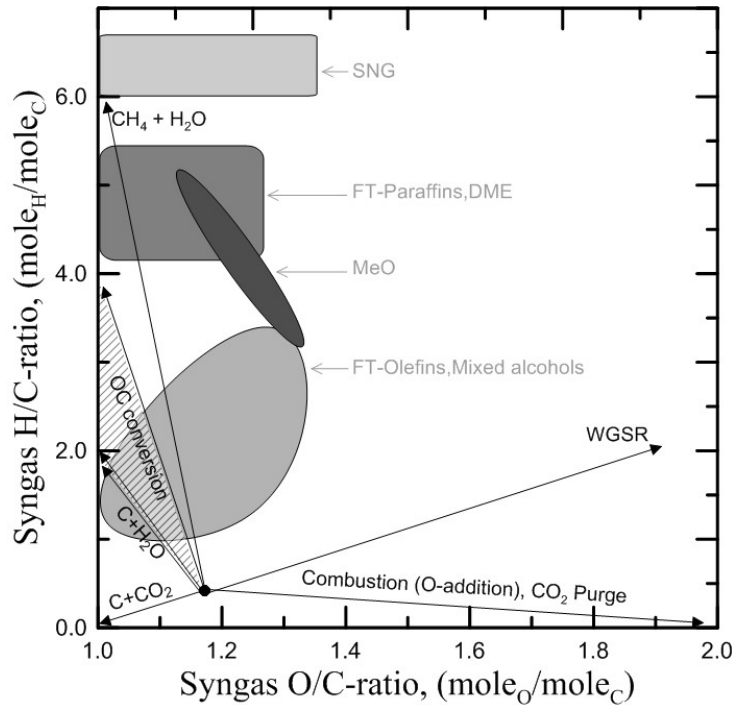


Figure 1.6: Illustration of the syngas composition and the changes in syngas composition based on the  $H_2$ ,  $CO$ , and  $CO_2$  levels resulting from the reactions in the gasifier (reactions R1–R10), as compared with the gas requirements shown in Figure 1.4.

To achieve an appropriate composition of the syngas two steps are used in the gas conditioning system, which is a reactor for WGSR and  $CO_2$  separation. Note that a secondary reforming step can be included in the gas conditioning to reform the gas, where reactions R2 and R5–R10 are the main reactions to consider. In terms of the impacts that these reactions have on syngas composition, it makes no difference whether they occur in the gasifier or in the reforming step, which means that Figure 1.6 can also be used to describe the reforming step.

## 1.4 GASIFICATION TECHNIQUES

In this section, short descriptions of the different gasification technologies that are relevant to biofuel production are given to exemplify how the design and operation of a gasifier can affect the loss-factors related to both the heating of the gasifier and to the yields of by-products from the gasifier. Three categories of gasifiers are considered here:

- Entrained flow (EF) gasifiers
- Fluidized bed (FB) gasifiers
- Dual fluidized bed (DFB) gasifiers

A list of the process parameters and schematics of the gasification techniques is presented in Table 1.4.

Table 1.4: Schematics of an EF gasifier, FB gasifier, and DFB gasifier, and the typical values for important process parameters.

	Autothermal (directly heated) Gasifiers	Allothermal (indirectly heated) Gasifiers
	Entrained flow (EF) gasifier	Dual fluidized bed (DFB) gasifier
Concept illustrations		
Temperature	>1300°C	800°–900°C
Pressure	Atmospheric or Pressurized	Atmospheric
Fuel feed	Powder or Slurry	Chips or Pellets
Gasification agent	Oxygen and Steam	Steam
Main source of heat	Partial combustion of gas	Combustion of part of the char and recirculated gas, if required
Other	Partial combustion of gas	Catalytic bed material can be applied

Gasification in an entrained flow (EF) gasifier is a well-established technique for the gasification of coal[20]. The technique is based on pneumatic feeding of fine particles and a high temperature ( $>1300^{\circ}\text{C}$ ), so as to ensure rapid conversion of the fuel particles. The high temperature means that high reaction rates and low yields of tar can be achieved. At this temperature, a considerable amount of the tar polymerizes into soot[5], and temperatures  $>1600^{\circ}\text{C}$  are required to avoid substantial soot formation, as shown in **Paper V**. At such high temperatures, the ash components of the fuel are in a molten state, and the lower part of the reactor involves a quenching step to remove the molten ash. The gasification medium is oxygen and steam, whereby the amount of oxygen is used to control the temperature of the gasifier. A major challenge that arises during the switch from coal to biomass in an EF gasifier concerns the fuel feed. The concept requires very small particles, but the grinding of biomass requires a lot of electricity (as much as  $0.08 \text{ MWe/MW}_{\text{th}}$  for achieving  $100\mu\text{m}$  particles[21]). To reduce the power consumption for grinding biomass, fuel preparation technologies, such as torrefaction[8, 21], are currently being researched, but torrefaction cause a loss of part of the fuel instead (the gas formed at the process temperature of  $200^{\circ}\text{C}$ – $300^{\circ}\text{C}$ ) and have not yet been implemented on a large scale. An alternative strategy to avoid the high cost of power consumption for grinding the biomass is to use the fluidized bed (FB) technology.

In an FB, silica sand or catalytic particles can be used as the bed material. The bed material is fluidized by adding the gasification medium, which is oxygen and/or steam, at the bottom of the reactor. The FB provides good mixing of the solid material and enables a long residence time for large fuel particles. In addition, the bed material has a high heat capacity and acts as a thermal flywheel that helps to stabilize the operation of the reactor. However, FBs are sensitive to agglomeration and sintering of the bed material, and the maximum temperature is limited by the type of bed material and the ash components of the fuel. Typically, a temperature  $>1000^{\circ}\text{C}$  ( $>900^{\circ}\text{C}$  when using silica sand) should be avoided; the temperature is regulated by adding oxygen to combust part of the fuel. Due to the significantly lower temperatures of FBs, as compared to that of an EF reactor, the yields of tar and other by-products are higher. However, by using a catalytic bed material the conversion of the by-products into syngas and can be increased and, to some extent, compensate for the lower temperature.

Both the FB gasifiers and EF gasifiers are autothermal (directly heated) gasifiers that require oxygen for sustaining the temperature of the process. Pure oxygen is used to avoid diluting the syngas with nitrogen, although, the production of oxygen is an energy-intensive process that decrease the overall efficiency and increase the operational costs. A design-option that removes the need for pure oxygen is to use an allothermal (indirectly heated) gasifier, where the temperature is sustained by delivering heat from another reactor in which air can be used for combustion without diluting the syngas.

The DFB technology facilitates allothermal gasification through the use of two FB reactors. The reactors are separated by loop seals, which enable transport of the bed material between the reactors while preventing cross-contamination of gases between the reactors. The reactors used in

a DFB gasifier are: 1) a combustor, which is fluidized with air and recycled flue gases; and 2) a gasifier, which is fluidized with steam (see schematics in Table 1.4). The fuel is fed into the gasifier, where the volatiles are released and a fraction of the char is gasified. The unconverted char follows the bed material to the second reactor where it is burned to produce heat. This heat is transferred back to the gasifier *via* the bed material to provide heat indirectly. Combustion in a separate reactor increases the flexibility of the system, as it enables combustion of by-products and/or auxiliary fuel if additional heat is required in the gasifier or other steps of the process.

With respect to the FB and DFB gasifiers, various bed materials can be used to increase the levels of the reactions in the gasifier. However, some materials (e.g., metal oxide-based materials) exhibit oxygen-carrying capabilities in addition to the ability to transfer heat. In a DFB system, this cause an oxygen transport from the combustor to the gasifier and have a negative effect on the efficiency. This is discussed further in Section 2.2 and in **Paper II**. Another parameter to consider is the pressure in the reactor. The concept behind the DFB is more complex than those of the other systems considered. While pressurization of a DFB process is unlikely to be used with the current technology, both FB and EF gasifiers can be pressurized and, thereby, reduced in size for a given throughput of fuel.

## LOSS-FACTORS FOR DIFFERENT GASIFICATION TECHNIQUES

The purpose of this section is to explain how the different features of the gasification technologies can affect the efficiency of a biomass to biofuel production unit in terms of the loss-factors related to heat production and the by-products from the gasifier, respectively.

The loss-factor related to the by-products is defined in Eq. (1.8), and the by-products to consider from the gasifier are char, OC,  $C_xH_y$ ,  $CH_4$ , and soot. DFB and FB gasifiers are restricted with respect to the temperature range due to sintering of the ash and bed material, and this favors the yields of the by-products OC,  $C_xH_y$ , and  $CH_4$ , for typical values and related loss-factors, see Table 1.5. The examples listed in Table 1.5 reveal that the loss-factors related to OC,  $C_xH_y$ , and  $CH_4$  are in the range of 1.2–1.9 for DFB and FB gasifiers, whereas they are approximately 0.6 for an EF gasifier. As an example, if MeOH is to be produced from wood pellets, the aforementioned loss-factors correspond to a loss in chemical efficiency of 0.28–0.45  $MJ_b/MJ_{daf}$  when using a lower-temperature reactor (FB or DFB), and about 0.14  $MJ_b/MJ_{daf}$  when using a high-temperature reactor (EF). This shows that there is a need for additional measures to reduce the yield of by-products, especially in DFB and FB gasifiers if MeOH is the end-product and the same trend holds true for all biofuels that utilize only the syngas. An exception is the production of SNG, in which  $CH_4$  is the main product and the presence of low-molecular-mass hydrocarbons,  $C_xH_y$ , in the product can be tolerated to some extent (if hydrogenated). The loss-factors related to by-products are thereby reduced to 0.1–0.6, which correspond to a loss-factor related to by-products of 0.02–0.14  $MJ_b/MJ_{daf}$  for all the considered gasification technologies. Thus, the need for additional measures is significantly lower for SNG, which makes SNG production an attractive choice, especially for DFB and FB gasifiers.

Table 1.5: Examples of the yields of by-products and the corresponding loss-factors.

	Dual Fluidized Bed DFB (~830°C, P <sub>atm</sub> )		Fluidized Bed <b>FB</b> (~900°C, P <sub>atm</sub> )		Entrained Flow EF (1350°C, P <sub>atm</sub> )	
	g/kg <sub>daf</sub>	$\mathcal{L}$	g/kg <sub>daf</sub>	$\mathcal{L}$	g/kg <sub>daf</sub>	$\mathcal{L}$
CH <sub>4</sub>	60–70	0.7–0.8	~70	0.8	~13	~0.15
C <sub>x</sub> H <sub>y</sub>	40–50	0.4–0.5	~24	0.2	~0	<0.10
OC	8–60	0.1–0.6	~20	0.2	~0	<0.10
Soot	n.a.		~8*	<0.1	~30	~0.23
Char	Function of the heat demand and degree of char conversion		n.a.		n.a.	
Lambda (oxygen)	0 with silica sand and a function of the oxygen-carrying capacity for MeO based materials		Function of the heat demand		Function of the heat demand	
References	Based on operation using silica sand, as presented in <b>Paper I</b> (upper limit), and bauxite, as presented in <b>Paper V</b> (lower limit).		Estimation for the Värnamo gasification plant[22]		Adapted from Qin et al[23]	

P<sub>atm</sub>, atmospheric pressure; n.a., not available

To reduce the yield of by-products, primary or secondary measures can be implemented. Primary measures refer to measures taken within the gasification reactor, such as the use of an active bed material in an FB or DFB reactors. As an example of this, a range of the yields are presented in Table 1.5 for the DFB gasifier, where the upper limit is based on operation with silica sand (low activity) as the bed material, and the lower limit is based on operation with bauxite (catalytic) as the bed material. Secondary measures refer to measures taken downstream of the gasifier, such as the inclusion of a reforming reactor. Implementing a secondary reforming reactor adds to the investment cost, so primary measures can be a cheaper alternative. However, a reactor that is optimized for conversion of by-products can be designed as a secondary measure, as discussed in detail in **Paper II**. Another secondary measure is to capture and recycle the by-products for combustion to cover part of the heat demand and thereby, the loss in chemical efficiency due to by-products.

The loss-factor related to the heat production is defined by Eq. (1.9) as a function of the amount of oxygen required. Expressed as the fraction of oxygen,  $\lambda$ , related to the stoichiometric amount of oxygen,  $\mu_{O_2,stoichiometric}$ , is estimated by:

$$\lambda \approx \frac{H_{gasif} + H_{gas} + v_{tot}}{\sigma LHV_{O_2,gas} + (1-\sigma)LHV_{O_2,char}} LHV_{daf} \frac{1}{\mu_{O_2,stoichiometric}} \left[ kg_{O_2} / kg_{O_2,stoichiometric} \right] \quad (1.10)$$

$$H_{gasif} \approx \frac{Y_{ch} X_{ch}^{\frac{131.3}{0.012}}}{LHV_{daf}} \left[ MJ / kg_{daf} \right] \quad (1.11)$$

where  $H_{gasif}$  and  $H_{gas}$  are the heat of reaction of the gasification and gas-phase reactions excluding the combustion, respectively,  $v_{tot}$  is the total heat demand of the process,  $\sigma$  is the fraction of the heat covered by combustion of gas, and  $LHV_{O_2,gas}$  and  $LHV_{O_2,char}$  are the lower heating values per unit of mass oxygen used for the combustion of the gas and char, respectively.

Note that, based on Eq. (1.8), the removal of one carbon atom is equivalent to the addition of an oxygen molecule, which means that the loss-factor based on the heat demand for a DFB gasifier can be estimated based on the oxygen required for the combustion, as in Eq. (1.9), assuming that the char is pure carbon.

The total heat demand for the gasifier in a biofuel production plant is based on the internal heat demand of the process,  $v_{int}$ , and the potential heat extraction,  $v_{extract}$ . The required heat extraction is a function of the external heat demands for the plant minus the heat from any axillary sources and from the combustion of by-products.

$$v_{tot} = v_{int} + v_{extract} \quad ( 1.12 )$$

$$v_{extract} = f(\text{external heat demands, auxiliary sources}) \quad ( 1.13 )$$

The internal heat demand, which includes the heat required to heat the fuel and the other process streams in the gasifier, must be covered by the heat production in the gasifier. The internal heat demand can be reduced, to some extent, by preheating the process streams or by drying the fuel, although in practice it can never be completely eliminated. The internal heat demand can be estimated based on the mass flows and temperatures of the gasifier, as described in **Paper I**. A higher temperature results in a higher heat demand, and the loss-factor based on the heat demand are higher for an EF than an FB or DFB, assuming equal mass flows. However, in a DFB, air is used instead of pure oxygen and heating of the nitrogen is required in addition to heating of the oxygen, and this increases the heat demand of the process. As an example to illustrate the impact of the temperature and the use of oxygen contra air, the loss-factors related to the heat demand for heating steam corresponding to 0.5 kg/kg<sub>daf</sub> and for heating oxygen/air from a pre-heated temperature of 500°C to the gasification temperature is compared. The oxygen/air amount is defined by the heat balance. Assuming that gas is combusted in the EF and FB processes and that char is combusted in the DFB process, the loss-factors are 0.24 for an EF (1600°C), 0.12 for an FB (900°C), and 0.23 for a DFB (900°C).

In a standalone plant, there might be a need to extract additional heat from the gasification process so as to avoid the need for an auxiliary combustor. The need for heat extraction is a function of the external heat demands (such as preheating of the process streams to the gasifier, steam production, and heating of downstream process steps), heat recovery and the level of integration, and auxiliary heat sources, such as the combustion of by-products or auxiliary fuel. The level of heat that can be recovered from the processes depends on the content of condensable compounds in the gas. The temperature cannot be reduced without removing these compounds or they will cause problems related to fouling. Instead, the gas is quenched to remove the problematic compounds. In an EF gasifier, molten ash with a melting temperature of around 1000°C is created, and therefore, it is necessary to quench the ash at this temperature. The gases from the DFB and FB gasifiers contain tar compounds, which can have dew-points of about

260°C (based on tar measurement is **Paper I**), and this can cause problems in the product gas heat exchanger. To remove the tar components, it is common practice to quench the gas in a scrubber. The higher the quenching temperature the less heat that can be recovered and reducing the tar concentration to enable further heat recovery is another important aspect in reducing the yield of tar contents in the gas, in addition to tar being a by-product. Another aspect that distinguishes the DFB technique is that the combustion is performed in a separate reactor, which generates a flue gas that can more easily be heat-exchanged than the raw gas.

For assessment of which process that is the most efficient in terms of both chemical efficiency and cost, a techno-economic analysis of the entire process chain is required. This is, however, outside the scope of the present work.

## 1.5 DEVELOPMENT TOWARDS A COMERCIAL SNG PLANT

The scope of present work is limited to DFB gasification, which is a highly promising technology for the production of biofuels that is approaching commercial implementation with the GoBiGas project initiated by Göteborgs Energi[24]. The overall goal of the GoBiGas project is to produce a total of 100–120 MW of SNG in two stages, with a demonstration plant of 20 MW SNG as the first stage and a commercial plant of 80–100 MW of SNG in a second step. Construction of the first stage of the 20-MW SNG was completed at the beginning of 2014 and the construction of the Chalmers gasifier was completed in 2008, Fig. 1.7. This enables parallel investigations in lab-scale, pilot-scale, and demonstration-scale to gain the required knowledge to construct a commercial plant. This work is focused on the experiments performed in the pilot plant, however, it includes also some lab reactor tests and initial results from the demonstration plant.

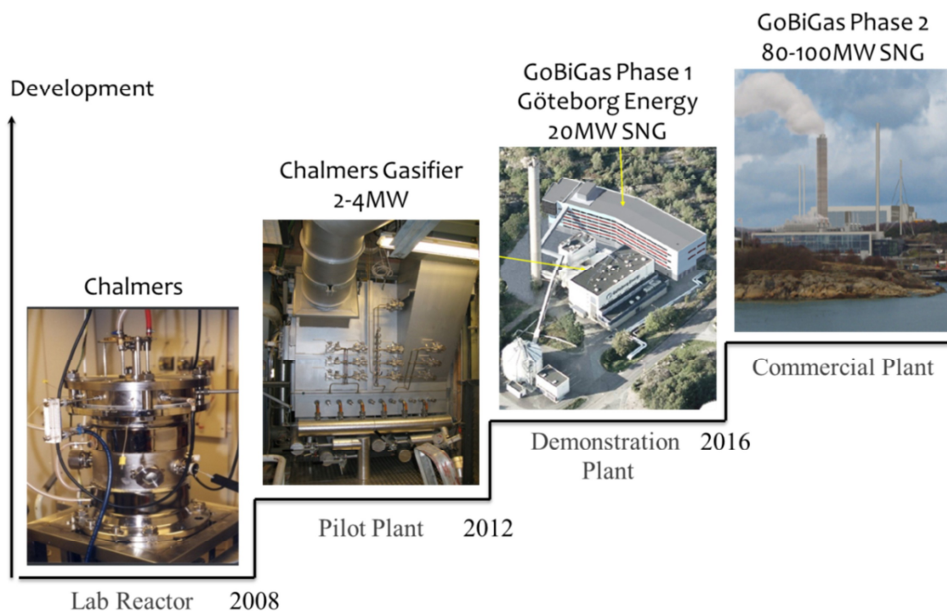


Figure 1.7: Milestones in the development of a commercial plant for SNG production using DFB gasification.

The use of a DFB gasifier for the production of SNG has a number of advantages, as described in Section 1.4. The choice of SNG avoids the need to convert the  $\text{CH}_4$ , which makes it feasible to use a DFB gasifier with a high yield of  $\text{CH}_4$  in the raw gas. The DFB gasification technology offers flexibility in terms of fuel properties, heat production, and the use of active bed materials. By separating the combustion, a stable gas quality from the gasifier is assured even with a change in the heat demand, as mixing of the raw gas and the flue gas from the combustion is avoided. With a separate combustion stage, the need for pure oxygen is removed and partial recovery of the losses in chemical efficiency due to by-products from the gasifier and off-gases from the gas conditioning and synthetic process can be achieved by combustion of these by-products. The potential efficiency of an SNG production plant has been addressed in a number of techno-economical investigations; for example, Heyne and Harvey[25] estimated a system efficiency level of 82%–84% for an SNG plant, however, the real system efficiency of the demonstration plant is yet to be evaluated.

To achieve a high efficiency level of biofuel production plants, and to reduce the investment cost, several aspects related to the gasification needs further consideration. The main factors to be investigated are related to fuel conversion, decreasing the levels of by-products, and the establishment of a simple yet comprehensive evaluation procedure, which can be used for optimization of gasification process.

## 1.6 AIM OF THE PRESENT WORK

The present work is motivated by the increasing, demands for, and political goals, to establish commercial production of biofuels. The current research on DFB gasification is conducted within the framework of the development of a commercial-scale SNG production plant, as currently planned in the GoBiGas project of Göteborgs Energi[24], with the goal of producing 100–120 MW of SNG. The conducted research is focused on DFB gasification, and the goal of this work is to contribute to the understanding and description of the DFB gasification process, so as to facilitate efficient conversion of biomass to syngas and  $\text{CH}_4$ . Towards this goal, the specific aims of this work are to:

- Establish an experimental evaluation procedure for the DFB gasification process (**Papers I, IV, V, and VI**).
- Investigate how to improve the fuel conversion by increasing the degree of OC conversion (**Papers I and II**) and increasing the degree of char conversion (**Paper III**).

## 1.7 METHODOLOGY

The methodologies applied here to improve the degree of fuel conversion and to establish a comprehensive evaluation procedure are illustrated in Figure 1.8. The work can be divided into three topics: fuel mixing; fuel conversion; and evaluation procedures.

In **Paper I**, the choice of parameters to be used in evaluating a DFB gasifier, and how to quantify these parameters to enable a first evaluation of the Chalmers gasifier, are discussed. In parallel, the char conversion rate of the Chalmers gasifier was investigated for **Paper III**, which was complemented with an investigation of the fuel mixing using a fluid-dynamically down-scaled cold flow model. These investigations underline the need for improved and simplified means to quantify all the compounds yielded by the gasifier, and they lead to further developments of the evaluation procedure in **Paper IV** and **Paper VI**.

The method developed in **Paper VI** allows simple quantification of the fuel conversion by combustion of the raw gas. **Paper IV** comprises a detailed investigation of how the loop seals of the gasifier are affected by changes in the bed material flux and changes in the type of bed material. An important aspect of the loop seals is what proportion of the steam that is fed to the loop seals that enters the gasifier, which is required to establish the mass balance of the gasifier. The method for combusting the raw gas is used in **Paper II** to investigate how the introduction of a catalytically active bed material affects the fuel conversion and gas composition. Finally, a refined method for online quantification of a range of important process parameters is established and presented in **Paper V**, which can also be viewed as a continuation of the development of the method described in **Paper VI**.

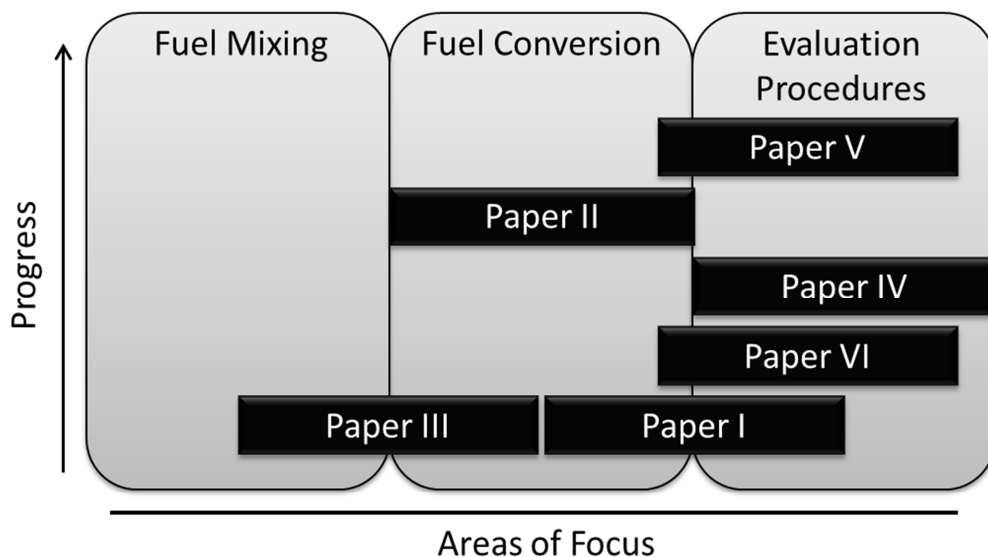


Figure 1.8: Areas of focus and the chronologic progress represented in the papers included in this thesis.

## 2 EVALUATION OF THE PERFORMANCE OF A DFB GASIFIER

---

DFB gasification involves multiple fluidized reactors and product streams, which are composed of numerous different components, which means that the evaluation of DFB gasifiers is complicated. A procedure for evaluating DFB gasifiers has been developed and implemented using the Chalmers 2–4-MW<sub>th</sub> gasifier. The evaluation involves the quantification of the gas composition, quantification of loss-factors related to the by-products and heat demands, and a description and quantification of the fuel conversion.

### 2.1 THE CHALMERS 2–4-MW<sub>TH</sub> GASIFIER

The Chalmers 2–4-MW<sub>th</sub> gasifier is connected to the 12-MW<sub>th</sub> Circulating Fluidized Bed (CFB) boiler at Chalmers University of Technology [26-28] (Fig. 2.1). For standard operation this corresponds to a fuel feed of roughly 400 kg/h to the gasifier and 1–2 trucks/day to the boiler. The furnace of the boiler (1) has a square cross-section of 2.25 m<sup>2</sup> and a height of 13.6 m; the fuel is fed from the side, at the top of the dense bottom bed in the furnace *via* the fuel chute (2). The solids circulate *via* a cyclone (4) through a particle distributor/loop pot (9). From the particle distributor, the solids can be directed differentially depending on the operational goal (e.g. including the gasifier or not). For standard operation of the boiler, the solids are directed straight back to the boiler. If additional cooling of the bed material is required, the solids are directed through an external particle cooler (10). When the external cooler is fluidized, the solids move passively through the cooler due to its vertical alignment. In addition, the Chalmers system has been retrofitted with an additional gasification reactor with a rectangular cross-section of 1.44 m<sup>2</sup> (11). By fluidizing the two loop seals, (items 12 and 13 in Fig. 2.1), the solids pass passively through the gasifier and provide heat to the fuel conversion process.

The fuel for the gasifier is stored in a silo (15), and this fuel is fed by a screw feeder and eventually introduced at the top of the gasifier bed *via* two in-series coupled rotary valves (14) (Fig. 2.2). Dried flue gases are used as purge gas to cool the rotary valves and to prevent gas exchange between the gasifier and the fuel silo. A high flow of purge gas with extraction in the intermediate section is used to remove any air or raw gas that enters through the rotary valves. To minimize the back-flow of raw gas, which contains tar that can cause fouling problems, a net flow of pure gas into the gasifier is required. However, the purge gas dilutes the gas with nitrogen and should, therefore, be adjusted to make up only a small percentage of the total gas and to avoid fouling-related problems.

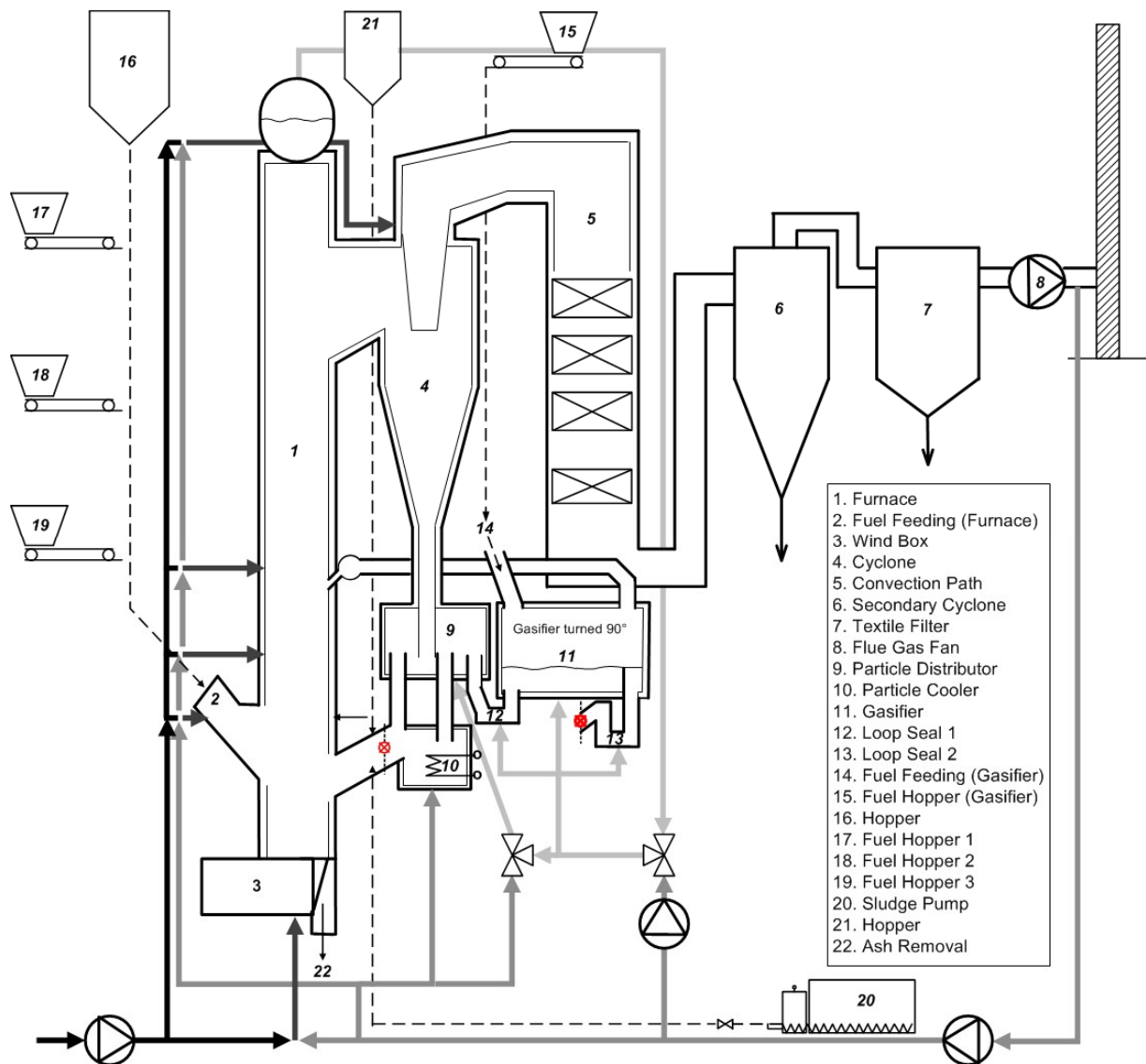


Figure 2.1: Schematic of the system at Chalmers University of Technology (*Paper I*).

The gasification reactor can be fluidized with either steam or flue gases. Steam is used for the gasification when fuel is fed into the gasifier, and flue gas is used to maintain the solids flow when the gasifier is operated without fuel. This enables cost-efficient heating of the gasifier through the bed material around the clock, even when no experiments are being conducted (e.g., during weekends). In this way, steady-state operation of the gasifier can be achieved quickly, as the bed material and brickwork in the gasifier are already heated prior to the start of the experiments. Typically, a period of 1–2 hours is sufficient for switching to steam, starting the fuel feed, and attaining steady-state operation.

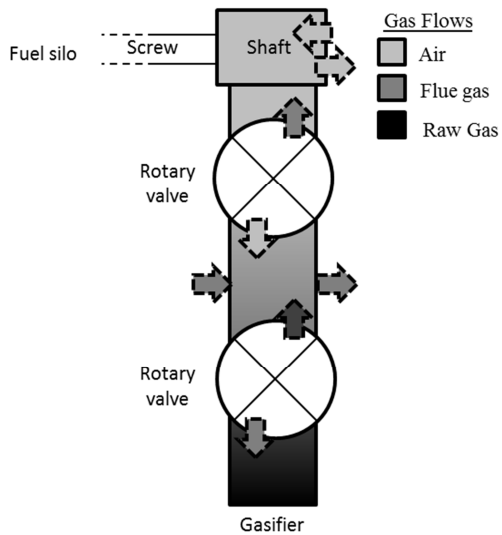


Figure 2.2: Schematic of the fuel feeding system.

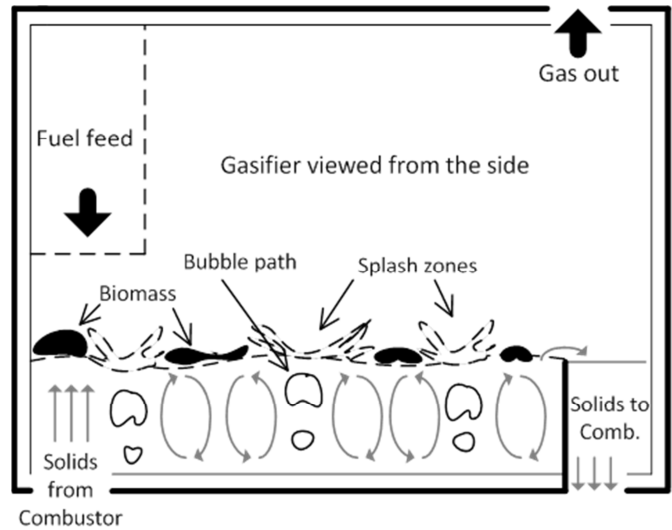


Figure 2.3: Schematic of the Chalmers gasifier (as viewed from the side).

The gasifier is operated within the fluidization regime of a bubbling bed ( $u/u_{mf} = 3-8$ ), and as illustrated in Figure 2.3, the solids enter through loop seal 1 (item 12 in Fig. 2.1) at the bottom of the fluidized bed in the gasifier and exit by flooding over a weir at the opposite side of the gasifier. The steam, which is added *via* evenly distributed nozzles at the bottom of the gasifier, creates bubble paths and splash zones. These bubble paths cause mixing of the fuel and the bed material, (indicated by gray arrows in Fig. 2.3, note that the number of bubble paths are reduced to give a clear illustration). The fuel enters through a downcomer onto the surface of the bed. The fuel is distributed mainly across the surface of the bed and between the splash zones formed as the bubbles erupt at the surface. Figure 2.4 shows the gasifier viewed from above, including a frame from video footage taken during the operation of the gasifier where the fuel can be seen as dark spots.

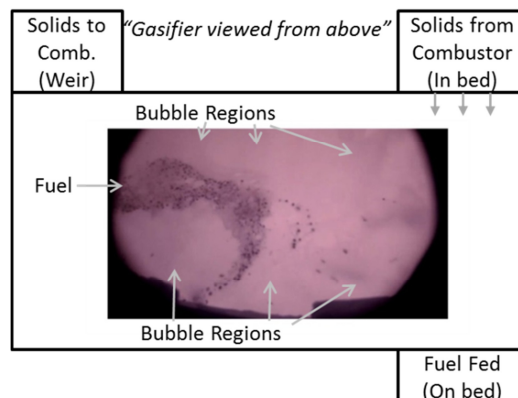


Figure 2.4: Video still of the bubbling bed during operation with a fluidization level of 0.14 m/s (gasifier viewed from above). From **Paper III**.

In the current setup, the major fraction of the raw gas is fed to the boiler for incineration and heat production. However, a small fraction of the gas (approximately 400 W) is sampled for analysis of the gas composition. For safety reasons, the Chalmers gasifier is operated at slightly below atmospheric pressure, and this level is maintained by the flue gas fan of the boiler (item 8 in Fig. 2.1). In contrast to a stand-alone plant, such as the plant in Güssing[29] or at GoBiGas[30], a large amount of additional fuel is fed into the combustion side of the Chalmers system. This means that a large surplus of heat is available for the gasifier, ensuring that the heat demand of the gasifier can be met across the whole range of operational settings and feedstocks.

The main operational parameters used to control the gasifier are summarized in Table 2.1. The fuel feed can be controlled over a wide range of values. The level of the fuel feed strongly affects important process parameters, such as the steam-to-fuel ratio (SFR), gas residence time, gas-steam mixing, and dilution level. For a large-scale unit, a high throughput of fuel is desirable to reduce the investment cost, and the most intensively investigated range of fuel feeding rates (300–450 kg/h), which can be translated into a throughput of 1.0–1.5 MW/m<sup>2</sup>. The amount of steam used for fluidization affects the SFR, gas residence time, and fluidization, and thereby, the mixing and residence time of the fuel particles, whereby high levels of steam increase the mixing, but decrease the residence time.

*Table 2.1: Summary of the main parameters used to control the operation of the gasifier*

Operational parameter	Notations	Means to control	Range of operation	Limitations
Fuel feed	$\dot{m}_{fuel}$	Rotational speed of a feeding screw	0–500 kg/h	The upper limit is defined by the temperature at the top of the combustor where the produced gas is combusted
Fluidization steam	$\dot{m}_{st,bed}$	Automatic valve controlled by an orifice plate-based measurement of the flow	120–360 kg/h	The lower limit is defined by the particles used and should be higher than the minimum fluidization velocity
Flow of bed material	$\dot{m}_{bm}$	The gas velocity through the bottom bed of the combustion reactor. This is controlled by splitting between the primary and secondary air and recirculation of flue gases	12000–25000 kg/h	At low levels, the temperature of the gasifier may become unstable; the upper limit is related to the gas velocity that can be achieved through the bottom bed of the combustion furnace.
Temperature	$T_{bed}$	Controlled by the temperature in the combustion zone and the flow of bed material.	750°–850°C (Silica sand)	The lower limit is set by the lowest temperature required in the combustor for sufficient combustion in combination with a low flow rate of the bed material. The upper limit is set to avoid sintering of the bed material and a different bed material might allow higher temperatures to be used.

The flow of bed material affects the temperature and residence time of the fuel particles, and as long as the heat transport to the gasifier is sufficient, a low flow rate of bed material can be applied to increase the average residence time of the bed material and the fuel particles. If a bed material that transports oxygen is used, the flow of bed material becomes a crucial parameter in controlling the amount of oxygen added to the gasifier. In general, oxygen transport should be restricted as much as possible, so as to ensure high efficiency. The flow rate of bed material is quantified by measuring the pressure difference over the bed in the furnace while defluidizing loop seal 2 (item 13 in Fig. 2.1) to drain the furnace of bed material, this is further described in **Paper I**. The temperature affects the reaction rates in the gasifier, in that a high temperature is beneficial in reducing the yields of undesired products, such as tar components. However, as higher temperatures increase the heat demand of the gasifier, the trade-off between the heat demand and the yields of undesired products needs to be considered.

## 2.2 PROCESS AND PERFORMANCE PARAMETERS

The operational parameters affect the fuel conversion and performance of the gasifier either directly or indirectly by affecting process parameters that are important for fuel conversion. In the present work, the fuel conversion is investigated in terms of the degree of conversion of the char and the degree of conversion of the OC (see Fig. 1.5). The yield of pyrolysis products,  $Y$ , and the degree of conversion,  $X$ , of the char and OC are described here as a function of a range of process parameters, together with the fuel properties, type of bed material, and layout of the process, which are summarized as the following simplified description of the fuel conversion:

$$Y_i = f(\text{Fuel Properties}, \bar{T}_{bed}, h_{eff}, \text{bed material}, \text{layout}), \quad i = ch, cg, \text{steam} \ \& \ OC \quad (2.1)$$

$$X_{ch} = f(\text{Fuel properties}, \bar{T}_{bed}, \bar{\tau}_f, SFR, \mu_p, \mu_o, \text{bed material}, u - u_{mf}, \text{layout}) \quad (2.2)$$

$$X_{OC} = f(\text{Fuel properties}, \bar{T}_{free}, \bar{\tau}_{rg}, SFR, \mu_p, \mu_o, \text{bed material}, u - u_{mf}, \text{layout}) \quad (2.3)$$

The process parameters, summarized in Table 2.2, in turn affect the performance of the gasifier, as well as the loss-factors related to by-products and the heat demand. Typical parameters used to describe the performance of a gasifier include: the cold gas composition; the cold gas efficiency; the tar concentration; the rate of carbon conversion; and the steam balance[31, 32]. While these parameters provide vital information for the processes downstream of the gasifier, they do not give all the information needed to describe the performance of the gasifier. In the present study, to carry out a more comprehensive evaluation of the performance of the system, the following additional performance parameters are used: gas yield; raw gas efficiency,  $\eta_{rg}$ ; conversion of char,  $X_{ch}$ ; the yield of OC from the gasifier; conversion of OC,  $X_{OC}$ ; and the heat demand of the gasifier. The performance parameters considered are summarized in Table 2.3, together with a short description of the areas in which the different parameters are used.

Table 2.2: Summary of process parameters considered in the present work and experimentally quantified.

Parameter	Notation (unit)	Comment
Steam-to-fuel ratio	$SFR$ ( $kg/kg_{daf}$ $_{fuel}$ )	Relates the total mass of steam added to the mass of daf fuel, which affects the amount of steam available for gasification, steam reforming, and WGSR
Effective heat transfer coefficient for fuel particles	$h_{eff}$ ( $W/m^2K$ )	The effective heating rate of the fuel particles affects the yields from pyrolysis and the time of pyrolysis, as illustrated in Fig. 1.2.
Average bed temperature	$\bar{T}_{bed}$ ( $^{\circ}C$ )	Important for the heating rate and the reaction rates for reactions that occur in the bed section of the gasifier, e.g., char gasification [Reaction (R4)]
Average gas temperature	$\bar{T}_{gas}$ ( $^{\circ}C$ )	Affects the rates of the reactions in the freeboard, such as the WGSR and steam reforming of the OC components
Average fuel residence time	$\bar{\tau}_f$ (s)	The fuel residence time is important for the level of char conversion
Average gas residence time	$\bar{\tau}_{gas}$ (s)	The average residence time of the gas is affected by both the release of gases from the fuel and the SFR
Gas velocity for fluidization	$u-u_{mf}$ (m/s)	The velocity of the gas used for fluidization affects the amount of particles thrown up in the freeboard and the mixing of the fuel particles
Purge gas amount	$\mu_p$ ( $kg/kg_{daf,fuel}$ )	If the amount of purge gas related to the fuel is significant it will affect the fuel conversion by diluting or reacting with the gas, depending on the composition of the flue gas.
Oxygen added	$\mu_O$ ( $kg/kg_{daf,fuel}$ )	Oxygen can be added to the process by transport together with the bed material, leakage or as part of the purge gas.

The experimental investigations of the present work are designed to elucidate how performance can be improved and loss-factors can be minimized by changing the operational parameters. Furthermore, the underlying process parameters are quantified to add to our understanding of the fuel conversion. Figure 2.5 illustrates the approach used for the analysis of the gasifier, including how the operational parameters affects the process parameters, which in turn affect the performance of the gasifier, and thereby, the loss-factors. To quantify experimentally these parameters, a comprehensive evaluation procedure was established, as described below.

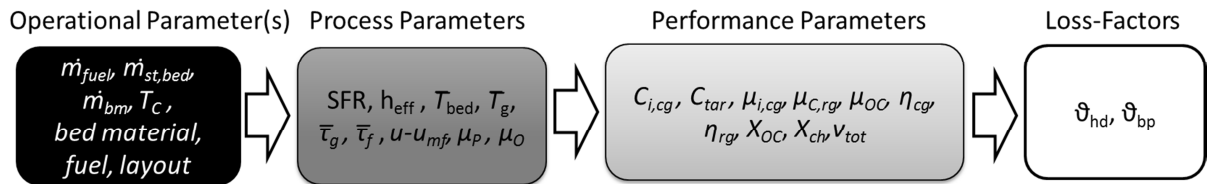


Figure 2.5: Illustration of the chain of impact in which operational parameters are used to change the process parameters, which in turn affect the performance parameters and loss-factors.

Table 2.3: Summary of performance parameters considered in the present work.

Performance Parameter	Notation (Unit)	Area of use
Cold gas composition	$C_{i, cg}$ (% vol)	The composition of the cold gas is important for downstream processes, such as a synthetic process, and for deriving important information, such as the H <sub>2</sub> /CO ratio.
Tar concentration and composition	$C_{tar}$ (g/ Nm <sup>3</sup> )	The concentration of the tar and the tar components themselves are important for establishing the dew-point of the tar and the average heating value of the tar.
Yields of cold gas components	$n_{i, cg}$ (mole/kg <sub>daf</sub> ) $\mu_{i, cg}$ (kg/kg <sub>daf</sub> )	Calculation of the cold gas efficiency, and the losses due to potentially undesired products. Enables quantification of the impacts of changes in the operational settings.
Cold gas efficiency	$\eta_{cg}$ (MJ/MJ <sub>daf</sub> )	The cold gas efficiency describes how much of the chemical energy in the fuel is retained in the cold gas.
Yield of tar	$\mu_{tar}$ (g/kg <sub>daf</sub> )	Enables quantification of the impacts of changes in the operational settings.
Carbon conversion	$\mu_{C, gas}$ (kg <sub>C, gas</sub> /kg <sub>C, daf</sub> )	Indirect measure of how much of the carbon in the fuel is not converted in the gasifier.
Yield of OC	$\mu_{OC}$ (g <sub>OC</sub> /kg <sub>daf</sub> )	The OC is a lumped group of undesired organic compounds that can cause a loss in the yield of biofuels
Raw gas efficiency	$\eta_{rg}$ (MJ/MJ <sub>daf</sub> )	The raw gas efficiency describes how much of the chemical energy in the fuel is retained in the raw gas.
Degree of char conversion	$X_{ch}$ (-)	Describes the extent to which a gasifier manages to convert the char.
Degree of OC conversion	$X_{ch}$ (-)	Describe the extent to which a gasifier manages to convert the OC.
Heat demand	$v_{int}$ (MJ/MJ <sub>daf</sub> )	Gives a measure of the degree of char conversion that is required to ensure a stable self-sustaining process.

## 2.3 EVALUATION PROCEDURES

This section provides a summary of the procedure employed for evaluating the process and performance parameters of the Chalmers DFB gasification system. The raw gas produced by the gasifier contains numerous components, ranging from permanent gases to large condensable organic components, which makes it challenging to quantify the yields of all the individual compounds. In the present work, the Chalmers gasifier was evaluated using the following steps:

- **Gas cleaning**
- Tar measurements using the **SPA method**
- **Tracer gas injections**
- Reformation of the raw gas by **combustion** or using a **high-temperature reactor (HTR)**
- Derivation of reference values from **pyrolysis** experiments
- Establishment of a **heat balance** in the gasifier
- Investigation of the average **fuel residence time** using a fluid-dynamically down-scaled, cold-flow model
- Measurement of the **pyrolysis time**

	Gas cleaning	SPA method	Helium tracing	HTR or Raw gas combustion.	Pyrolysis	Heat balance	Cold-flow model	Time for pyrolysis
<b>Performance Parameters:</b>								
Cold gas concentration (Vol%)								
Tar concentration (g/Nm <sup>3</sup> )								
Gas split in loop seals								
Yields of cold gas components								
Yield of tar								
Carbon conversion								
Yield of OC								
Raw gas efficiency								
Degree of char conversion								
Degree of OC conversion								
Total heat demand								
<b>Process Parameters:</b>								
Steam-to-fuel ratio								
heating rate during pyrolysis								
Purge gas								
Average gas residence time								
Average fuel residence time								
Oxygen added								

Figure 2.6: Summary of the investigated parameters and the evaluation steps used for the quantifications, as indicated by the filled cells.

Figure 2.6 lists the evaluation step required for the quantification of different process and performance parameters. The following sections give a short description of each of the evaluation steps, together with some results from the evaluation that exemplify the usefulness of the different evaluation steps.

## GAS CLEANING

Online measurements of the cold gas composition require the extraction of a continuous slipstream of raw gas, which is cleaned in a gas conditioning system (Fig. 2.7). In this setup, the number of particles in the raw gas is initially decreased using a mounted-beam separator at the exit of the gasifier [(A) in Fig. 2.7], and eventually, before the gas enters the conditioning system, more particles are removed by a ceramic filter (B) that is maintained  $>350^{\circ}\text{C}$ . Potential catalytic effects of the filter on the raw gas were investigated by analyzing the tar content and gas composition before and after the filter. No significant change in the gas nor the tar composition was observed (for further details, see Israelsson et al.[33]). After the filter, the raw gas is quenched in isopropanol and cooled to  $-2^{\circ}\text{C}$ , to separate all the condensable compounds (D–H). The flow of raw gas through the gas conditioning system is controlled by a membrane gas pump (I), together with a pressure-regulated valve (G), which is used to sample approximately 2 l/min of cold dry gas. The volume of cold gas flowing through the system is monitored *via* a volumetric flow gas meter, thermocouple, and pressure sensor (J and R), which also allow for a rough estimation of the amount of condensate, measured on a scale and related to the flow of cold gas ( $\text{g}/\text{Nm}^3_{\text{cg}}$ ).

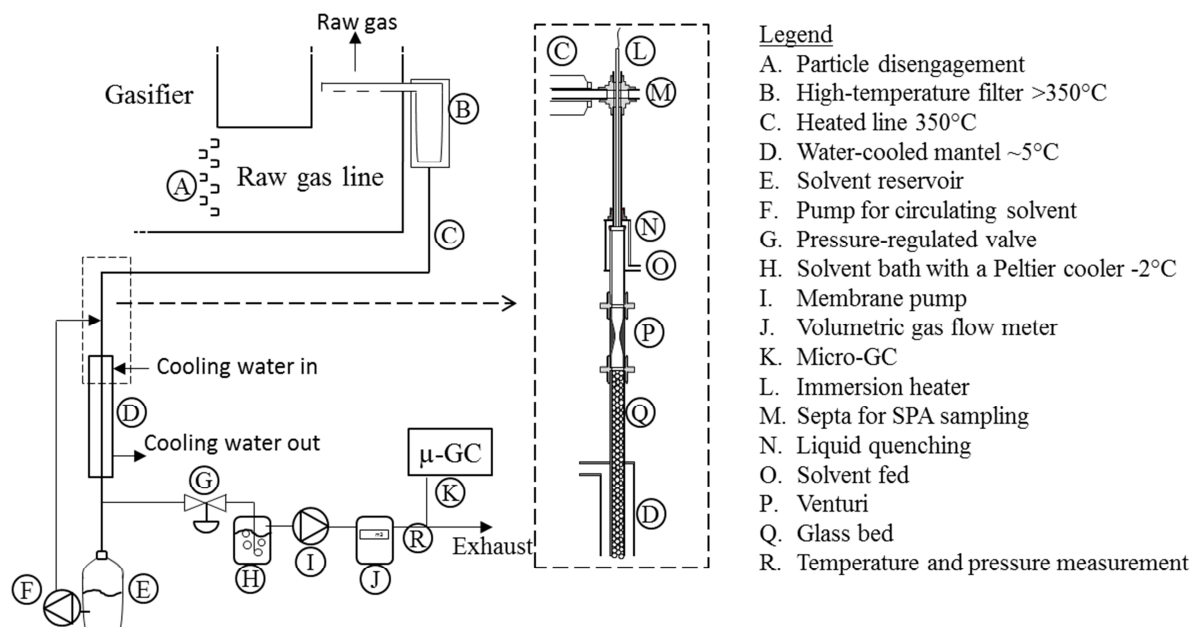


Figure 2.7: Schematic of the gas cleaning system for the cooling and cleaning of the raw gas. A, Illustrated from above; B–R, side-views (Paper I).

A micro-gas chromatograph ( $\mu$ -GC) at position (K) is used for measuring the concentrations of the cold gas components. The  $\mu$ -GC is a Varian CP4900 equipped with one molecular sieve column with argon (Ar) as the carrier gas to include measurements of helium (He), and one Polarplot Q column with He as the carrier gas. A three-point calibration method was used for calibration, which is renewed each week, and the gas species that are measured with this GC setup were: He, H<sub>2</sub>, CO, CO<sub>2</sub>, CH<sub>4</sub>, N<sub>2</sub>, O<sub>2</sub>, and C<sub>x</sub>H<sub>y</sub> components. The method applied allows for sampling at intervals of 180 seconds.

The analysis of the composition of the cold gas used to quantify the H/C-ratio and O/C-ratio of the syngas, so as to compare it with the pyrolysis gas, is presented as an example in Figure 2.8. This shows that a significant change occurred in the syngas composition that can be related to a combination of the WGSR and conversion of char, OC, C<sub>x</sub>H<sub>y</sub> or CH<sub>4</sub>. As discussed for Fig. 1.6 the position over the WGSR vector for the pyrolysis gas indicates that the Chalmers gasifier decrease the loss-factors comparing to the pyrolysis case.

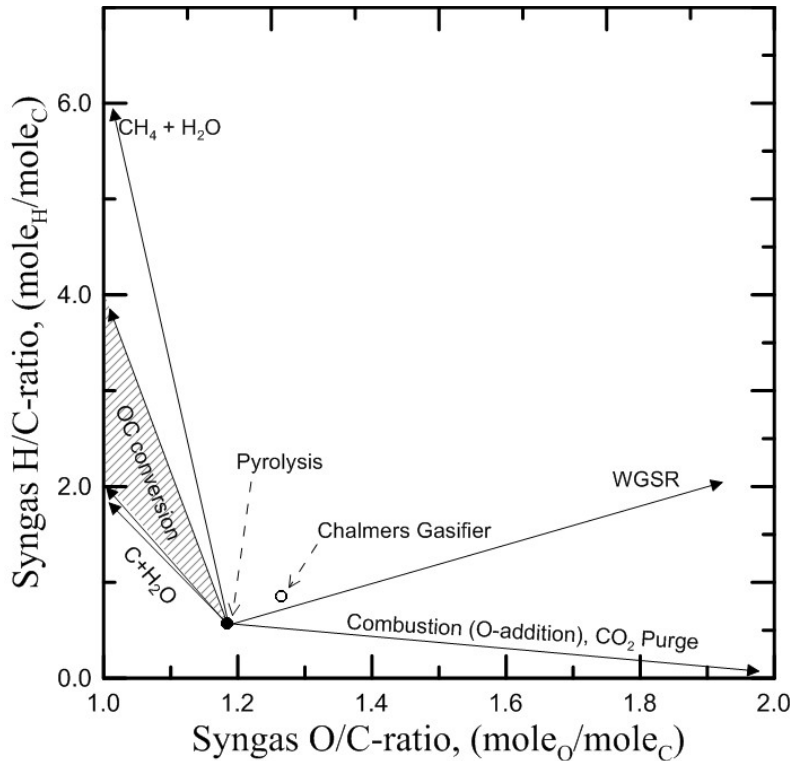


Figure 2.8: Example on how the H/C-ratio and the O/C-ratio of the syngas from the Chalmers gasifier using wood pellets ( silica sand and 835°C) is compared with the composition of the syngas from pyrolysis of wood pellets at 830°C

## SPA METHOD

The tar was measured using the solid-phase adsorption (SPA) method proposed by Brage et al[34] and implemented as proposed by Israelsson et al.[33] In summary, a known volume of the raw gas (100 ml) was extracted at a temperature of 350°C through the amine phase, in which tar compounds are adsorbed. Subsequently, the tar components were desorbed using a solvent and analyzed in a GC using a flame ionization detector (FID). For each measurement, four to six samples were taken with the amines and three injections into the GC-FID were made for each dissolved sample.

The SPA method enables the quantification of individual species, as illustrated in Figure 2.9, which shows the compositions of the tar during operation at three different fluidization levels, referred to as Cases A, B, and C, respectively, and presented in **Paper I**. The figure includes the compounds that were used to calibrate the GC-FID (indicated with labels), with the light compounds with low retention times located on the left, and larger compounds with long retention times located on the right. The unlabeled stacks represent unknown compounds that were detected between known compounds and lumped into a single group. Known compounds constitute 70-80%<sub>mass</sub>[33] of the detected compounds, and a satisfying standard deviation was achieved for phenol and larger compounds (to the right of the graph).

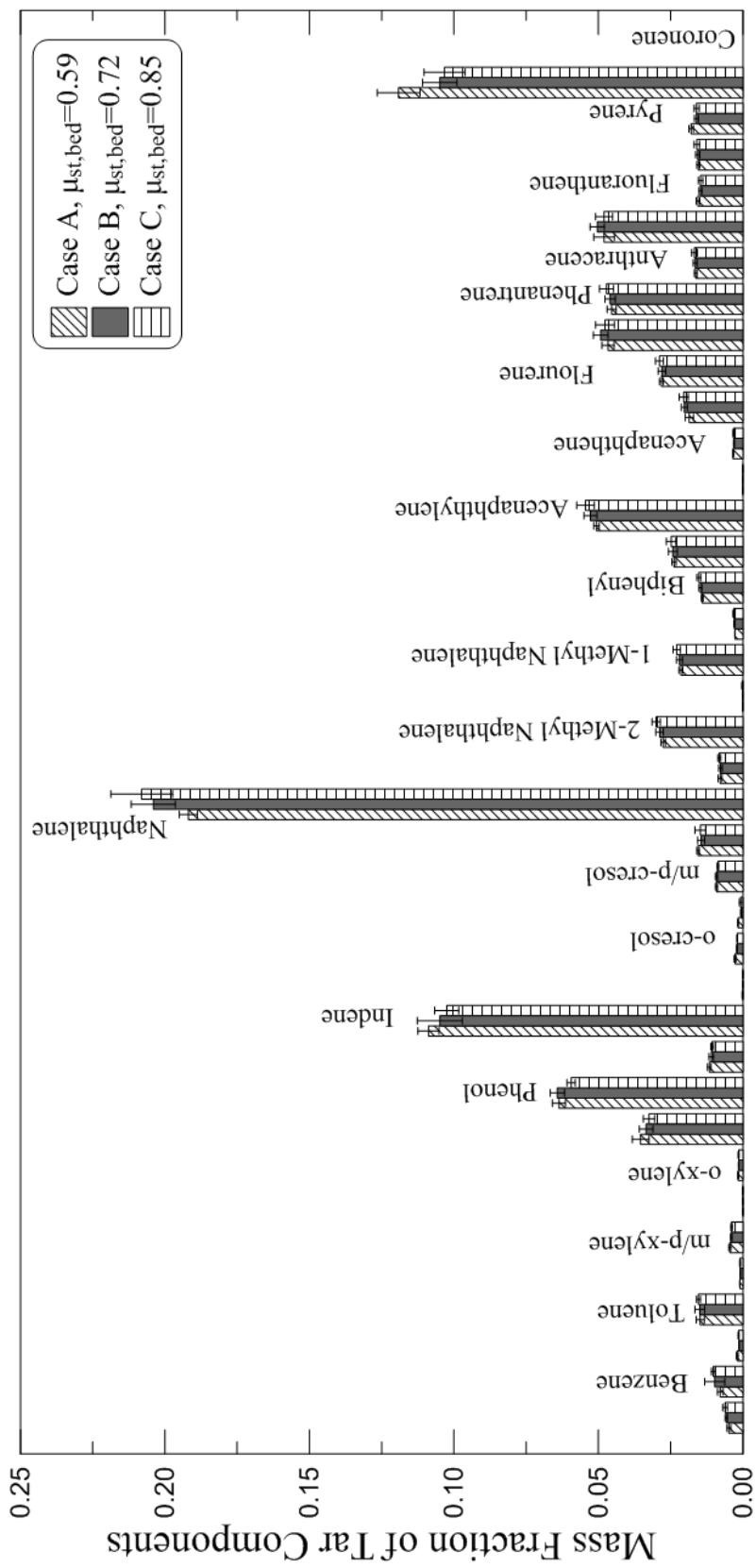


Figure 2.9: Mass fractions of tar components in Cases A, B, and C. Identified species are labeled in the figure and shown in the order in which they were analyzed by the GC-FID, with the general trend of higher dew-points to the right of the graph. The unlabeled stacks represent the sums of unknown compounds analyzed at time-points between the known compounds. The error bars indicate the standard deviations of the levels between samples taken during the same measurement.

Benzene, toluene and xylene (BTX compounds) were detected only at low levels; it has been shown by others (e.g.[35, 36]) that the SPA method is less effective for the quantification of BTX compounds than for larger compounds. This contributes to the phenomenon whereby parts of the raw gas are not measured, as they are not covered either by the SPA method or by analysis of the cold gas, as elaborated below. The biggest difference in the compositions of the cases shown in Figure 2.9 is the fraction of unknown compounds that are larger than pyrene that decreases, and naphthalene that increases, when more steam is used for fluidization. The dew-point of tar is controlled mainly by the presence of large components, such as pyrene and coronene. Although no coronene was detected, several unknown components were found after pyrene, which together with pyrene define the dew-point. The dew-point was estimated to be  $<260^{\circ}\text{C}$ [37] for all the cases, and tended to decrease as the level of steam was increased.

A common way to present the total amount of tar in a gasifier is in terms of  $\text{g}/\text{Nm}^3_{\text{cg}}$ . However, the use of this unit can be dubious, as a change in the operation of the gasifier most likely changes the yield of cold gas. This can make any discussion regarding the change in the amount of tar in terms of  $\text{g}/\text{Nm}^3_{\text{cg}}$  misleading if the change in the volume flow of cold gas is not considered. Changes in the concentration of the tar are important with respect to the dew-point of the tar, although if the purpose is to investigate the function of the gasifier, a better approach is to quantify the yield, for instance in units of  $\text{kg}/\text{kg}_{\text{daf}}$ . In the present work, this was achieved using a trace gas (He) to quantify the volume flow of cold gas.

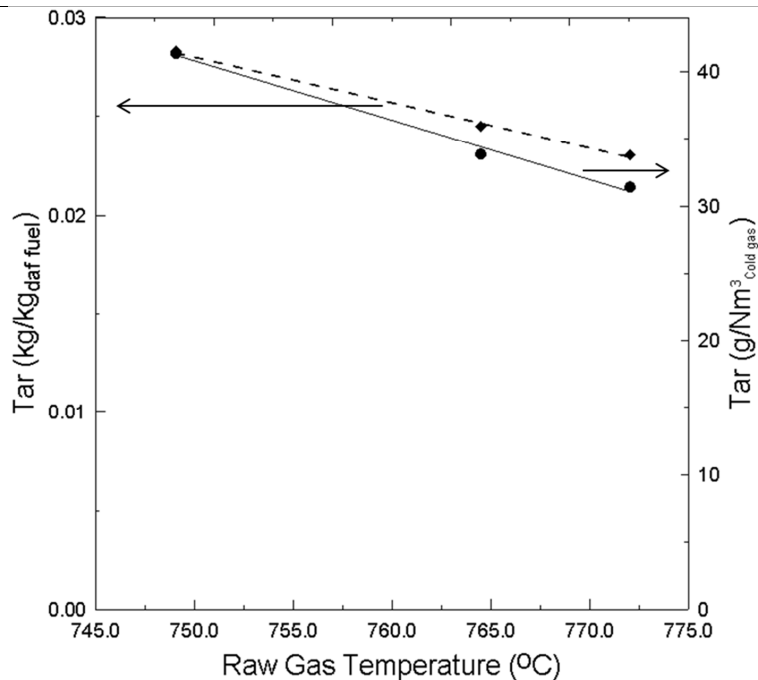


Figure 2.10: Example on how the yield of tar (left y-axis;  $\text{kg}/\text{kg}_{\text{daf}}$ ) and the concentration of tar (right y-axis;  $\text{g}/\text{Nm}^3$ ) change as a function of the raw gas temperature. The ranges of the y-axes are set so that the low-temperature points match, so as to highlight the increasing gap.

Figure 2.10 shows an example of the discrepancy between the change in the tar yield and the tar concentration. This difference arises as the volume flow of cold gas increases as the tar yield decreases. Thus, evaluating the amount of tar in terms of  $\text{g}/\text{Nm}^3_{\text{cold gas}}$  may result in an overestimation of the decrease in tar as the temperature increases. This is one of the advantages of the He tracing approach, which is described below.

## HELIUM TRACING

Using a Bronkhorst mass flow controller (MFC F-202AV) to inject high-quality helium into the steam ducts of the gasifier and loop seals, investigations using He tracing is performed. Figure 2.11 shows a section of the process previously described in Figure 2.1, and it illustrates four points of injection to the process. The He tracing system is used to:

- Enable quantification of the total yields of gas components, tar, and the components of the reformed raw gas, as described below; and
- Investigate the function of the particle seals and the amount of steam that enters the gasifier (**Paper IV**).

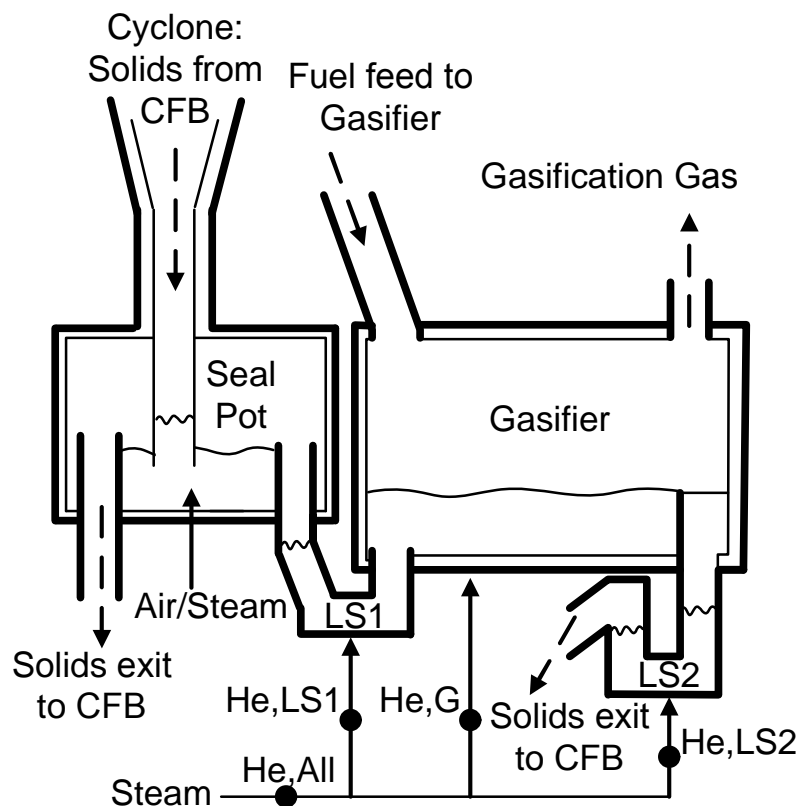


Figure 2.11: Schematic of the Gasifier and loop seals. LS1 and LS2 represent loop seals 1 and 2, respectively. The in- and out-going mass flows are indicated by arrows, and the positioning of the He-injection points are indicated by black dots.

The molar yields of gas components,  $n_{i,cg}$ , are quantified by injecting a known amount of He,  $\dot{V}_{He}$ , and then measuring the concentration of He in the cold gas,  $C_{He}$ . As He is inert and passes through the reactor unconverted, the measured concentration of He reflects the volume flow of gas, which enables calculation of the yield of the cold gas components, by assuming that the ideal gas law can be applied, as follows:

$$\dot{n}_i = \frac{\dot{V}_{He}}{C_{He,G}} C_i \frac{P}{\mathcal{R}T} \quad , i = \text{measured gas components} \quad (2.4)$$

where  $P$  is the pressure,  $T$  is the temperature, and  $\mathcal{R}$  is the general gas constant.

Figure 2.12 and 2.13 show examples of the measured gas concentrations and gas yields, as presented in **Paper I**. Figure 2.12 shows the composition of the cold gas measured from the Chalmers gasifier in terms of volume percentage, revealing a distinct decrease in mainly CO and increases in  $H_2$  and  $CO_2$  as the responses to an increase in the amount of steam used for fluidization. The values with 0.0 steam are based on laboratory-scale pyrolysis test results for a reference composition, further described below. Figure 2.13 displays the corresponding yields, calculated based on helium injections and related to the feed of dry ash-free fuel. Here, it can be seen that the CO yield is more or less stable, while the yields of  $H_2$ ,  $CO_2$ , and  $CH_4$  increase with the amount of steam used for fluidization. In **Paper I**, the increasing yields of the cold gas components were identified to be a consequence of conversion of OC components during reaction with steam. As an example of

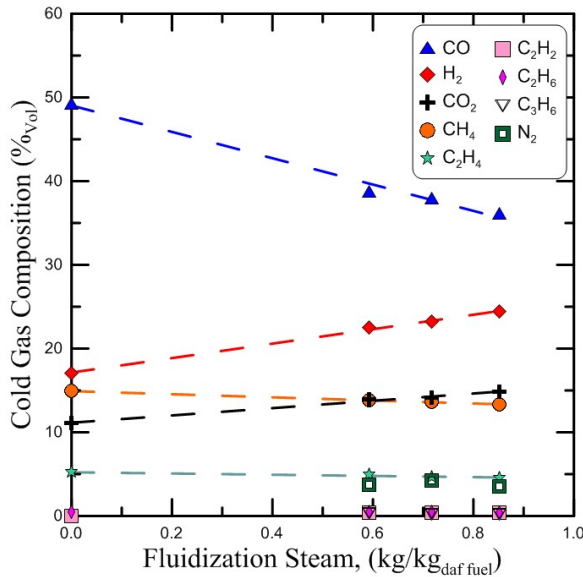


Figure 2.12: Gas composition as a function of the level of fluidization steam. The standard deviation from the mean value of the gas measurements for each case was  $<2\%_{rel}$  ( $<5\%_{rel}$  for the pyrolysis case with  $0\text{ kg/kg}_{daf}$  of steam).

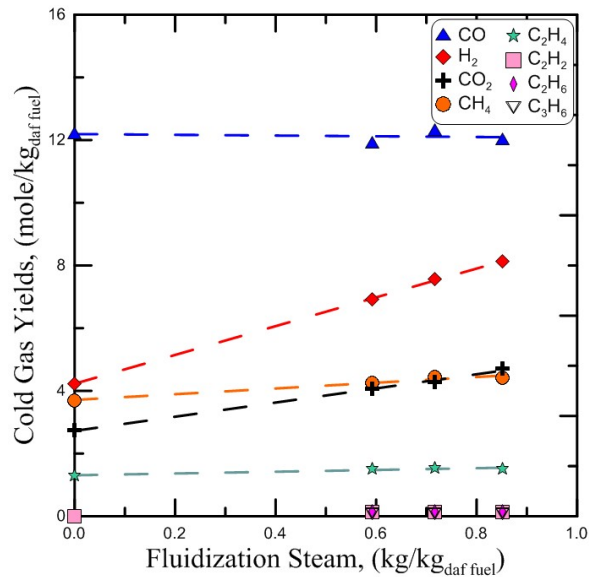


Figure 2.13: Gas yield as a function of the level of fluidization steam. The purge gas is subtracted to show the gas yielded from the fuel conversion.

the usefulness of quantifying the yield in addition to the cold gas composition, a global reaction that can be established to describe the OC conversion based on the yield is here presented as (normalized to 1 mole of C in the OC):



Another use for the He injections is in investigations of the dynamics of the loop seals and the fraction of steam that enters the gasifier (**Paper IV**). The concentration of He in the gasification gas when He is injected into the steam duct to the gasifier (injection point He,G in Fig. 2.11) is denoted as  $C_{He,G}$ .

The value of  $C_{He,G}$  is used as a reference concentration to establish the volume flow of gas,  $\dot{V}_{gas}$ , under the assumption that no steam (or He) added to the gasifier escapes through the loop seals. The reference concentration allows calculation of the fraction of steam that enters the gasifier *via* LS1,  $X_{st,LS1}$ , and LS2,  $X_{st,LS2}$ :

$$X_{st,i} = \frac{\dot{V}_{gas}C_{He,i}}{\dot{V}_{He,i}} = \frac{\dot{V}_{He,G}C_{He,i}}{\dot{V}_{He,i}C_{He,G}}, \quad i = \text{LS1,LS2} \quad ( \text{ 2.5 } )$$

where  $\dot{V}_{He,i}$  is the volumetric flow rate of injected He at point He,i. To assess the validity of the assumption that none of the steam injected into the gasifier (He,G) escapes through the loop seals, two experiments are performed. The fraction of the total amount of steam that enters the gasifier,  $X_{st,All}$ , was quantified in two ways: 1) based on the mass flow of steam,  $\dot{m}_{st}$ , and the fraction entering the gasifier,  $X_{st}$ , as quantified by Eq. (1); and 2) by injecting He into the main steam duct (at point He,All). These two approaches can be compared through Eq. (2.6), where the left-hand side is based on the first approach and the right-hand side is based on the second approach.

$$\frac{X_{st,LS1}\dot{m}_{st,LS1} + \dot{m}_{st,G} + X_{st,LS2}\dot{m}_{st,LS2}}{\dot{m}_{st,LS1} + \dot{m}_{st,G} + \dot{m}_{st,LS2}} = X_{st,All} = \frac{\dot{V}_{He,G}C_{He,All}}{\dot{V}_{He,All}C_{He,G}} \quad ( \text{ 2.6 } )$$

Figure 2.14 shows the He concentrations and fractions that result from injecting a known amount (50 nl/min) of helium into the gasifier (He,G in Fig. 2.14), the main steam duct (He,All), loop seal 1 (He,LS1), and loop seal 2 (He,LS2). The measured concentration of He in the gasification gas is used to determine the gas split through Eq. (1). The results are summarized in Table 2.4, whereby the fraction of steam to the gasifier [0.85; calculated using the right-hand side of Eq. (2)] can be compared with the fraction of steam to the gasifier [0.87; calculated using the right-hand side of Eq. (2), based on the fractions of steam entering the gasifiers through the loop seals]. The results are in good agreement, which confirms that it is valid to assume that all the He injected into the gasifier ends up in the gas from the gasifier.

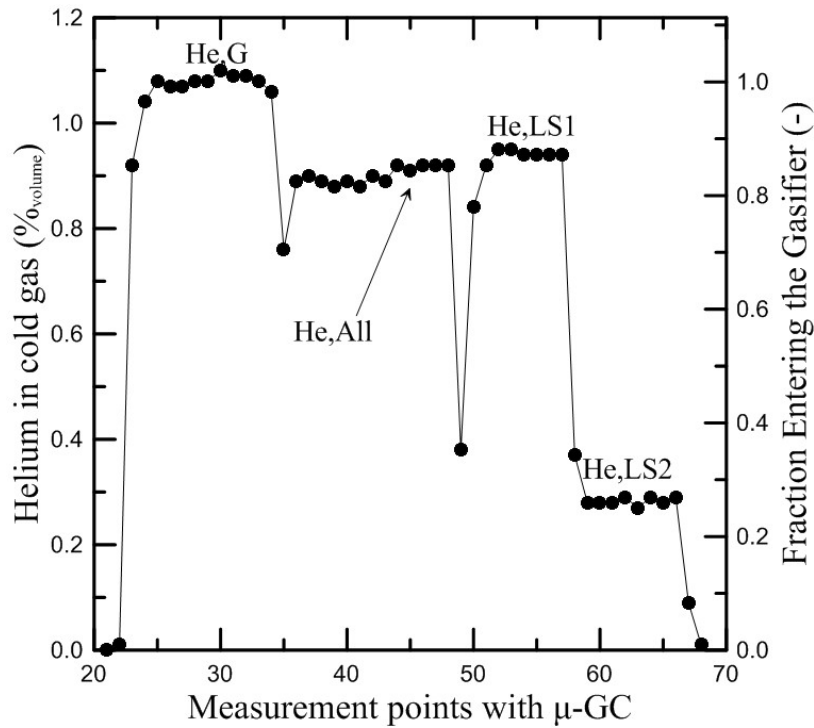


Figure 2.14: The measured He concentrations (left y-axis) and the calculated fractions of steam entering the gasifier (right y-axis) based on the injection of He at positions He,G, He,all, He,LS1, and He,LS2, respectively.

Table 2.4: Total amounts of steam entering the gasifier, calculated based on He injections into the loop seals [Eq. (1)] and compared with the total amount of steam entering the gasifier, based on He injection into the main steam duct [Eq. (2)]. The compared values are highlighted in bold text.

Injection point	Gasifier (He, G)	Main duct (He,All)	Loop seal 1 (He,LS1)	Loop seal 2 (He,LS2)	All; Eq. (2)
Steam flow (kg/h)	211	300	45	44	300
Mean He concentration (vol%), with the standard deviation in brackets	1.082 (9)	0.918 (4)	0.943 (5)	0.283 (8)	-
Calculation of the steam fraction	Reference level	Right hand side of Eq. (2.6)	Eq. (2.5)	Eq. (2.5)	Left-hand side of Eq. (2.6)
Steam fraction to the gasifier (Fraction of He)	1	<b>0.85</b>	0.86	0.26	<b>0.87</b>

This method can be used for the determination of the aeration gas split, i.e., the tendency for the aeration gas (steam) supplied to the loop seal to follow the direction of the bed material. The split of the steam is used for studying the dynamics of the loop seal (**Paper IV**) and to quantify the steam that enters the gasifier from the loop seals. This must be quantified to know the SFR of the gasifier. As an example, the amount of steam added to the loop seals correspond to 15%–35%<sub>mass</sub> of the total H<sub>2</sub>O added to the gasifier and loop seals. Therefore, it is important to know how the gas split is affected by the operation of the gasifier.

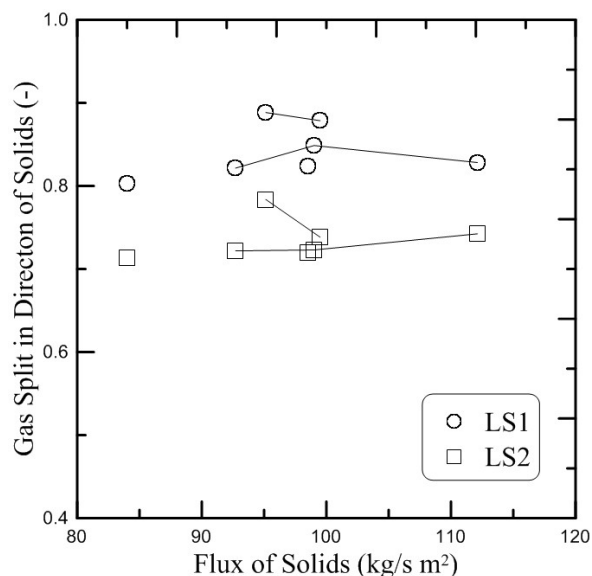


Figure 2.15: Fraction of steam entering the gasifier as a function of the flux of solids.

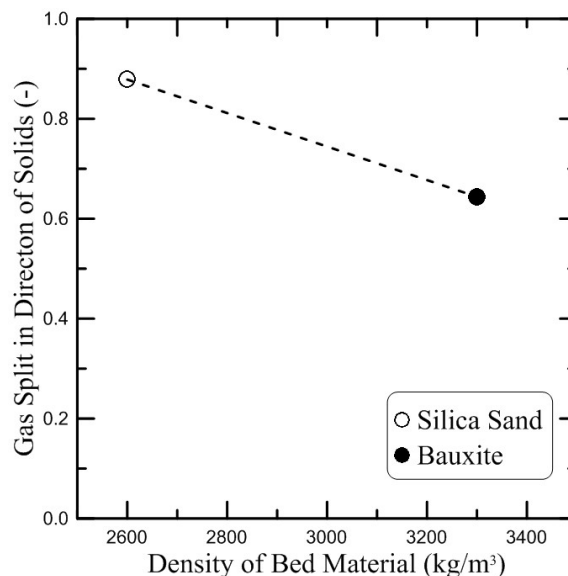


Figure 2.16: Fraction of steam entering the gasifier as a function of the density of the bed material particles.

The measured gas split of the loop seals of the Chalmers system are affected little by changes in the operational parameters of the gasifier (Table 2.1). For example, Fig. 2.15 shows that the mass flow of bed material, which is expressed as solids flux through the loop seals, can be changed within a wide range without any significant impact on the gas split.

However, it is concluded in **Paper IV** that the gas split in loop seal 1 is affected by the density of the bed material, and that when a switch is made from silica sand particles (lower density) to bauxite particles (higher density) the gas split in the direction of the solids is decreased, Fig. 2.16. This change roughly corresponds to a change in the SFR of 1.5%–3.5%. More importantly, it is concluded that there is no carryover of gas through loop seal 1, which would otherwise cause a dilution of the gas. The dynamics of the loop seal are further studied in **Paper IV** with a three-dimensional computational fluid dynamics (CFD) model, which confirms the trend observed when changing the density of the particle.

## RAW GAS COMBUSTION AND HIGH-TEMPERATURE REACTOR

By reforming the raw gas, either through combustion (**Paper VI**) or in a HTR (**Paper V**), the organic components of the gas are converted to light gas components that can be analyzed with online instruments, such as a  $\mu$ -GC or an instrument that uses nondispersive infrared (NDIR) detectors. By introducing air and the raw gas into a heated environment (800°–950°C), the raw gas is combusted and this enables measurements of the total carbon content of the gas based on the CO<sub>2</sub> content of the gas, as described in **Paper VI**. This enables a convenient measurement of the total amount of carbon in the raw gas, illustrated in Fig. 2.17.

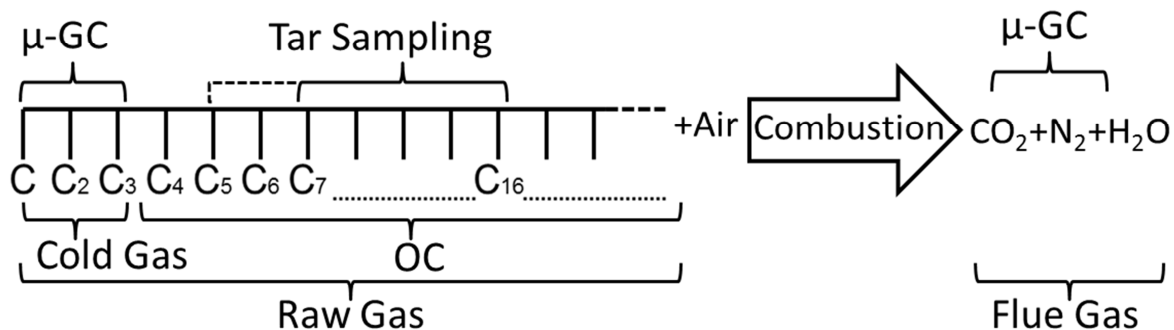


Figure 2.17: Illustration of the combustion of the carbon-containing compounds of the raw gas (C-C<sub>16</sub>, where...represent all compounds between the adjacent ones). The dotted line for 'Tar Sampling' indicates that only some of these components are sampled.

The carbon-containing compounds in the raw gas comprise a range of compounds sorted according to the number of carbon atoms in the molecules (C-C<sub>16</sub>- etc.); the lumped groups in which the components are included are illustrated below, and the components included in the cold gas and tar analyses are indicated above the compounds. As previously described, the cold gas components are measured in a  $\mu$ -GC and the tar components are sampled using the SPA method. This leaves a gap in the analysis both for compounds C<sub>3</sub>-C<sub>7</sub> and for compounds with molecular size larger than C<sub>16</sub> (pyrene). By adding air and combusting the raw gas, the complexity of the gas is considerably reduced and it can be analyzed without the need for additional analytic methods, since the dry flue gas can be analyzed with a  $\mu$ -GC. As an example, it is shown in **Paper I** that only 35% of the carbon in the OC could be sampled with the SPA method with those specific operational conditions. The experimental setup used for the combustion of the raw gas is illustrated in Fig. 2.18 and are described in detail in **Paper VI**

A drawback associated with the combustion approach is the dilution of the gas by the nitrogen that is added together with the combustion air, as this complicates the quantification of the oxygen and nitrogen concentrations in the raw gas. To avoid dilution of the reformed gas with nitrogen, the method is further developed in **Paper V**, and in this case, the method is based on high-temperature reforming of the gas at 1700°C (Fig. 2.19). The new approach offers simplification of the operation and is less labor-intensive than the combustion approach. At 1700°C, organic compounds are thermally cracked and reformed into a mixture of H<sub>2</sub>, CO, CO<sub>2</sub>, H<sub>2</sub>O, N<sub>2</sub> (if present in the raw gas), and soot.

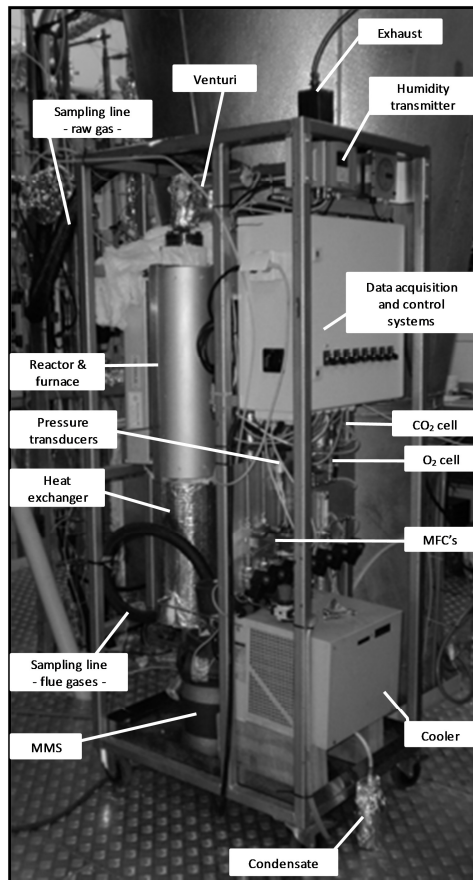
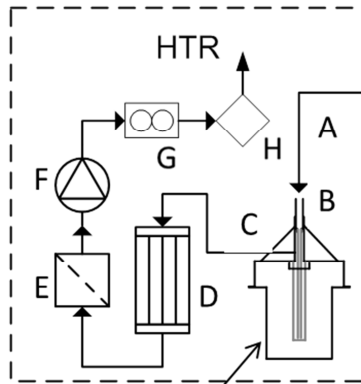
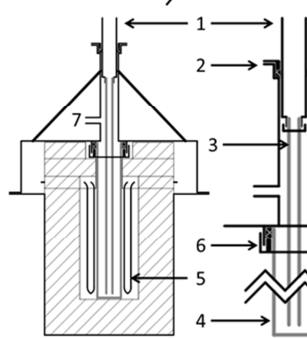


Figure 2.18: Schematics of the combustion reactor used for reforming the raw gas into flue gas.



Legend

- A. Raw gas line, 350 °C
- B. HTR, 1700 °C
- C. SPA sampling
- D. Particle filter
- E. Condenser
- F. Gas pump
- G. Flow meter
- H. μ-GC



Legend

- 1. Steel adaptor
- 2. Connection flange
- 3. Inner Al<sub>2</sub>O<sub>3</sub> tube
- 4. Outer Al<sub>2</sub>O<sub>3</sub> tube
- 5. Electrical heaters
- 6. Pack box
- 7. Gas outlet

Figure 2.19: Schematic of the HTR used for reforming the raw gas into cold gas components.

Reforming the raw gas through combustion or the HTR enables online quantification of several performance parameters and process parameters. The following section describes how a set of parameters is quantified based on data obtained from the HTR. The parameters quantified using the HTR are:

- Carbon conversion
- Oxygen transport
- Yield of OC
- Raw gas efficiency

Carbon conversion

By reforming the gas in combination with helium tracing, the carbon conversion in the gasifier is quantified as described above [Eq. (2.4)]. Quantification of the carbon conversion gives an indirect measure of the carbon loss due to unconverted fuel and soot (if the soot is removed prior to the conversion).

### Oxygen transport

The level of oxygen transport can have a strong impact on the efficiency of biofuel production. Therefore, when evaluating different bed materials the oxygen transport is a crucial parameter. Oxygen added to a gasifier can be determined using the HTR and the following equation:

$$\dot{n}_{O,add} = \Delta H_{daf,HTR} * \left[ \frac{O}{H} \right]_{H_2O} - \Delta O_{Fuel,HTR} + \Delta C_{Fuel,HTR} * \left( \left[ \frac{O}{C} \right]_{UC} - \left[ \frac{H}{C} \right]_{UC} * \left[ \frac{O}{H} \right]_{H_2O} \right) \quad ( 2.7 )$$

where  $\Delta H_{daf,HTR}$ ,  $\Delta O_{daf,HTR}$ , and  $\Delta C_{daf,HTR}$  denote the differences in the molar flow rates of C, O, and H, respectively, as determined by the levels in the fuel feed and the dried gas exiting the HTR. The terms in parentheses in Eq. (2.7) denote the molar ratios of the unconverted part of the fuel (UC) and the oxygen to hydrogen ratio of water (1:2). The first two terms in Eq. (2.7), which relate to hydrogen and oxygen, simply describe the differences in the oxygen and hydrogen levels between the fuel and the HTR gas. The third term, which concerns carbon, describes the effects of the oxygen and hydrogen within the char that is exiting the gasifier. If the difference in hydrogen levels between the fuel and the HTR gas is twice the difference in the oxygen levels, the increase in oxygen level can be explained by the WGSR and therefore, oxygen addition is not occurring. Contrarily, if the difference in hydrogen levels between the fuel and the HTR gas is less than twice that of the difference in the oxygen levels, oxygen addition is taking place. The importance of oxygen transport is discussed further in **Paper II** and in Section 3.1.

### Yield of OC

To quantify the yield of OC, two analytic systems are used in parallel to measure: 1) the cold gas from the gas cleaning system (Fig. 2.7); and 2) the syngas from the HTR (Fig. 2.19). With He injection into the gasifier (He,G in Fig. 2.11), the carbon yields in the cold gas and raw gas can be calculated [Eq. (2.4)]. The difference in the yield is defined as the yield of OC, and based on the carbon balance, the yield of carbon in the OC is calculated as:

$$\mu_{C,OC} = \mu_{C,rg} - \mu_{C,cg} \quad ( 2.8 )$$

where  $\mu_{C,rg}$  is the yield of C in the raw gas, and  $\mu_{C,cg}$  is the yield of C in the cold gas. As an example, the yields of carbon in the cold gas and the raw gas when operating the Chalmers gasifier with bauxite are illustrated in Figure 2.21 over a set of nine measurements in the  $\mu$ -GC (27-min sampling). The difference indicated by a two-way arrow in Figure 2.21 represents the yield of OC.

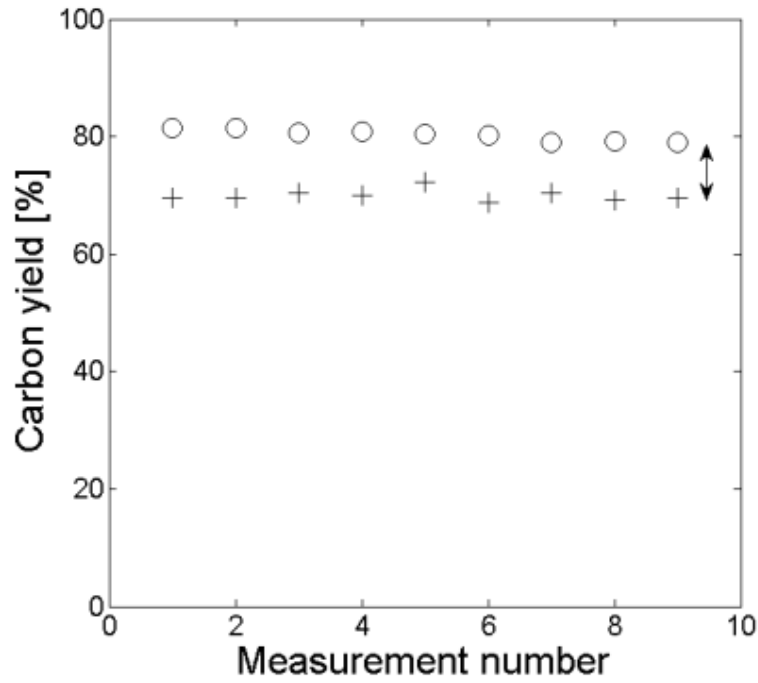


Figure 2.21: Yields of carbon in the cold gas (+) and raw gas (o), The yield of OC is indicated by a two-way arrow.

#### Raw gas efficiency and heating value of the gas

Once the yield of OC and yield of cold gas are quantified, it is possible to calculate the raw gas efficiency and heating value of the raw gas as follows:

$$LHV_{rg} = \frac{\sum \dot{n}_{i,cg} * LHV_{i,cg} + \mu_{OC} * LHV_{OC}}{\dot{V}_{rg}} \quad ( 2.9 )$$

$$\eta_{rg} = \frac{\mu_{rg} LHV_{rg}}{LHV_{fuel}} \quad ( 2.10 )$$

where  $\dot{V}_{rg}$  is the total volumetric flow of the raw gas [in  $Nm^3/s$ ], consisting of the cold gas flow, the steam flow, as determined using the mass balance (**Paper V**), and the flow of condensable species, which are assumed to be free of oxygen. As an example, the estimated chemical efficiencies of the Chalmers gasifier using bauxite as bed material are 73.5% for the raw gas and 61.4% for the cold gas. Thus, roughly 12% of the chemical energy of the fuel can be found as OC components.

## PYROLYSIS YIELDS

As described in section 1.1, the biomass is converted by drying, pyrolysis, and subsequent secondary conversion of the char and OC. As such, the yields during pyrolysis represent the starting point for the char conversion and reforming of volatile components, which distinguishes gasification from pyrolysis. The yields during pyrolysis were investigated in collaboration with the University of Aveiro, and the part of the facility that was utilized for the experiments described in this work is illustrated in Fig. 2.22, as previously described by Neves.[38] The bench-scale fluidized bed reactor [(A) in Fig. 2.22] with electrical heaters (B) was used to pyrolyse the fuel. The reactor was fluidized with nitrogen and a 1–3 wood pellets were introduced into the reactor. The gas exited through a heated quartz thimble filter (C) into an impinging train that was cooled with ice-water (D) to clean the gas. The remaining OC was removed with paper filters (E) before the gas was collected in a gas-sampling bag. To avoid unnecessary dilution of the pyrolysis gas, a three-way valve (F) was used to connect and disconnect the sampling bag. The sampled gas composition was analyzed using the  $\mu$ -GC described in the gas cleaning section, and by injecting a known amount of He into the bag, the yields could be calculated and are presented as a function of temperature in Figure 2.23.

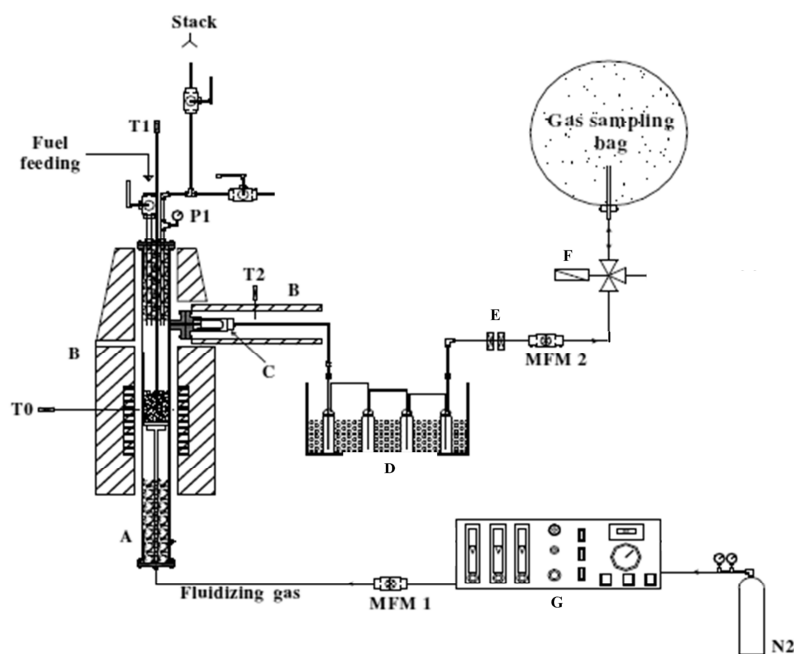


Figure 2.22. Outline of the bench-scale fluidized bed pyrolysis facility at the University of Aveiro. Adapted from Neves[38].

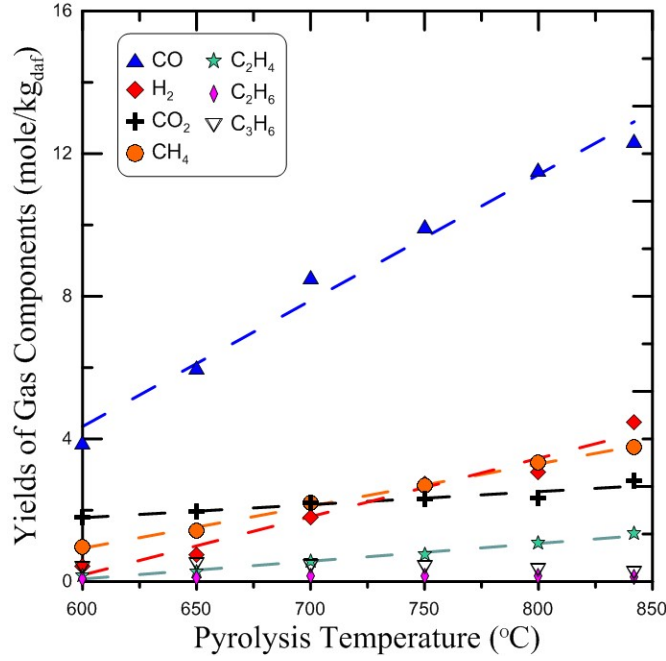


Figure 2.23: Yields of cold gas components as a function of temperature

The char, which was collected after cooling the reactor, was weighed to estimate the yield of char and sent for analysis of the elemental composition. This is described in greater detail by Neves[38] who investigated the yield of char. The char yield at 830°C was  $Y_{ch} = 0.16 \text{ kg/kg}_{\text{daf}}$  for wood pellets and the composition was 93.1% carbon, 1.2% hydrogen, 5.3% oxygen, and 0.4% nitrogen. The yield of soot was measured as the increase in weight of the quartz thimble filter; at 830°C, it was  $0.004 \text{ kg/kg}_{\text{daf fuel}}$ . The yield of C in the OC from pyrolysis of wood pellets at 830°C was  $Y_{OC,C} = 0.094 \text{ kgC/kg}_{\text{daf fuel}}$ , which is in line with the values listed in the literature for the given conditions[6] and was estimated based on the carbon balance and the yield of carbon in the OC is according to:

$$Y_{C,OC} = Y_{C,daf} - Y_{C,ch} - Y_{C,cg} - Y_{C,soot} \quad ( 2.11 )$$

Once the yields from the pyrolysis are known, the fuel conversion in a gasification reactor can be quantified in terms of the degree of char conversion,  $X_{ch}$ , and degree of OC conversion,  $X_{OC}$ :

$$X_i = \frac{\mu_i}{Y_i} = \frac{\mu_{C,i}}{Y_{C,i}} \text{ . with } i = ch, OC \quad ( 2.12 )$$

## HEAT DEMANDS

By estimating the internal heat demands of the process, a simplified heat balance is established:

$$1 = v_{tot} + \eta_{rg} \quad ( 2.13 )$$

The calculations of the total heat demand,  $v_{tot}$ , is described in detail in **Paper I** and are not repeated here. In summary, by measuring the in- and out-going streams of the gasifier and the temperatures, the heat demands are quantified. With the total heat demand ( $v_{tot}$ ), known the raw gas efficiency can be estimated according to Eq. (2.13), and the degree of char conversion required to attain this raw gas efficiency and to have sufficient char to combust to cover the heat demands is estimated as follows:

$$(1 - X_{ch})\Delta h_{comb} = X_{ch}\Delta h_{gasif} + v_{tot} \quad ( 2.14 )$$

where  $\Delta h_{comb}$  is the heat of reaction for the combustion of pure carbon with oxygen (-393.5 kJ/mole)[39] and  $\Delta h_{gasif}$  is the heat of reaction for the gasification reaction of pure carbon with steam (+131.3 kJ/mole)[39]. The maximum theoretical raw gas efficiency of a DFB gasification system is by definition equal to unity, assuming no heat losses and thermally neutral conversion of the volatile fraction, which means that the maximum theoretical char conversion in the gasifier,  $X_{ch,max}$ , according to:

$$(1 - X_{ch,max})\Delta h_{comb} = X_{ch,max}\Delta h_{gasif} \quad ( 2.15 )$$

This calculation gives a maximum theoretical char conversion of  $X_{ch,max} \approx 0.75$  for any fuel. Figure 2.24 illustrates how the heat demands can be used for estimating the raw gas efficiency and the degree of char conversion required to cover the heat demands. The solid line indicates steady-state operation of the gasifier, whereby the char that leaves the gasifier unconverted is just sufficient to cover the heat demands of the process. The raw gas efficiency at  $X_{ch}=0$  is defined by the char yield of the fuel, and the maximal char conversion is calculated using Eq. (2.15). The dotted line indicates an arbitrary internal heat demand, meaning that the area above indicates the fraction of the heating value of the fuel that is converted into sensible heat (white area), and the area below indicates the fraction of the heating value of the fuel that is retained as chemically stored energy in the gas (gray area). This example shows that a char conversion value of approximately 0.15 is required for steady-state operation with a heat demand of 0.2, which roughly corresponds to the heat demand of a gasifier for the production of SNG with an efficiency of 75%, as estimated in **Paper I** based on a techno-economic analysis conducted by Gassner et al.[40] If the degree of conversion is higher, additional fuel is needed in the combustion chamber to maintain the temperature of the system, whereas if the degree of conversion is lower, a surplus of heat is produced and cooling is required. This gives an example on how the heat demands can be used to estimate the desired degree of char conversion. If the degree of char conversion in a gasifier can be estimated, this balance can be used to calculate the need for auxiliary fuel combustion.

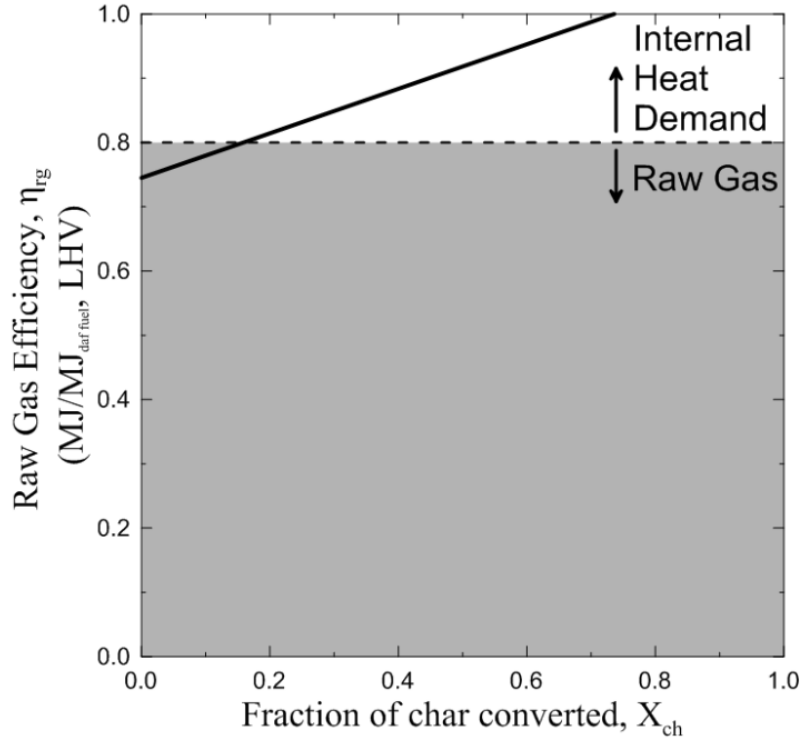


Figure 2.24: Illustration of how the internal heat demand (white area) acts as a limiting factor for the raw gas efficiency (gray area), as compared with the theoretical raw gas efficiency for biomass.

## FUEL RESIDENCE TIME

The average residence time of solids in a fluidized bed is determined in a fluid dynamically down-scaled cold reactor model, which has previously been presented by Sette et al.[41, 42]. Using tracer particles, the transient tracer concentration,  $C(t)$ , at the outlet is used to quantify the average residence time,  $\bar{\tau}_f$ :

$$\bar{\tau}_f = \int_0^{\infty} t \cdot E(t) dt \quad ( 2.16 )$$

$$E(t) = \frac{c(t)}{\int_0^{\infty} c(t) dt} \quad ( 2.17 )$$

$$F(t) = \int_0^t E(t) dt \quad ( 2.18 )$$

where  $E(t)$  is the fraction of particles that has left the reactor at time  $t$ , and  $F(t)$  is the cumulative fraction of particles. In the present work, the cumulative fraction of particles leaving the reactor as a function of residence time was investigated for six cases, with and without a baffle, which is further described in Section 3.2, and for three levels of fluidization.

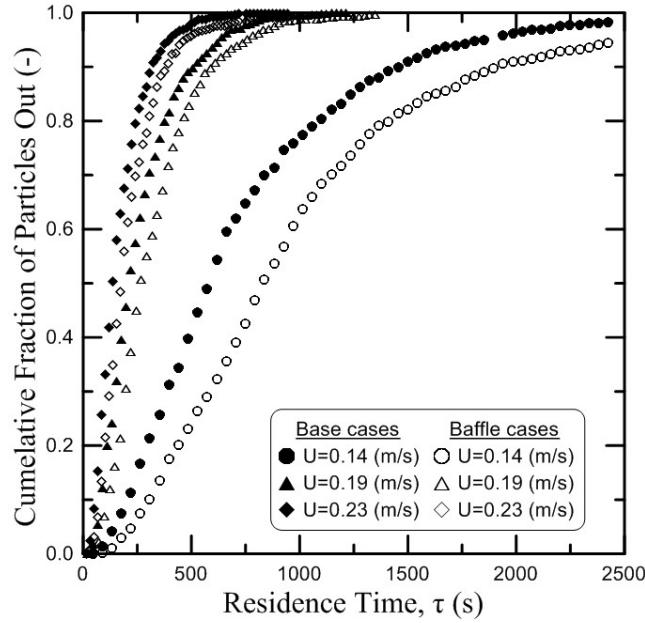


Figure 2.25: Cumulative fractions of particles leaving the gasifier as a function of time, for three fluidization velocities, as derived using Eq. (2.18).

As shown in Figure 2.25, the cumulative fraction of particles that has left the reactor after a specific time is higher with high levels of fluidization, meaning that the average residence time of the fuel particles is lower at higher levels of fluidization. Furthermore, by introducing a baffle across the surface of the bed, the average residence of the fuel particles increases, especially at low levels of fluidization.

## TIME FOR PYROLYSIS

The time for devolatilization for wood pellets in the Chalmers gasifier was estimated by abruptly terminating the fuel feed to and monitoring the decline in the level of  $\text{CH}_4$  in the cold gas as an indicator of the level of volatiles. The time delay for the reactor and measurements system was assessed by abruptly terminating the purge gas, i.e., the dry flue gas, and monitoring the change in  $\text{CO}_2$  concentration, which represents the unit-impulse response function. Thus, the true change in the normalized concentration of  $\text{CH}_4$  can be calculated by convolution[43] of the normalized measured concentrations:

$$C_{\text{CH}_4}(t) = \int_{-\infty}^{\infty} C_{\text{CH}_4}(\tau - t) C_{\text{CO}_2}(\tau) d\tau \quad ( 2.19 )$$

where  $\tau$  is a time-scale, and  $t$  is the time. Figure 2.26 show the normalized concentrations of  $\text{CH}_4$  and  $\text{CO}_2$ , as well as the convolution of the two concentrations, which for simplicity is normalized to its maximum value.

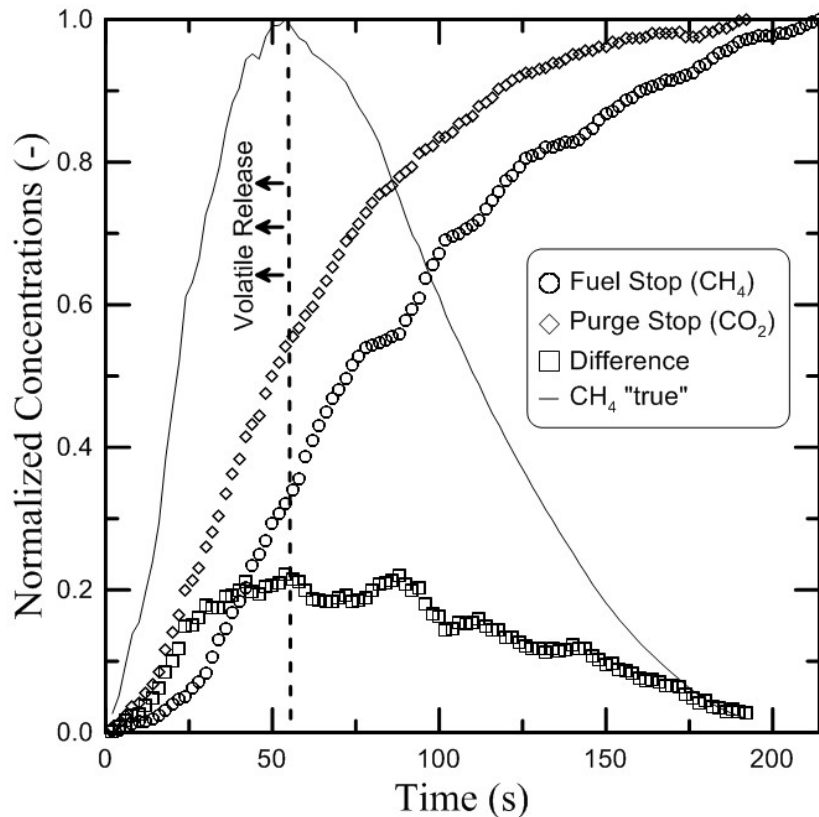


Figure 2.26: Normalized concentrations of  $\text{CH}_4$  and  $\text{CO}_2$  as the fuel feed and purge gas feed, respectively, are terminated. Also shown are the differences between the values and the convoluted function.

Figure 2.27 shows the normalized release of volatiles when the fuel feed to the Chalmers gasifier is stopped, and compares this to the release of volatiles from bench-scale fluidized bed pyrolysis experiments, as described by Neves[38]. There are no major differences between the heating rates of the fuel in the large-scale continuous system and the small-scale batch experiments. Thus, the batch pyrolysis experiments are well suited to investigations of devolatilization time in large bubbling fluidized beds. Further it suggests that the average effective heating rate of the fuel particles in the Chalmers gasifier can be estimated by the calculated effective heating rate of a single fuel particle in a fluidized bed, see for instance[44].

Comparing the fractions of particles that are expected to have left the reactor within the period of devolatilization (from the cold-model experiments), it is concluded that for the specific cases,  $<3\%$  of the fuel particles leave the reactor before at least 75% of the volatiles have been released. This indicates that  $<1\%_{\text{mass}}$  of the volatiles leave the gasifier in an unreleased form and can thus be neglected.

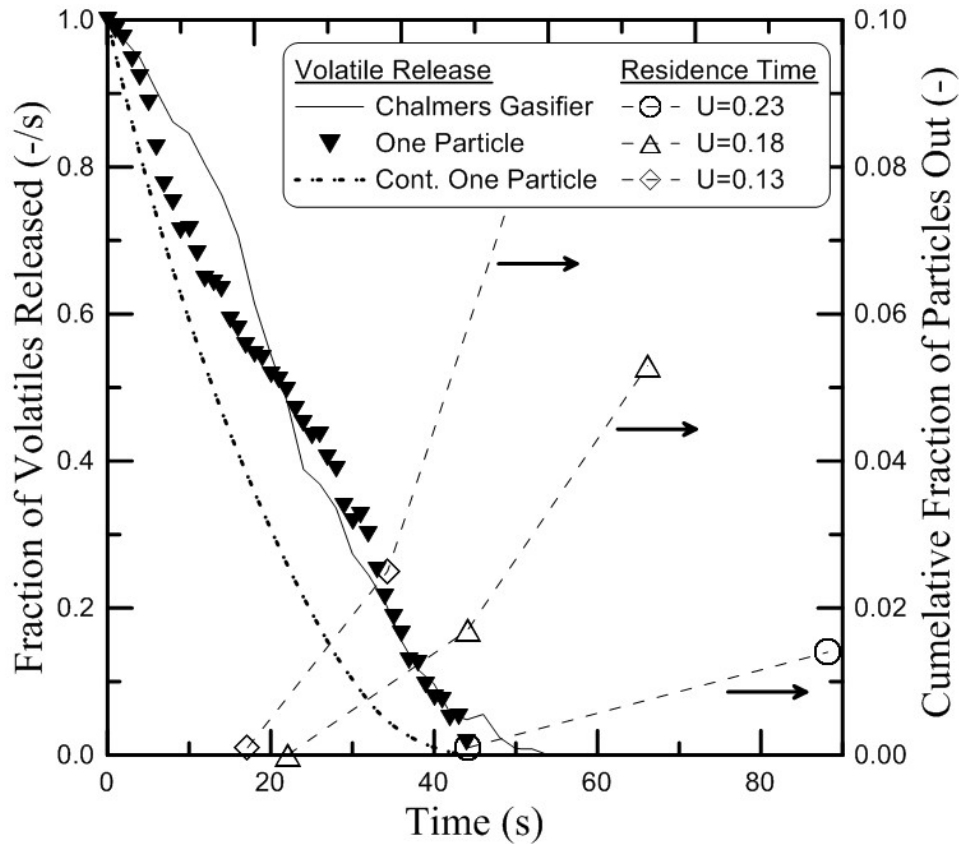


Figure 2.27: Fractions of unconverted volatiles (left y-axis) as a function of time, based on measurements with a single particle and the Chalmers gasifier. This is compared with the fractions of fuel particles that have left the reactor (right y-axis), so as to illustrate the potential for unconverted volatiles to leave the reactor together with the char.

## 2.4 CONCLUSIONS

The proposed evaluation process enables a comprehensive evaluation of DFB gasifiers, as exemplified by implementation in the Chalmers 2–4-MW<sub>th</sub> gasifier. The evaluation procedures enable the quantification of important parameters concerning the gas quality, potential losses related to by-products and heat demands, and the level of conversion of undesired products from the pyrolysis. From this study, the following conclusions are drawn:

- By quantifying the H/C-ratio and O/C-ratio of the syngas, changes in the syngas composition can be used to carry out a qualitative evaluation of how the operational parameters influence the fuel conversion.

- The yield of tar and the dew-point of the tar are crucial parameters in the avoidance of fouling problems downstream of the gasifier, and the SPA method provides a convenient sampling procedure to quantify the tar (in  $\text{g/Nm}^3$ ). However, to assess the impact that a change in the operation of the gasifier has on the tar yield, the change in the volume flow of gas must be considered, so as not to overestimate the impact.
- The volume flows and yields of syngas,  $\text{CH}_4$ ,  $\text{C}_x\text{H}_y$ , and tar can be quantified accurately from a slipstream with injection of a known mass flow of helium.
- By reforming the raw gas to syngas (or flue gas), the carbon conversion, oxygen transport, yield of organic compounds, and heating value of a gasifier can be quantified online, providing crucial information on the rate of fuel conversion and facilitating further efforts to improve the performance of the gasification process.
- Investigation of the yields during pyrolysis of a specific fuel provides valuable reference information for quantifying the degree of conversion of different components in the gasifier and how these components affects the syngas yield and composition.
- By quantifying the heat demands and establishing a heat balance, the degree of char conversion required to maximize the raw gas efficiency can be estimated.
- The degree of char conversion in a gasifier depends on the char reactivity and the average residence time of the fuel particles, which can be estimated using a fluid-dynamically down-scaled, cold-flow model. Using the cold-flow model, the impacts of the level of fluidization, cross-flow of bed material, and the use of a baffle can be described, revealing that the average residence time can be increased by a low level of fluidization, or low flow of bed material, or by the use of a baffle.
- The time it takes a fuel particle to undergo pyrolysis in the Chalmers gasifier was estimated by abruptly terminating the fuel feed to the gasifier. A comparison with the average residence time of a fuel particle confirms that the fraction of particles that leaves the reactor before all the volatile components have been released is negligible. The time required for the pyrolysis of a single fuel particle (based on the results of the reference pyrolysis experiments) is similar to the time needed for pyrolysis in the Chalmers gasifier. This finding suggests that the effective heat transfer for an average fuel particle in the continuous feed to the Chalmers gasifier can be estimated in an equivalent way as for a single particle.



### 3 FUEL CONVERSION IN DFB GASIFIERS

This section summarizes the work conducted on the fuel conversion and performance of a DFB gasifier. The conversion of char and OC are summarized separately, and the published analyses are here complemented with analyses of the impacts that different measures have on the loss-factors [Eqs. (1.8) and (1.9)] and how the H/C-ratio and O/C-ratio of the syngas are affected by the different measures.

#### 3.1 OC CONVERSION

Unconverted organic compounds, and especially tar components, not only create problems by fouling downstream equipment, but also constitute a potential loss. It is desirable to understand how a DFB gasifier can be operated so to have a high rate of conversion of the OC. For this purpose, the impact that the level of steam used for fluidization (**Paper I**) and the impact that the use of metal oxide-containing materials (**Paper II**) have on the yield of OC is investigated.

#### EFFECT OF THE LEVEL OF FLUIDIZATION STEAM

In **Paper I**, three levels of fluidization are investigated in the Chalmers gasifier, and the effects are summarized in Fig. 3.1. Increasing the level of fluidization affects a range of process parameters, and the combined effect is to increase conversion of the OC, H<sub>2</sub>, CO<sub>2</sub>, and CH<sub>4</sub>. However, it also increases the heat demand of the gasifier, so that the loss-factor related to the heat demand,  $\vartheta_{hd}$ , increases while the loss-factor related to the by-products,  $\vartheta_{bp}$ , decreases.

Three levels of fluidization are investigated, and increasing the amount of steam used for fluidization gives a higher SFR, average temperature of the gas, and fluidization velocity, as well as lower gas residence times for both the fuel and the gas (Table 3.1). This suggests that a more detailed investigation is needed to distinguish the respective impacts of  $SFR$ ,  $\bar{T}_{gas}$ ,  $\bar{\tau}_{gas}$ , and  $u-u_{mf}$ . However, the overall effect can be described as a function of the amount of fluidization steam in relation to the daf fuel,  $\mu_{st,bed}$ .

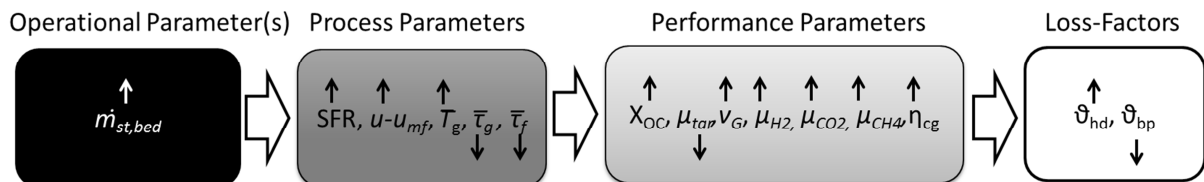


Figure 3.1: Illustration of the chain of impact when the mass flow of fluidization steam is changed. The arrows indicate the impacts that the changes have on the process parameters, which in turn affect the performance parameters and loss-factors. The parameters that remain constant are not included.

Table 3.1: Summary of process parameters resolved from cases with different levels of fluidizing steam.

Parameter	Notation (unit)	$\mu_{st,bed} = 0.59$	$\mu_{st,bed} = 0.72$	$\mu_{st,bed} = 0.85$
		kg/kg <sub>daf fuel</sub>	kg/kg <sub>daf fuel</sub>	kg/kg <sub>daf fuel</sub>
Steam-to-fuel ratio	SFR (kg/kg <sub>daf fuel</sub> )	0.84	0.92	1.06
Average gas temperature	$\bar{T}_{gas}$ (°C)	791	797	801
Average fuel residence time	$\bar{\tau}_f$ (s)	~257*	~170*	~120*
Average gas residence time	$\bar{\tau}_{gas}$ (s)	3.9	3.6	3.3
Gas velocity for fluidization	$u-u_{mf}$ (m/s)	0.16	0.20	0.25

\* Extrapolated values based on the cold flow experiments presented in **Paper III**.

The yields of OC and tar are illustrated as a function of the level of steam used for fluidization in Figure 3.2, which also includes the yield of OC during pyrolysis as a reference level (indicated by zero fluidization steam). The results show that the yields of OC and tar (sampled using the SPA method) decrease with the level of fluidization. The yield of OC corresponds to a degree of OC conversion  $X_{OC} = 0.20\text{--}0.36$ .

Increasing the level of fluidization affects the fluid dynamics in the reactor, and additional steam results in a more violent fluidization, which means that more of the bed material particles are thrown into the freeboard section of the reactor and the mixing of steam and volatiles is increased. Furthermore, the partial pressure of the steam is increased, which can benefit the steam reforming of the OC. However, more steam entails a reduction in the residence time of the raw gas in the reactor (~3.9 s at the lowest level to ~3.3 s at the highest level of fluidization), which can have a negative effect on the conversion level. In summary, it can be concluded that for the present reactor and operating parameters, the combined increases in the mixing, heat transfer, and partial pressure of steam have a greater influence on OC conversion than the residence time.

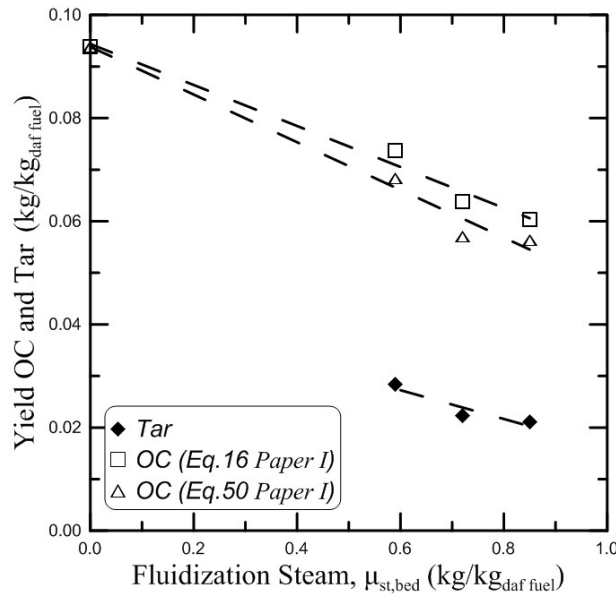


Figure 3.2: Levels of tar and OC as a function of the amount of fluidizing steam, where the OC levels are estimated from both the amount of carbon in the cold gas,  $\Delta$ , and the fraction of tar in the OC determined from Case 3,  $\square$ .

An increase in the conversion of OC gives a lower loss-factor. Comparing the lowest and highest levels investigated, the value of  $\vartheta_{bp}$  is decreased by 0.12. However, heat is required to produce the steam and to heat the steam to the temperature of the reactor. The increase in the internal heat demand results in an increase in the loss-factor of about 0.08. Thus, the increase in the internal heat demand is sufficiently low to facilitate increased chemical efficiency of biofuel production. However, producing the steam creates a heat demand external to the gasifier, and a sufficient level of heat must be available to produce the steam. The level of steam used for fluidization affects the yields of gas components by conversion of the OC. Based on the findings presented in **Paper I**, the OC conversion is described by a simplified global reaction:



By comparing the H/C-ratio and O/C-ratio of the syngas for the investigated cases, the change in composition can be compared with the effects of different reactions (Fig. 3.3). The change in the syngas composition indicates a decrease in the loss-factor related to the by-products, which concurs well with the measured decrease in the yield of OC. Thus, by measuring only the syngas composition, the effect that a change in the operational parameters has on fuel conversion can be detected qualitatively.

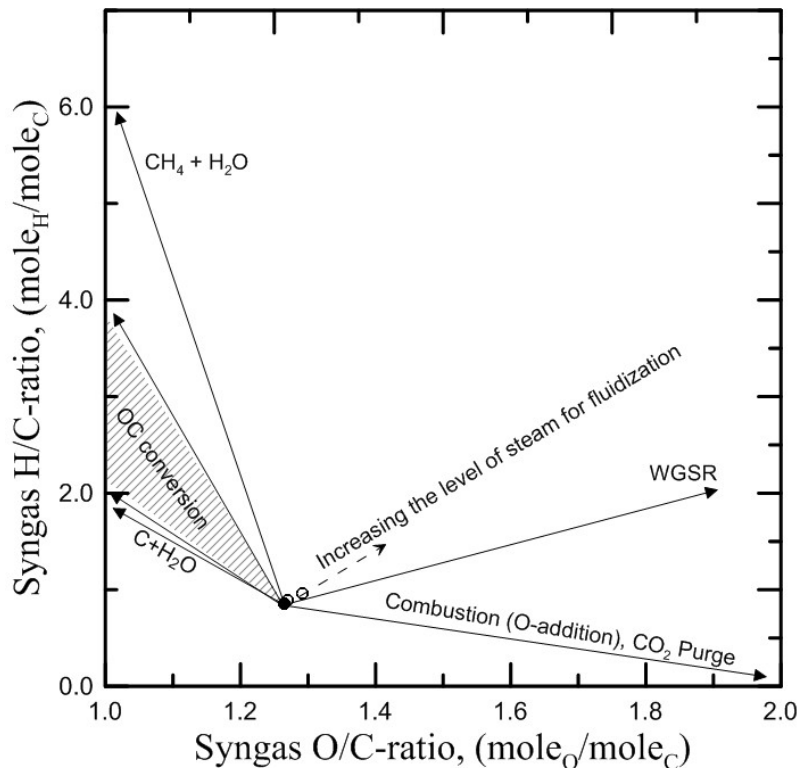


Figure 3.3: Change in the syngas composition, with the case with the lowest level of fluidization used as reference (filled dot) and the two cases with higher levels of fluidization (open dots), and compared with the syngas change due to the different reactions introduced in Figure 1.6.

## USING CATALYTIC BED MATERIALS TO REDUCE THE OC YIELD

Different methods that use catalytic materials (such as alkali metals, non-metal oxides, and supported metal oxides) have been reported as strategies to improve the conversion of OC[45-47]. For FB gasification processes, much research has been devoted to the use of metal oxide (MeO) compounds to promote OC conversion[47]. MeO materials (such as Ni-, Fe-, and Mg-based materials) can be applied as a primary measure in DFB gasifiers to substitute part or all of the bed material with the catalyst. Alternatively, the catalyst can be applied as a secondary measure, in the form of either a fixed bed or a second DFB system downstream of the gasifier, such as is used in the Chemical Looping Reforming (CLR) concept[48-50].

MeO materials have the ability to adsorb oxygen under oxidizing conditions and to release oxygen under reducing conditions, and both of these conditions exist in a DFB gasifier. These properties of MeO can induce a net transport of oxygen between two reactors without any exchange of the other gases[51]. In a DFB gasifier, the transported oxygen participates in the combustion of part of the gas and reduces the efficiency of the gasifier, as well as reducing the heating value of the gas to such an extent that it requires consideration[52]. Thus, the use of an MeO material involves a trade-off between increased conversion of OC and a decrease in the heating value of the gas, as well as an increased O/C-ratio for the gas. The bed materials tested in the Chalmers gasifier are:

- Silica sand, used as reference with no catalytic or oxygen transporting abilities
- Ilmenite mixed in silica sand (1%, 2% and 12%<sub>mass</sub> of ilmenite)
- Bauxite
- Olivine[53]

### Ilmenite

The impacts that the use of MeO materials have on the process parameters, performance parameters, and loss-factors were investigated by adding different fractions of ilmenite to the silica sand used as the bed material. Ilmenite, which is a natural occurring ore that contains iron-titanium oxide ( $\text{FeTiO}_3$  in its most reduced state), has previously been implemented in a laboratory-scale CLR reactor for the reduction of tar components and has proven to be an efficient catalyst for this purpose[54, 55].

Different levels of ilmenite was mixed with silica sand to investigate the effects that increased fractions of ilmenite have on the process, summarized in Figure 3.4. The amount of oxygen added to the gasification gas increases with the fraction of ilmenite, which results in decreased yields of  $\text{CH}_4$  and  $\text{CO}$  and increased yield of  $\text{CO}_2$ , while the level of  $\text{H}_2$  is more or less constant within the investigated range. Owing to the oxygen transport, the cold gas efficiency is decreased and the loss-factor related to heat demand increases. However, the catalytic properties of the ilmenite also cause an increase in the degree of OC conversion, which decreases the loss-factor related to the by-products.

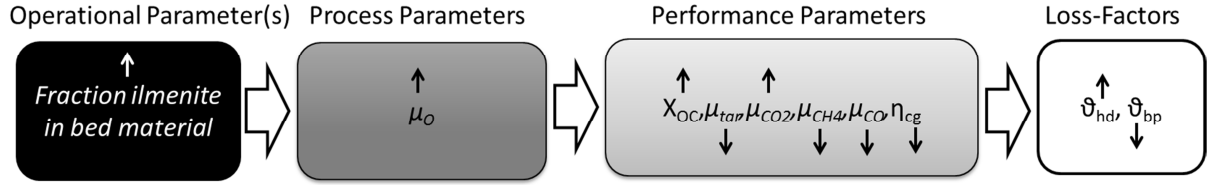


Figure 3.4: Illustration of the chain of impact when the fraction of ilmenite in the bed material is changed. The arrows indicate the impacts that the changes have on the process parameters, which in turn affect the performance parameters and loss-factors. The parameters that remain constant are not included.

The oxygen transport is quantified by combustion of part of the raw gas, as described in Section 2.3 [Eq. (2.5)] and **Paper VI**. The amount of oxygen added to the process is presented in Table 3.2 as a ratio of the stoichiometric oxygen amount, where a value of 1 would represent complete combustion. The effect of ilmenite was investigated by mixing various amounts of ilmenite (0%, 1%, 2%, 12% on a mass basis) with the silica sand used as the inert reference material. The remaining process parameters were kept constant, as presented in **Paper II**, in which an additional level of fluidization is analyzed. By relating the total oxygen transport to the bed material flow and the fraction of ilmenite in the bed material, the oxygen-carrying capacity of the ilmenite was estimated to be  $0.028 \text{ kg}_{\text{Oxygen}}/\text{kg}_{\text{ilmenite}}$ , which is in line with the results presented in the literature[56, 57].

The impact that the use of an MeO material has on the theoretical yield of carbon in the end-product can be evaluated based on the changes in the loss-factors  $\Delta\vartheta_{hd}$  and  $\Delta\vartheta_{bp}$ , and if

$$\Delta\vartheta_{bp} < -\Delta\vartheta_{hd}$$

then the negative effect of the oxygen transport is greater than the positive effect of OC conversion. Correspondingly, if

$$\Delta\vartheta_{bp} > -\Delta\vartheta_{hd}$$

then the positive effect of catalytic conversion of the OC has a greater impact on the potential chemical efficiency of biofuel production than the negative effect of oxygen transport.

The yield of tar was measured with the SPA method, and the tar yield was found to decrease with the fraction of ilmenite in the bed material (Fig. 3.5). At most, a decrease in the tar yield of ~50% was achieved by using a low level of fluidization and 12% ilmenite.

Table 3.2: Summary of the process parameters for the investigated steady-state cases.

Parameter	Notation	Case low0	Case low1	Case low2	Case low12
Oxygen transport	$\lambda_{O,G}$	0	0.013 <sup>a</sup>	0.026 <sup>a</sup>	0.133 <sup>a</sup>

<sup>a</sup> Based on the estimated oxygen-carrying capacity  $R_O X_{MeO,G} = 0.028$ , see **Paper II**.

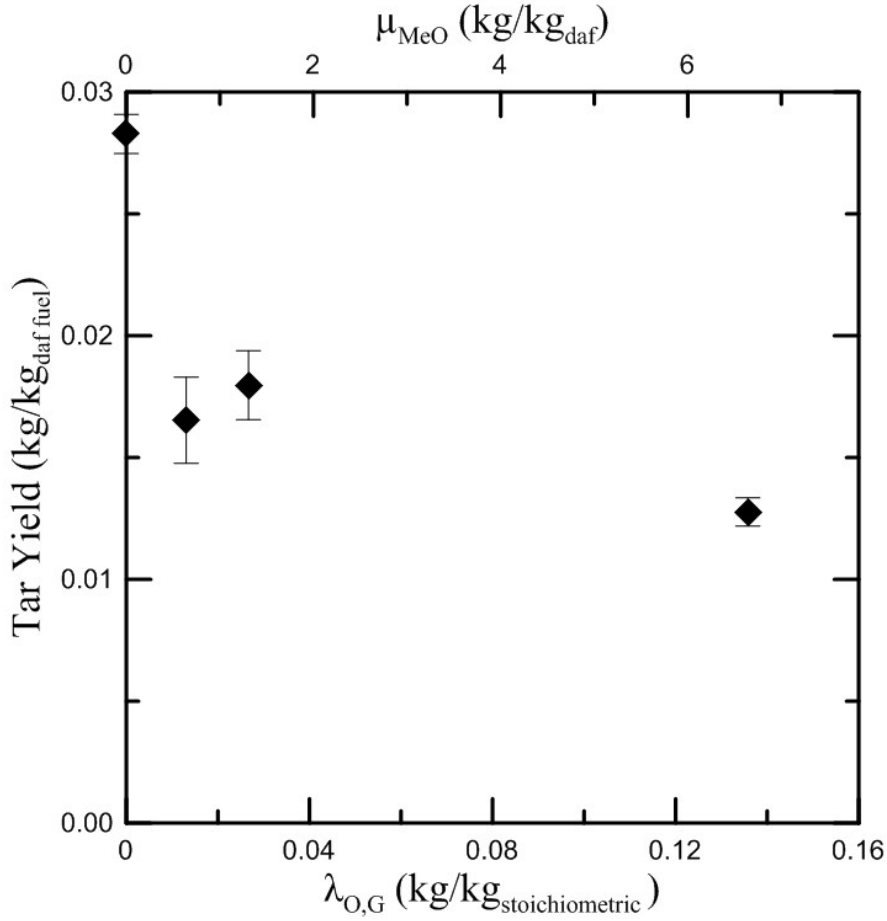


Figure 3.5: Yield of tar as a function of the amount of transported oxygen, expressed as a fraction of the stoichiometric amount (lower x-axis) and the amount of ilmenite (upper x-axis).

Comparing the case with 12% ilmenite with the sand reference case and relating the decrease in  $\mathcal{G}_{bp}$  to the decrease in the yield of tar to the change in  $\mathcal{G}_{hd}$  due to the oxygen transport, it is clear that:

$$(4-2(O/C)_{tar}+(H/C)_{tar})\Delta\dot{n}_{C,tar}/\dot{n}_{C,daf}=0.12 < 0.28 = 2\dot{n}_{O,transport}/\dot{n}_{C,daf}.$$

This shows that the introduction of ilmenite had a negative effect on the potential chemical efficiency of biofuel production. It can be concluded that the level of oxygen transport caused by ilmenite is excessive compared with its effect on the tar yield. For this reason, potential measures for achieving lower oxygen transport while using MeO material are discussed in **Paper II**. In summary, restriction of oxygen transport could be achieved by reduction of the material prior to the gasifier or by implementation of the MeO in a secondary system. However, as such measures add to the complexity of the system, it might be more worthwhile to identify a material with a low oxygen-carrying capacity and high reactivity towards tar. It should be noted that to some extent, an increase in char conversion would compensate for the decrease caused by the oxygen transport, as discussed in **Paper II**.

### Comparing different bed materials

In **Paper V**, the results are presented from the operation of the Chalmers gasifier with 100% bauxite as an alternative MeO-based bed material. The measured oxygen-carrying capacity of the bauxite was  $0.0023 \text{ kg}_O/\text{kg}_{\text{Bauxite}}$ , which is almost one-tenth of the oxygen-carrying capacity of ilmenite. With 100%<sub>mass</sub> bauxite as bed material the oxygen transport contributes to the loss-factor related to the heat demand with  $2\Delta\dot{n}_{\text{oxygen transport}}/\dot{n}_{C,daf} = 0.23$ , which is lower than the corresponding value for 12% ilmenite. Bauxite has a positive effect on both OC conversion and char conversion. Using the silica sand as reference allows comparisons of the bed different materials based on the syngas composition, including ilmenite (**Paper II**), bauxite (**Paper V**), and Norwegian olivine (investigated by Marinkovic and Seemann[53]).

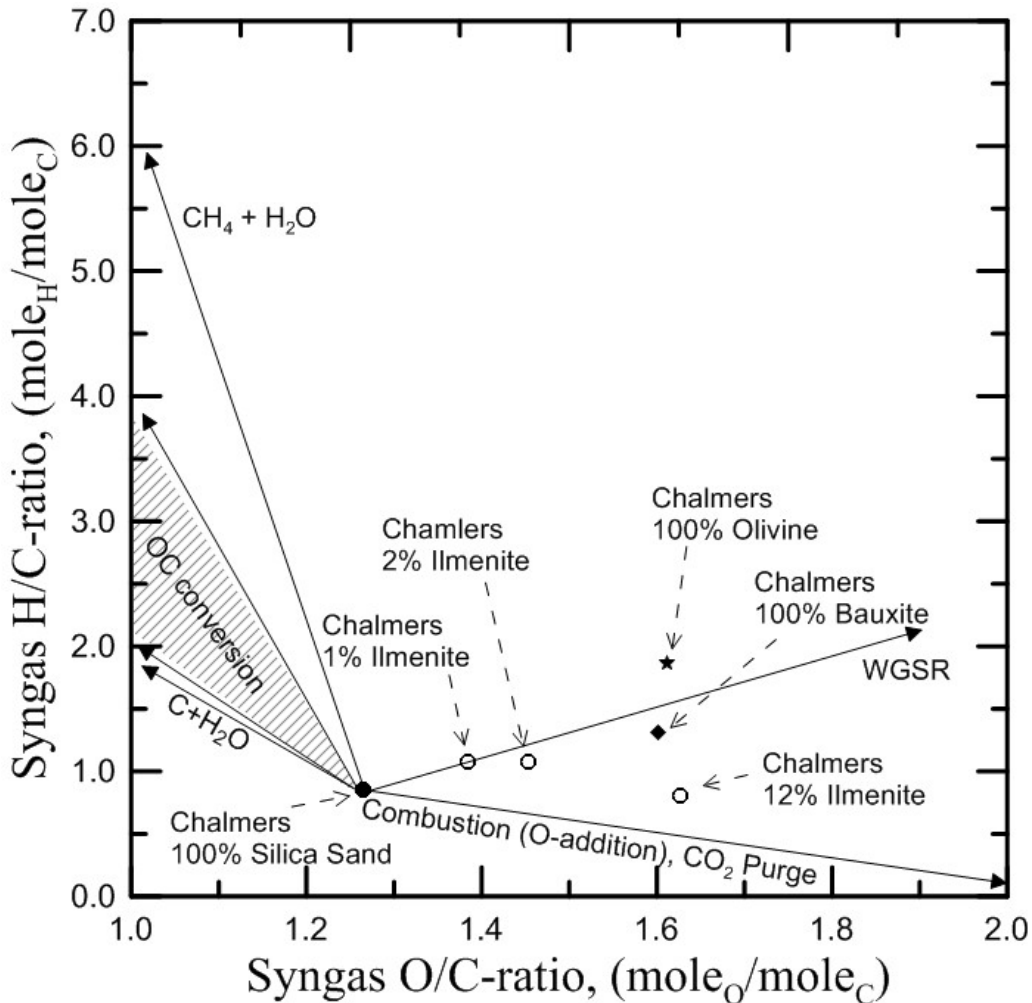


Figure 3.6: Changes in the syngas composition for the reference case with silica sand (filled dot), the three cases with ilmenite (open dots), and a case with bauxite (filled diamond), and compared with the syngas changes due to different reactions, as introduced in Figure 1.6.

Using silica sand as reference the WGSR vector can be used as a reference line to indicate if the loss-factors has been reduced (coordinates above the WGSR line) or increased (coordinates below the WGSR line). This was further described for Fig. 1.6. The syngas compositions from the ilmenite cases show that the sum of the loss-factors is similar for the silica sand cases with 1% or 2% ilmenite. The effect of the high level of oxygen transport with ilmenite is clearly indicated as the syngas composition of the 12% ilmenite case is located well below the WGSR vector, indicating an increase in the sum of the loss-factors, as validated by the quantification above.

The syngas compositions detected using 100% bauxite in the Chalmers gasifier show that the sum of the loss-factors is similar to that in the reference case. For a known level of oxygen transport, this indicates that the increase in the loss-factor related to the heat demand is compensated by a decrease in the loss-factor related to the by-products. Thus, the use of bauxite efficiently reduces the yield of by-products with little loss of efficiency. The tar yield, as sampled with the SPA method, is reduced from 28 g/kg<sub>daf</sub> for the silica sand case to 19 g/kg<sub>daf</sub> for the bauxite case. The use of bauxite as a bed material to reduce the tar yield shows promise and should be investigated further. The use of olivine show a clear decrease in the loss-factors with a value well above the WGSR vector and thus a substantial conversion of char and or OC are indicated. Due to this clear effect on the fuel conversion olivine has been tested in several plants and are the bed material used in the GoBiGas gasifier.

### Olivine in Different Gasifiers

The bed material used in the GoBiGas gasifier is Austrian olivine, which is a magnesium iron silicate-containing ore. Olivine is a well-established material for use in DFB gasifiers due to its catalytic effects[58, 59] and its resistance to agglomeration[60]. The Olivine bed material requires activation to increase the catalytic activity of the material[58, 59]. Figure 3.7 shows the compositions of the syngas from the GoBiGas gasifier before and after the activation of the bed material, using the composition of the syngas from pyrolysis of wood pellets at 830°C as the reference composition. The differences show that activation of the bed material increases both the WGSR and conversion of char and/or OC. A significant decrease in the amount of tar was validated with the SPA method, showing a tar concentration of ~20 g/Nm<sup>3</sup> before activation and ~5 g/Nm<sup>3</sup> after activation of the bed material (excluding BTX components). This underlines the usefulness of a graph like the one in Figure 3.7 for detecting differences in the reactivity of the bed material, and it is currently used to monitor the reactivity of the bed material in the GoBiGas gasifier.

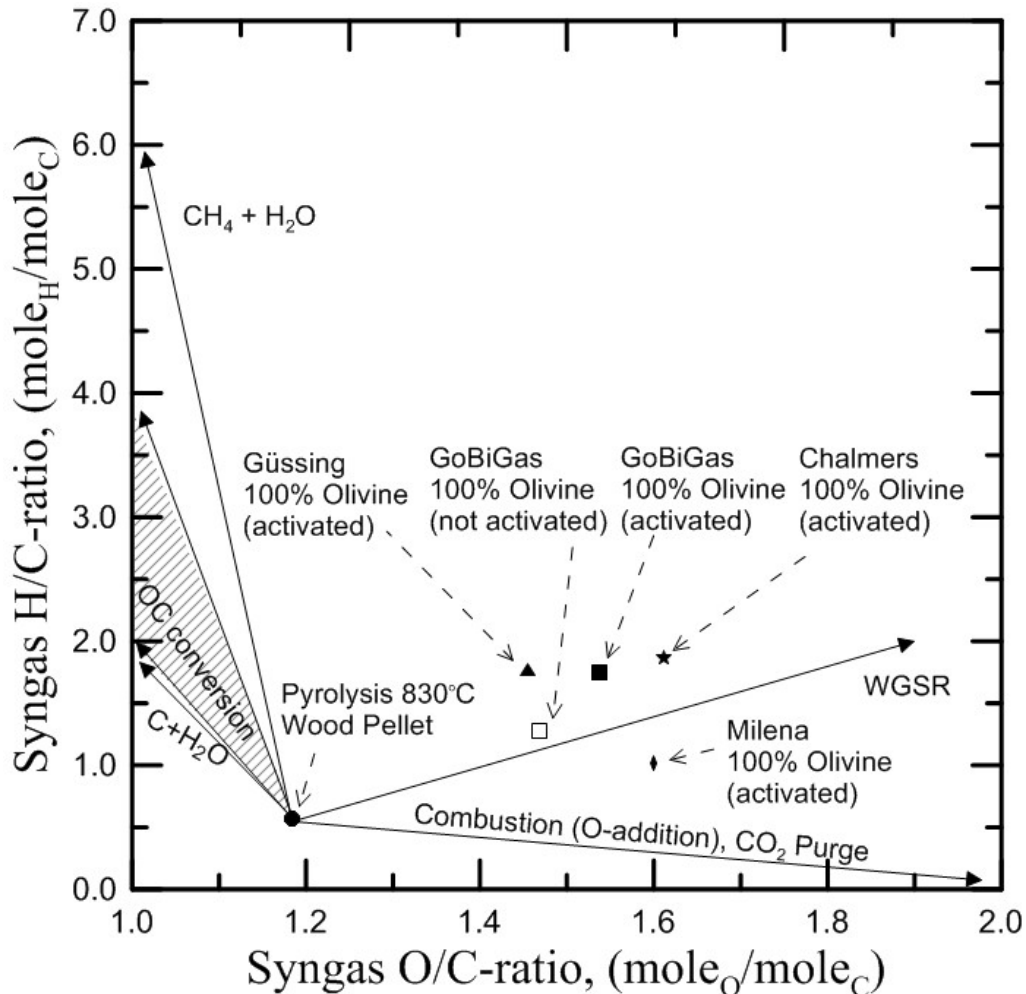


Figure 3.7: Syngas compositions for the: 1) pyrolysis gas[38] (filled dot, used as reference), 2) GoBiGas before activation (open square); 3) GoBiGas after activation (filled square); 4) Güssing[58] (filled triangle); 5) Milena gasifier[59] (filled diamond); and 6) Chalmers gasifier[53] (filled star). The syngas changes (indicated with arrows) due to different reactions are introduced in Figure 1.6.

In addition, the syngas composition from the GoBiGas gasifier is compared with the syngas compositions from the gasifier in Güssing[58] and the Milena gasifier[59], when using Austrian olivine as bed material, and the Chalmers gasifier using Norwegian olivine. The gasifier in Güssing, the Chalmers gasifier and the GoBiGas gasifier show a similarity in the syngas composition. The discrepancy can be related to differences in the fuel properties (wood pellets in GoBiGas and Chalmers cases, and wood chips in Güssing case) and differences in the operational parameters and the layout of the processes. The composition of the syngas from the Milena gasifier differs considerably from the compositions of the syngases from the other gasifiers, and the positioning below the WGSR vector indicates that a much higher level of added oxygen, which can be due to oxygen transport and leakage, or a high level of  $\text{CO}_2$  used as purge gas. Further investigation is required to define the factors in the design and/or operation that cause these differences in the composition of the syngas.

In summary, further investigations of different bed materials, layouts of the gasifier, and operation of the gasifier should be conducted to produce further improvements. For such investigations, the proposed analysis based on the O/C-ratio and H/C-ratio of the syngas provides a simple and quick qualitative estimation, while the comprehensive evaluation procedure provides the means to quantify the gasifier performance.

### 3.2 CHAR CONVERSION

This section summarizes the work that focuses on the degree of char conversion. The char consists, by definition, of the fraction of the fuel that remains in the solid phase after pyrolysis. The char from biomass contains primarily carbon and small fractions of hydrogen and oxygen, as well as ash components. In **Paper III**, the degree of conversion of the char,  $X_{ch}$ , in the gasifier due to gasification with steam (R4) with and without a baffle are investigated:

The average degree of char conversion is affected by the average residence time and the average reactivity of the char. To increase the average residence time of the fuel particles, a baffle was introduced into the fluidized bed of the gasifier. The baffle was partially immersed into the bed to hinder fuel particles from passing the baffle without entering dense part of the bubbling bed, as illustrated in Figure 3.9.

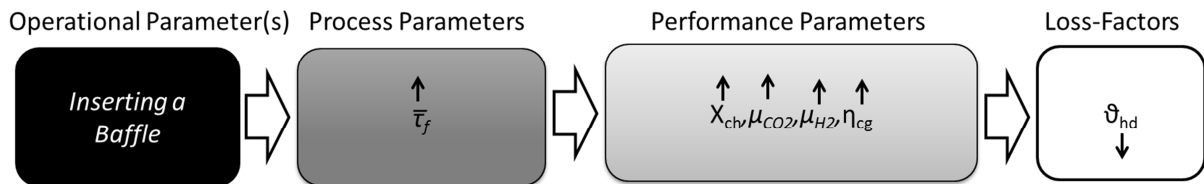


Figure 3.8: Illustration of the chain of impact when introducing a baffle. The arrows indicate the impact that the change has on the process parameters, which in turn affects the performance parameters and loss-factors. The parameters that remain constant are not included.

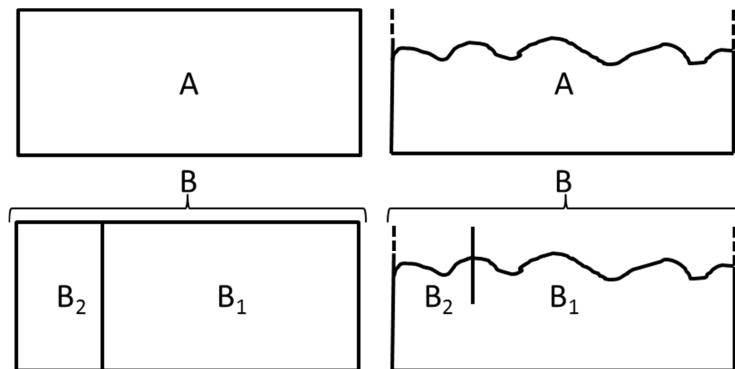


Figure 3.9: Splitting of the bed surface into sections, as viewed from above (left) and as viewed from the side (right). A is the reference layout without the baffle and B is the layout with the baffle.

Table 3.3: Average residence time of fuel particles with and without a baffle for three different levels of fluidization, as defined by Eq. (2.16) (see also Fig. 2.25).

Parameter	Notation	Base 1	Base 2	Base 3	Baffle 1	Baffle 2	Baffle 3
Fluidization velocity	$u$ (m/s)	0.14	0.19	0.23	0.14	0.19	0.23
Average fuel particle residence time	$\bar{\tau}_f$ (s)	632*	271*	176*	854*	334*	210*

\* measured in the cold flow model.

The degree of char conversion in the gasifier depends on the average residence time of the char particles and the effective reactivity of the char  $r_{eff}$ :

$$r_{eff} = -\frac{1}{M_{ch}} \frac{dm_{ch}}{dt} = \frac{1}{1-X_{ch}} \frac{dX_{ch}}{dt} \quad (3.1)$$

where  $M_{ch}$  is the mass of the char inventory in the gasifier,  $dm_{ch}/dt$  is the rate of the mass of char converted with time, and  $dX_{ch}/dt$  is the rate of change in the degree of char conversion. The average residence time is investigated using the cold flow model, as described in Section 2.3, and this enables an analysis of the char conversion in the Chalmers gasifier. From Table 3.3, it is concluded that the level of fluidization has a strong effect on the residence times of the fuel particles, which increase with lower levels of fluidization. It is also concluded that the baffle increases the average residence time, but not to the same extent as the level of fluidization.

The change that occurs in the composition of the syngas when using the baffle, as compared to the reference case, is illustrated in Figure 3.10. This shows that introducing the baffle has a stronger impact on the production of syngas than the fluidization level, which indicates that the baffle affects not only the average residence time of the fuel, but also the reactivity of the char. This is confirmed by the degree of char conversion, as quantified in **Paper III**, showing that the char conversion is increased by 8%–15% for all the fluidization levels when the baffle is added.

The reactivity of char is dependent upon the fuel properties, the temperature, the partial pressure of the reactant (in this case, steam), and the partial pressure of the inhibiting species, which is primarily  $H_2$  when considering steam gasification[3, 61]. With constant fuel properties and temperatures in the presence and absence of the baffle, the results indicate that the baffle affects the average partial pressure of  $H_2O$  and/or  $H_2$  in the vicinity of the char particles. Thus, by forcing the char particles into the dens part of the bed, higher char reactivity is achieved, since the partial pressure of  $H_2O$  is higher and the partial pressure of  $H_2$  is lower than in the average raw gas or in the volatiles.

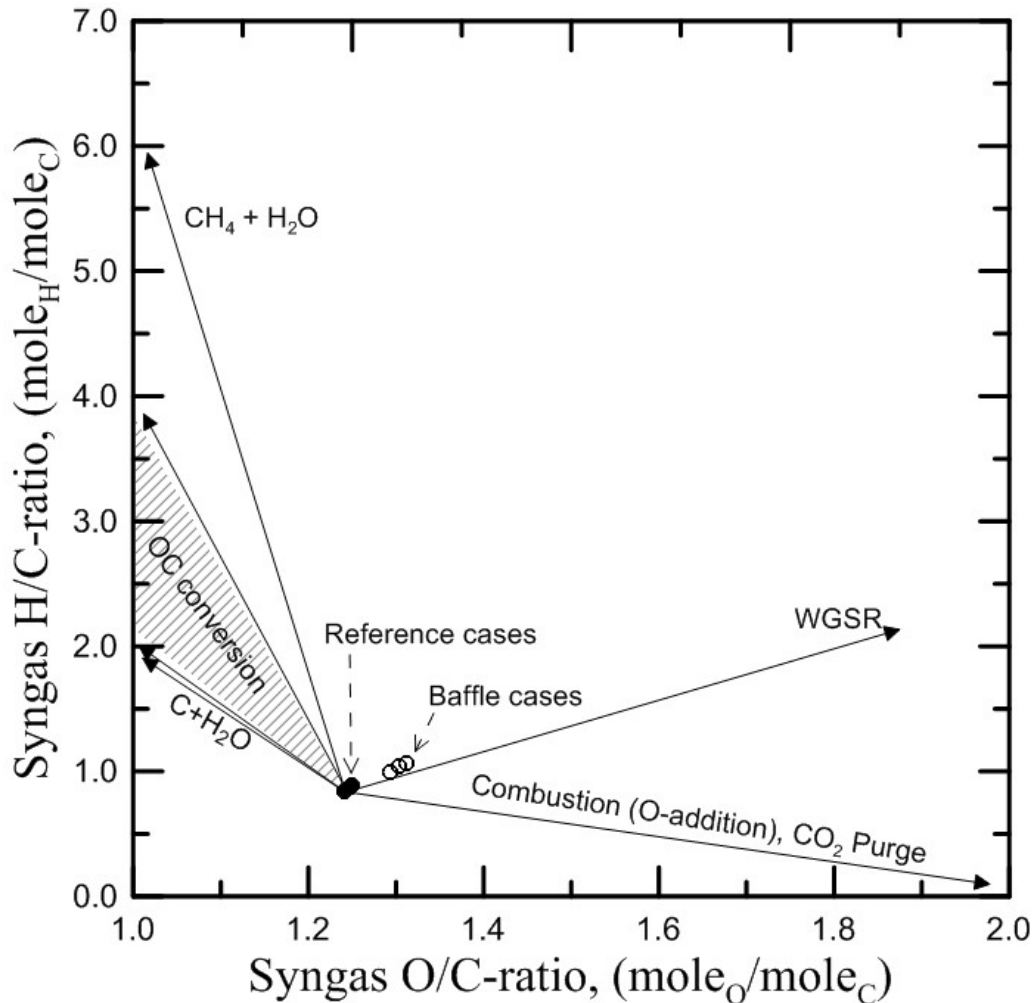


Figure 3.10: Changes in the syngas compositions for the case with silica sand as reference (filled dots) and the three cases with the baffle (open dots), as compared with the syngas changes due to the different reactions (introduced in Fig. 1.6).

This is confirmed by estimating the effective reactivity of the char with a Langmuir-Hinshelwood expression based on data from Barrio et al[62] and the partial pressures of  $H_2O$  and  $H_2$  in the emulsion phase of the bubbling bed, the raw gas, and the volatiles released from the biomass. Figure 3.11 shows the normalized char reactivity as a function of the partial pressure of  $H_2$ , for different partial pressures of  $H_2O$  and a temperature of  $820^\circ C$ . Unity represents the reactivity in pure steam without any  $H_2$ . The partial pressures of  $H_2O$  and  $H_2$  that are typical for the raw gas, volatiles, and bed section are indicated as shaded fields in the figure. This shows that local variations in the partial pressures of  $H_2$  and  $H_2O$  can have a substantial impact on char reactivity, and that it is crucial to separate the char from the volatiles to increase the char reactivity.

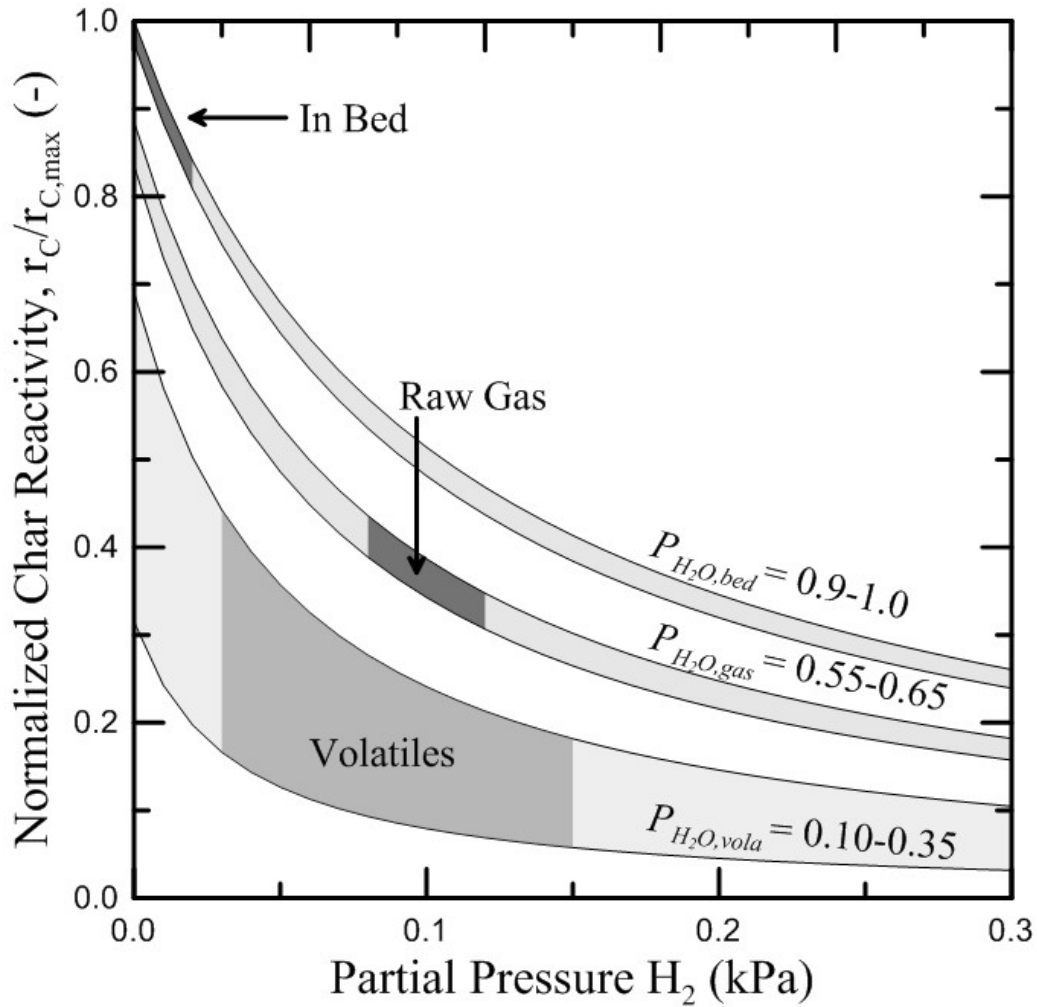


Figure 3.11: Normalized char reactivities as a function of the partial pressure of  $H_2$  and different levels of  $H_2O$  typical for different locations in the gasifier. Based on the Langmuir-Hinshelwood model presented by Barrio et al.[62].

In summary, introducing a baffle across the surface of the bed is effective for increasing the degree of char conversion. The increase in char conversion is mainly due to increased char reactivity, which can be achieved by an increase in the concentration of  $H_2O$  and a decrease in the concentration of  $H_2$  in the vicinity of the char particles. Further research is required to design a layout for the gasifier that offers robust operation and ensures a degree of char conversion that matches the heat demands of the process (as described in Section 2.3).

### 3.3 CONCLUSIONS

The effects of changing the fluidization level, the type of bed material, and the layout of the reactor were investigated in present work, and it is concluded that:

- Increasing the steam improves the conversion of OC components, which decrease the losses related to the by-products. Increasing the steam also increases the internal heat demand and, thereby, increases the loss related to the heating of the process. The current results show that as long as sufficient heat is available external to the gasifier to produce the steam, increasing the level of steam has a positive effect on the potential chemical efficiencies of the end-product.
- Introducing a catalytic oxygen-carrying material, such as a metal oxide-containing material, can decrease the yield of by-products but it can also increase the loss related to the heating of the system. The materials tested in the Chalmers gasifier were ilmenite and bauxite, and it can be concluded that ilmenite has too high an oxygen-carrying capacity to be used as a primary tar reduction measure without a major penalty in terms of chemical efficiency. In contrast, bauxite, which has a lower oxygen-transporting capacity, shows good potential, and it should be subjected to further research.
- Initial results from the GoBiGas gasifier, in which olivine is used as a bed material, show that the activation of the olivine reduced the tar concentration from about 20g/Nm<sup>3</sup> to 5 g/Nm<sup>3</sup>.
- By adding a baffle that spans the surface of the bubbling bed of the gasifier, the average residence time of the fuel particles is prolonged and the fuel particles are forced into the dense part of the bubbling bed to pass the baffle. Our results show that char conversion is increased by 8%–15% following the introduction of a baffle.
- The impacts that the investigated changes have on the composition of the syngas are compared with the theoretical changes in the composition of the syngas based on the H/C-ratio and O/C-ratio. It is shown in this thesis that this type of comparison can be used for qualitative evaluations of the change in performance between different operational cases based solely on measurements of the H<sub>2</sub>, CO, and CO<sub>2</sub> concentrations. The approach also offers a quick and relatively easy method for detecting unwanted changes in the fuel conversion in a gasifier.

## 4 CONCLUDING REMARKS AND OUTLOOK

---

A comprehensive procedure for the evaluation of a DFB gasifier, which consists of eight steps, is presented in this work. The multitude of equipment and methods required for a comprehensive evaluation makes the procedure complex and demanding in terms of both resources and labor. Although some procedural modifications of the evaluation are suggested in this work, there is a need for further developments that will simplify the evaluation of DFB gasifiers both in terms of quantifying the fuel conversion and improving the monitoring of the process. The present work shows how the syngas composition, expressed as the H/C-ratio and the O/C-ratio, can be used as indicators to detect transient behavior in a gasifier and as a valuable tool for optimizing the operation of a gasifier.

The chemical efficiency of a DFB gasifier is dependent upon the fuel conversion in the reactor, and the main aspects to consider are the heat demand and the production of by-products, such as tar components. A low yield of tar is a crucial for a gasifier, as tar causes fouling of downstream equipment and constitutes a by-product. Therefore, it will be important in future studies to find ways to reduce the tar yield so as to improve the efficiency and reduce the operational costs. A promising approach is to use catalytic metal oxide (MeO)-based bed materials to reduce the tar yield, e.g., by using bauxite or olivine, although further research on catalytic bed materials is required. Important aspects to consider concerning bed materials are their catalytic capabilities, oxygen-carrying capacities, interactions with the fuel ash, cost, and environmental impacts upon disposal.

The application of system integration and heat recovery is important for establishing a low heat demand in the gasifier, as the latter restricts the chemical efficiency of the gasifier. With a low heat demand in the gasification process, it becomes important to gasify part of the char. The important aspects of char conversion comprise the reactivity, temperature, and residence time of the char particles. To increase understanding of how the degree of char conversion can be controlled, future research should focus on how the reactivity of the char and the average residence time of the char particles are affected by changing the fluidization and the layout of the gasification reactor. A major aim of such research should be to separate the devolatilization and gasification processes, to increase the steam-char contacts and reduce inhibition of the gasification by volatile components.



## 5 NOMENCLATURE

---

$\Delta C_{daf,HTR}$	Change in the amount of mole C from the biomass to the gas out of the HTR
$\Delta H_{daf,HTR}$	Change in the amount of mole H from the biomass to the gas out of the HTR
$\Delta O_{daf,HTR}$	Change in the amount of mole O from the biomass to the gas out of the HTR
$C(t)$	Concentration of tracer particles at time t
$C_{He}$	Concentration of He in the cold gas (Vol%)
$CH_iO_j$	Average composition of biomass normalized with the mole amount of carbon
$CH_kO_l$	Average composition of a biofuel normalized with the mole amount of carbon
$C_{i,cg}$	Concentration of component i in the cold gas (Vol%)
$C_i$	Organic compound with j C molecules
$C_t$	Concentration of tar in (g/Nm <sup>3</sup> )
$C_xH_y$	Organic compounds with 2 or 3 atoms of carbon
$C_zH_vO_w$	Average composition of the raw gas
$E(t)$	Fraction of particles out of a reactor at time t (-)
$F(t)$	Cumulative fraction of particles out of a reactor at time t (-)
$H_{gasif}$	Heat of reaction for the gasification reaction (MJ/kg)
$H_{gas}$	Heat of reaction for the reforming of the gas (MJ/kg)
$He,all$	Helium injection to the gasifier,LS1, and LS2 at the same time
$He,G$	Helium injection to the gasifier
$He,LS1$	Helium injection to LS1
$He,LS2$	Helium injection to LS2
$h_{eff}$	Effective heating rate (W/m <sup>2</sup> K )
$LHV_b$	Lower heating value of a biofuel (MJ/kg)
$LHV_{daf}$	Lower heating value of a dry-ash-free fuel (MJ/kg)
$LHV_{O_2,ch}$	Lower heating value of char per mass unit of O <sub>2</sub> (MJ/kgO <sub>2</sub> )
$LHV_{O_2,gas}$	Lower heating value of gas per mass unit of O <sub>2</sub> (MJ/kgO <sub>2</sub> )
$\dot{m}_{bm}$	Mass flow of bed material (kg/h)
$\dot{m}_{fuel}$	Mass flow of fuel (kg/h)
$\dot{m}_{st,bed}$	Mass flow of steam (kg/h)
$\dot{m}_{st,i}$	Mass flow of steam to i=G,LS1,LS2,all (kg/h)
$\dot{n}_C$	Molar flow of Carbon (mole/s)

$\dot{n}_H$	Molar flow of Hydrogen (mole/s)
$\dot{n}_O$	Molar flow of Oxygen (mole/s)
$\dot{n}_{O,add}$	Molar flow of Oxygen added to a gasifier (mole/s)
$OC^*$	OC with an altered composition
$P$	Pressure (kPa)
$P_{atm}$	Atmospheric pressure (kPa)
$\mathcal{R}$	General gas constant ( $m^3\text{bar}/\text{mole K}$ )
$R_{O}X_{MeO,G}$	Oxygen-carrying capacity of a MeO material to the gasifier ( $kg_O/kg_{MeO}$ )
$t$	Time (s)
$T$	Temperature ( $^{\circ}\text{C}$ )
$\bar{T}_{bed}$	Average temperature of the bed section of the gasifier ( $^{\circ}\text{C}$ )
$T_C$	Temperature in the combustion reactor ( $^{\circ}\text{C}$ )
$\bar{T}_{gas}$	Average temperature of the gas in the freeboard section of the gasifier ( $^{\circ}\text{C}$ )
$\dot{V}_{He}$	Volume flow of helium ( $m^3/s$ )
$\dot{V}_{rg}$	Volume flow of raw gas ( $m^3/s$ )
$X$	Degree of conversion (-)
$X_{ch}$	Degree of conversion of char (-)
$X_{ch,max}$	The maximum degree of char conversion in a adiabatic gasifier (-)
$X_{st,i}$	Fraction of steam entering the gasifier from $i=LS1,LS2,all$ (-)
$Y$	Yields from pyrolysis ( $kg/kg_{daf}$ )
$Y_{C,gas}$	Yield of C in the cold gas from pyrolysis ( $kg_C/kg_{daf}$ )
$Y_{C,daf}$	Yield of C in the cold gas from pyrolysis ( $kg_C/kg_{daf}$ )
$u-u_{mf}$	Superficial fluidization velocity minus the minimum fluidization velocity (m/s)

## ABBREVIATIONS

Ar	Argon
BTX	Benzene, toluene and xylene
C	Elemental carbon
$C_2H_6$	Ethane molecule
CFB	Circulating fluidized bed
CFD	Computational fluid-dynamics
$CH_4$	Methane molecule

CLR	Chemical looping reforming
CO	Carbon monoxide molecule
CO <sub>2</sub>	Carbon dioxide molecule
DFB	Dual fluidized beds
DME	Dimethyl ether
EF	Entrained flow
FB	Fluidized bed
FID	Flame ionization detector
FT	Fischer-Tropsch
G	Gasifier
H	Elemental hydrogen
H <sub>2</sub>	Hydrogen molecule
H <sub>2</sub> O	Water molecule
HTR	High temperature reactor
LHV	Lower heating value
LS1	Loop seal 1
LS2	Loop seal 2
MeO	Metal-oxide material
MeOH	Methanol
NDIR	Non-dispersive infrared
N <sub>2</sub>	Nitrogen molecule
O	Elemental oxygen
OC	Organic compounds with more than 3 carbon atoms
SFR	Steam-to-fuel ratio
SNG	Substitute natural gas
SPA	Solid phases adsorption
WGSR	Water-gas-shift reaction

## GREEK LETTERS

$\alpha_i$	Mole amounts of component i to balance chemical reactions
$\delta_{bp}$	Loss-factor related to by-products
$\delta_{hd}$	Loss-factor related to the heat demand
$\delta_i$	Loss-factor related to component i
$\eta_b$	Chemical efficiency of a biofuel (MJ/MJdaf)
$\eta_{cg}$	Chemical efficiency of the cold gas (MJ/MJdaf)
$\eta_{rg}$	Chemical efficiency of the raw gas (MJ/MJdaf)
$\lambda$	Fraction of the stoichiometric amount of oxygen ( $\text{kg}_{\text{O,add}}/\text{kg}_{\text{stoichiometric}}$ )
$\mu$	Mass per kg of dry-ash-free fuel ( $\text{kg}/\text{kg}_{\text{daf}}$ )
$\mu_{C,b,theo}$	Mass of C in a biofuel per mass unit of C in the dry-ash-free fuel, no losses ( $\text{kgC}/\text{kgC}_{,\text{daf}}$ )
$\mu_{C,b}$	Mass of C in a biofuel per mass unit of C in the dry-ash-free fuel ( $\text{kgC}/\text{kgC}_{,\text{daf}}$ )
$\mu_{C,cg}$	Mass C in cold gas per kg of dry-ash-free fuel ( $\text{kg}/\text{kg}_{\text{daf}}$ )
$\mu_{C,rg}$	Mass C in raw gas per kg of dry-ash-free fuel ( $\text{kg}/\text{kg}_{\text{daf}}$ )
$\mu_{i,cg}$	Mass of component i in cold gas per kg of dry-ash-free fuel ( $\text{kg}/\text{kg}_{\text{daf}}$ )
$\mu_{\text{O}}$	Mass of oxygen added to the gasifier per kg of dry-ash-free fuel ( $\text{kgO}/\text{kg}_{\text{daf}}$ )
$\mu_{\text{O}_2,\text{stoichiometric}}$	Mass O <sub>2</sub> per kg of dry-ash-free fuel required for stoichiometric combustion ( $\text{kg}/\text{kg}_{\text{daf}}$ )
$\mu_{\text{OC}}$	Yield of OC per kg of dry-ash-free fuel ( $\text{kg}/\text{kg}_{\text{daf}}$ )
$\mu_p$	Mass of purge gas added to the gasifier per kg of dry-ash-free fuel ( $\text{kg}/\text{kg}_{\text{daf}}$ )
$\mu_{\text{tar}}$	Yield of tar per kg of dry-ash-free fuel ( $\text{kg}/\text{kg}_{\text{daf}}$ )
$\nu$	Heat demand (MJ/MJdaf)
$\nu_{\text{extract}}$	Required heat extraction (MJ/MJdaf)
$\nu_{\text{int}}$	Internal heat demand (MJ/MJdaf)
$\sigma$	Fraction gas combusted by oxygen added to a gasifier (-)
$\bar{\tau}_f$	Average residence time of the fuel (s)
$\bar{\tau}_g$	Average residence time of the gas (s)

## 6 REFERENCES

---

- [1] The Swedish Government, "En sammanhållen klimat och energipolitik - klimat," vol. prop. 2008/09:162 (government bill) Ministry of the Environment, ed.
- [2] A. V. Bridgwater, "Renewable fuels and chemicals by thermal processing of biomass," *Chemical Engineering Journal*, vol. 91, pp. 87-102, 2003.
- [3] C. Di Blasi, "Combustion and gasification rates of lignocellulosic chars," *Progress in Energy and Combustion Science*, vol. 35, pp. 121-140, // 2009.
- [4] T. A. Milne, N. Abatzoglou, and R. J. Evans, *Biomass gasifier" tars": their nature, formation, and conversion*: National Renewable Energy Laboratory Golden, CO, 1998.
- [5] A. Jess, "Mechanisms and kinetics of thermal reactions of aromatic hydrocarbons from pyrolysis of solid fuels," *Fuel*, vol. 75, pp. 1441-1448, 1996.
- [6] D. Neves, H. Thunman, A. Matos, L. Tarelho, and A. Gomez-Barea, "Characterization and prediction of biomass pyrolysis products," *Progress in Energy and Combustion Science*, 2011.
- [7] P. H. Brunner and P. V. Roberts, "The significance of heating rate on char yield and char properties in the pyrolysis of cellulose," *Carbon*, vol. 18, pp. 217-224, // 1980.
- [8] M. J. C. van der Stelt, H. Gerhauser, J. H. A. Kiel, and K. J. Ptasinski, "Biomass upgrading by torrefaction for the production of biofuels: A review," *Biomass and Bioenergy*, vol. 35, pp. 3748-3762, 10// 2011.
- [9] D. Mohan, C. U. Pittman Jr, and P. H. Steele, "Pyrolysis of wood/biomass for bio-oil: A critical review," *Energy and Fuels*, vol. 20, pp. 848-889, 2006.
- [10] R. Rauch, J. Hrbek, and H. Hofbauer, "Biomass gasification for synthesis gas production and applications of the syngas," *Wiley Interdisciplinary Reviews: Energy and Environment*, pp. n/a-n/a, 2013.
- [11] NNFCC, "Review of Technologies for Gasification of Biomass and Wastes," NNFCC project 09/008, 2009.
- [12] I. Tomoyuki, "Methanation," in *Encyclopedia of Catalysis*, ed: John Wiley & Sons, Inc., 2002.
- [13] I. Czekaj, F. Loviat, F. Raimondi, J. Wambach, S. Biollaz, and A. Wokaun, "Deactivation process of Ni/Al<sub>2</sub>O<sub>3</sub> Catalyst during methanation by biomass-derived synthesis gas," in *Proceeding of the EUROPACAT VIII conference, catalyst deactivation, regeneration and recycling session, Turku Fair Centre, Turku/Åbo, Finland*, 2007.
- [14] J. Kopyscinski, M. C. Seemann, R. Moergeli, S. M. A. Biollaz, and T. J. Schildhauer, "Synthetic natural gas from wood: Reactions of ethylene in fluidised bed methanation," *Applied Catalysis A: General*, vol. 462-463, pp. 150-156, 2013.
- [15] M. Seemann, S. Biollaz, C. Aichernig, R. Rauch, H. Hofbauer, and R. Koch, *Methanation of bio-syngas in a bench scale reactor using a slip stream of the FICFB gasifier in Güssing*: na, 2004.

- [16] T. Ogawa, N. Inoue, T. Shikada, O. Inokoshi, and Y. Ohno, "Direct Dimethyl Ether (DME) synthesis from natural gas," in *Studies in Surface Science and Catalysis*. vol. Volume 147, B. Xinhe and X. Yide, Eds., ed: Elsevier, 2004, pp. 379-384.
- [17] D. W. van Krevelen, *Coal: Typology, Chemistry, Physics, Constitution*: Elsevier Publishing Company, 1961.
- [18] O. S. Bruinsma, R. S. Geertsma, P. Bank, and J. A. Moulijn, "Gas phase pyrolysis of coal-related aromatic compounds in a coiled tube flow reactor: 1. Benzene and derivatives," *Fuel*, vol. 67, pp. 327-333, 1988.
- [19] O. S. Bruinsma, P. J. Tromp, H. J. de Sauvage Nolting, and J. A. Moulijn, "Gas phase pyrolysis of coal-related aromatic compounds in a coiled tube flow reactor: 2. Heterocyclic compounds, their benzo and dibenzo derivatives," *Fuel*, vol. 67, pp. 334-340, 1988.
- [20] C. Higman and M. Van der Burgt, *Gasification*: Gulf professional publishing, 2011.
- [21] A. Van der Drift, H. Boerrigter, B. Coda, M. Cieplik, K. Hemmes, R. Van Ree, *et al.*, "Entrained flow gasification of biomass," *Energy Centre of Netherlands*, 2004.
- [22] J. Brandin and T. Liliedahl, "Unit operations for production of clean hydrogen-rich synthesis gas from gasified biomass," *Biomass and Bioenergy*, vol. 35, pp. S8-S15, 2011.
- [23] K. Qin, W. Lin, P. A. Jensen, and A. D. Jensen, "High-temperature entrained flow gasification of biomass," *Fuel*, vol. 93, pp. 589-600, 3// 2012.
- [24] I. Gunnarsson, "The GoBiGas Project," in *International Seminar on Gasification*, 2011, pp. 6-7.
- [25] S. Heyne and S. Harvey, "Assessment of the energy and economic performance of second generation biofuel production processes using energy market scenarios," *Applied Energy*, vol. 101, pp. 203-212, 1// 2013.
- [26] H. Thunman, L.-E. Åmand, B. Leckner, and F. Johnsson, "A cost effective concept for generation of heat, electricity and transport fuel from biomass in fluidized bed boilers – using existing energy infrastructure," ed: Proceedings of the 15th European Biomass Conference & Exhibition - From research to market Deployment, Berlin, Germany, 7-11 May 2007, 2007.
- [27] M. Seemann and H. Thunman, "The new Chalmers research-gasifier," in *the 20th International Conference on Fluidized Bed Combustion*, 2009, pp. 659-663.
- [28] B. Leckner, M. R. Golriz, W. Zhang, B. A. Andersson, and F. Johnsson, "Boundary layers-first measurements in the 12 MW CFB research plant at Chalmers University," in *International Conference on Fluidized Bed Combustion*, 1991, pp. 771-776.
- [29] H. Hofbauer, "Scale up of fluidized bed gasifiers from laboratory scale to commercial plants: steam gasification of solid biomass in a dual fluidized bed system," 2006, pp. 21-24.
- [30] I. Gunnarsson, "The GoBiGas Project," 2011.
- [31] R. Reimert, F. Marschner, H.-J. Renner, W. Boll, E. Supp, M. Brejc, *et al.*, "Gas Production, 2. Processes," in *Ullmann's Encyclopedia of Industrial Chemistry*, ed: Wiley-VCH Verlag GmbH & Co. KGaA, 2000.
- [32] P. Basu, *Biomass gasification and pyrolysis: practical design and theory*: Academic press, 2010.
- [33] M. Israelsson, M. Seemann, and H. Thunman, "Assessment of the solid-phase adsorption method for sampling biomass-derived tar in industrial environments," *Energy and Fuels*, vol. 27, pp. 7569-7578, // 2013.

- [34] C. Brage, Q. Yu, G. Chen, and K. Sjöström, "Use of amino phase adsorbent for biomass tar sampling and separation," *Fuel*, vol. 76, pp. 137-142, 1997.
- [35] S. Osipovs, "Sampling of benzene in tar matrices from biomass gasification using two different solid-phase sorbents," *Analytical and Bioanalytical Chemistry*, vol. 391, pp. 1409-1417, // 2008.
- [36] S. Osipovs, "Comparison of efficiency of two methods for tar sampling in the syngas," *Fuel*, vol. 103, pp. 387-392, // 2013.
- [37] S. V. B. Passen. (2005). *"Thersites": website for tar dew point calculations*. Available: [www.thersites.nl](http://www.thersites.nl)
- [38] D. Neves, "Evaluation of thermochemical biomass conversion in fluidized bed," Phd, Department of Environment and Planning and Centre of Environmental and Marine Studies, University of Aveiro, 2013.
- [39] P. J. Linstrom, W. G. Mallard, and (eds.). NIST Chemistry WebBook [Online]. Available: <http://webbook.nist.gov/chemistry/>
- [40] M. Gassner and F. Maréchal, "Thermo-economic process model for thermochemical production of Synthetic Natural Gas (SNG) from lignocellulosic biomass," *Biomass and Bioenergy*, vol. 33, pp. 1587-1604, 2009.
- [41] E. Sette, S. Aimé, D. Pallares, and F. Johnsson, "Analysis of lateral fuel mixing in a fluidodynamically down-scaled bubbling fluidized bed," presented at the Fluidization XIV Conference 2013.
- [42] E. Sette, A. Gómez García, D. Pallares, and F. Johnsson, "Quantitative evaluation of inert solids mixing in a bubbling fluidized bed," in *21st International Conference on Fluidized Bed Combustion*, 2012.
- [43] F. J. Kuchuk, M. Onur, and F. Hollaender, "Chapter 3 - Convolution," in *Developments in Petroleum Science*. vol. Volume 57, F. H. Fikri Kuchuk and O. Mustafa, Eds., ed: Elsevier, 2010, pp. 51-114.
- [44] G. I. Palconok, "Heat and mass transfer to a single particle in fluidized bed," Chalmers University of Technology, 1998.
- [45] A. Nzihou, B. Stanmore, and P. Sharrock, "A review of catalysts for the gasification of biomass char, with some reference to coal," *Energy*, vol. 58, pp. 305-317, 9/1/ 2013.
- [46] P. Simell, P. Ståhlberg, E. Kurkela, J. Albrecht, S. Deutsch, and K. Sjöström, "Provisional protocol for the sampling and analysis of tar and particulates in the gas from large-scale biomass gasifiers. Version 1998," *Biomass and Bioenergy*, vol. 18, pp. 19-38, 2000.
- [47] Y. Richardson, J. Blin, and A. Julbe, "A short overview on purification and conditioning of syngas produced by biomass gasification: Catalytic strategies, process intensification and new concepts," *Progress in Energy and Combustion Science*, vol. 38, pp. 765-781, 12// 2012.
- [48] F. Lind, M. C. Seemann, and H. Thunman, "Continuous catalytic tar reforming of biomass derived raw gas with simultaneous catalyst regeneration," *Industrial & Engineering Chemistry Research*, 2011.
- [49] A. Dutta, M. Talmadge, J. Hensley, M. Worley, D. Dudgeon, D. Barton, *et al.*, "Techno-economics for conversion of lignocellulosic biomass to ethanol by indirect gasification and mixed alcohol synthesis," *Environmental Progress and Sustainable Energy*, vol. 31, pp. 182-190, // 2012.

- [50] M. Rydén, A. Lyngfelt, and T. Mattisson, "Synthesis gas generation by chemical-looping reforming in a continuously operating laboratory reactor," *Fuel*, vol. 85, pp. 1631-1641, // 2006.
- [51] A. Lyngfelt, B. Leckner, and T. Mattisson, "A fluidized-bed combustion process with inherent CO<sub>2</sub> separation; Application of chemical-looping combustion," *Chemical Engineering Science*, vol. 56, pp. 3101-3113, // 2001.
- [52] R. J. Lancee, A. I. Dugulan, P. C. Thüne, H. J. Veringa, J. W. Niemantsverdriet, and H. O. A. Fredriksson, "Chemical looping capabilities of olivine, used as a catalyst in indirect biomass gasification," *Applied Catalysis B: Environmental*, vol. 145, pp. 216-222, // 2014.
- [53] M. Jelena and M. Seemann, "Role of inorganics in the Indirect Biomass Gasification while using olivine as bed material," *To be submitted*.
- [54] F. Lind, N. Berguerand, M. Seemann, and H. Thunman, "Ilmenite and Nickel as Catalysts for Upgrading of Raw Gas Derived from Biomass Gasification," *Energy & Fuels*, vol. 27, pp. 997-1007, 2013/02/21 2013.
- [55] Z. Min, M. Asadullah, P. Yimsiri, S. Zhang, H. Wu, and C. Z. Li, "Catalytic reforming of tar during gasification. Part I. Steam reforming of biomass tar using ilmenite as a catalyst," *Fuel*, vol. 90, pp. 1847-1854, // 2011.
- [56] A. Cuadrat, A. Abad, J. Adánez, L. F. de Diego, F. García-Labiano, and P. Gayán, "Behavior of ilmenite as oxygen carrier in chemical-looping combustion," *Fuel Processing Technology*, vol. 94, pp. 101-112, 2// 2012.
- [57] H. Leion, A. Lyngfelt, M. Johansson, E. Jerndal, and T. Mattisson, "The use of ilmenite as an oxygen carrier in chemical-looping combustion," *Chemical Engineering Research and Design*, vol. 86, pp. 1017-1026, 9// 2008.
- [58] R. Rauch, C. Pfeifer, K. Bosch, H. Hofbauer, D. Swierczynski, C. Courson, *et al.*, "Comparison of different olivines for biomass steam gasification," *Science in thermal and chemical biomass conversion*, vol. 1, pp. 799-809, 2004.
- [59] A. Grootjes, C. Meijden, H. Visser, and A. Drift, "Improved Gasifier availability with bed material and additives," 2013.
- [60] M. Öhman, A. Nordin, B. J. Skrifvars, R. Backman, and M. Hupa, "Bed agglomeration characteristics during fluidized bed combustion of biomass fuels," *Energy & Fuels*, vol. 14, pp. 169-178, 2000.
- [61] M. Keller, H. Leion, T. Mattisson, and A. Lyngfelt, "Gasification inhibition in chemical-looping combustion with solid fuels," *Combustion and Flame*, vol. 158, pp. 393-400, 3// 2011.
- [62] M. Barrio, B. Gøbel, H. Rimes, U. Henriksen, J. E. Hustad, and L. H. Sørensen, "Steam Gasification of Wood Char and the Effect of Hydrogen Inhibition on the Chemical Kinetics," in *Progress in Thermochemical Biomass Conversion*, ed: Blackwell Science Ltd, 2008, pp. 32-46.